STEADY STATE AND DYNAMIC PERFORMANCE OF ANISOTROPIC RELUCTANCE MOTOR

BY

S. CHANDRASEKHARA RAO

A THESIS

PRESENTED IN PARTIAL FULFILLMENT OF

THE REQUIREMENTS FOR THE DEGREE

OF

MASTER OF SCIENCE IN ELECTRICAL ENGINEERING

AT

NEWARK COLLEGE OF ENGINEERING

Newark, New Jersey

ABSTRACT

The paper deals with a special type of reluctance motor called Anisotropic rotor reluctance motor. As the name implies, advantage is taken of the internal anisotropy of the rotor magnetic structure. Axially laminated grain oriented silicon steel is used in the rotor. This unconventional configuration of assembly of rotor laminations results in a high ratio of direct axis to quadrature axis reluctance. Compared to the conventional reluctance motor, pull out torque of more than three times and a power factor as high as in an induction motor is obtained. Several motors of ratings up to 60 HP. were built and tested.

The superiority of these over the conventional or the commercially available "Synduction Motor" is established both theoritically and by test results. Combined with the ease of manufacturing almost akin to the squirrel cage induction motor, a high power factor and pull-out and pull-in performance, the Anisotropic motor poses a serious challange to the brushless synchronous motor for constant speed applications.

In industrial applications, like textile mill applications and computer power supplies where reliable power drives are required, this new type of Anisotropic motor is expected to find greater demand in the future.

APPROVAL OF THESIS

STEADY STATE AND DYNAMIC PERFORMANCE

OF ANISOTROPIC RELUCTANCE MOTOR

BY

S. CHANDRASEKHARA RAO

FOR

DEPARTMENT OF ELECTRICAL ENGINEERING

NEWARK COLLEGE OF ENGINEERING

BY

FACULTY COMMITTEE

APPROVED: _____

_____

_____

NEWARK, NEW JERSEY

PREFACE

The purpose of this thesis is to make theoretical evaluation of the performance of the commercially available Synduction motor and the new axially laminated Anisotropic motor. This has been followed by construction and testing the Anisotropic design. Considerable work has been done on establishing dynamical equations of the motor performance and solution to the dynamical equation using a computer.

I would like to thank Messrs. E. P. Schinman, B. Barron, and S. Garnett for encouraging me in building several units of different ratings of the Anisotropic motor.

My special thanks are to Prof. K. Denno for allowing me to work on this subject and especially for encouraging me to make theoretical study on the dynamic performance. Thanks are also due to Mr. N. S. Vishwanath for running a computer program for the solution to the dynamical equation.

Finally, the author wishes to express deep appreciation for the meticulous typing work done by Mrs. Pauline R. Schirner.

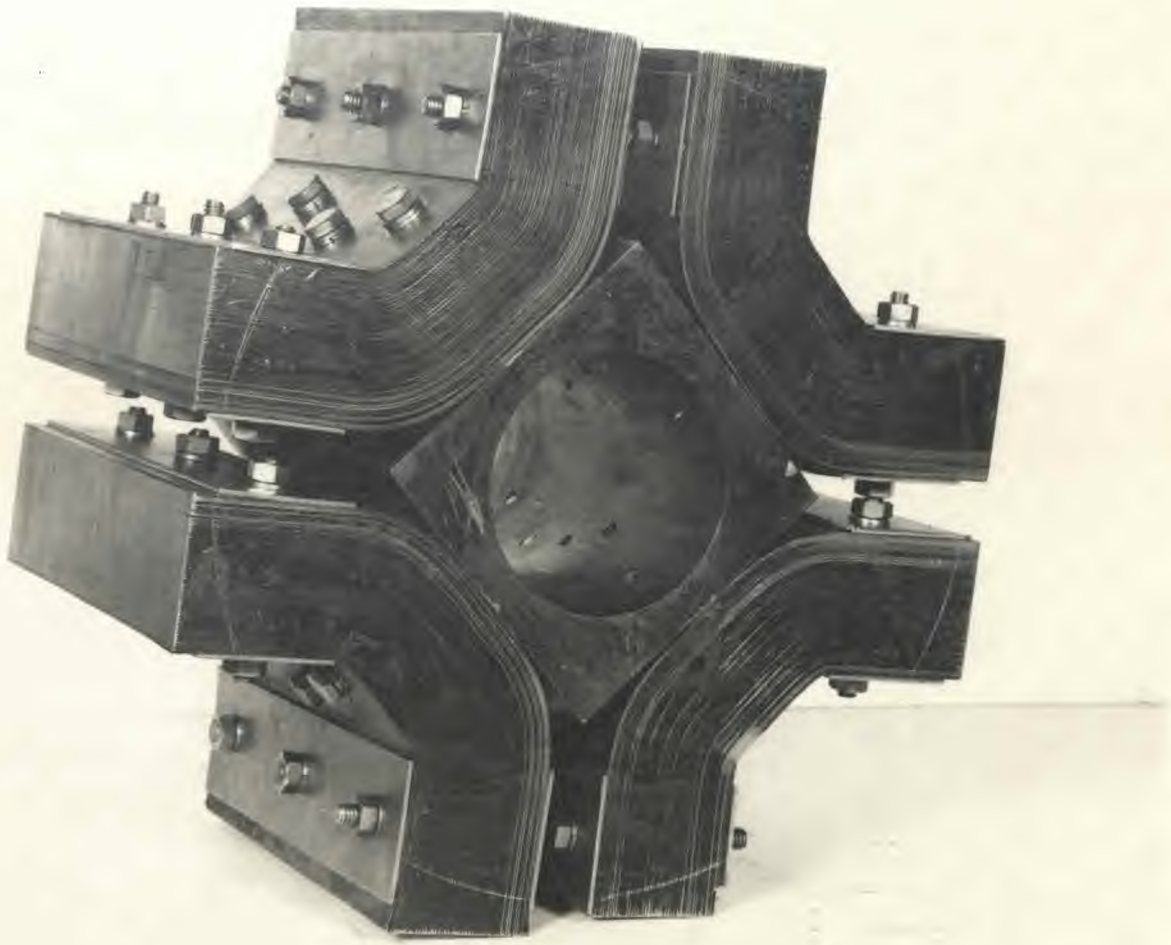

LAMINATION ASSEMBLY OF ANISOTROPIC ROTOR

DIE CAST ANISOTROPIC ROTOR

LAMINATION OF SYNDUCTION MOTOR

TABLE OF CONTENTS

LIST OF FIGURES

LIST OF FIGURES

CHAPTER 1

INTRODUCTION

The advantages of using a reluctance motor in place of excited field synchronous motors are well known. Lack of any field winding, ease of synchronization and resynchronization in case of pull out are some of the advantages in performance. Also reluctance motors are cheap, robust, and reliable when compared to excited field synchronous motors. On the other hand, lower specific output and poor power factor limit the application of these motors. The reluctance torque in any synchronous machine accounts for not more than 30% of total pull out torque. Even with the improved saliency by optimizing pole span/pole pitch ratio pull out torques obtained are far below that for excited field machines.

During the last few years, attention has been given to further improve the performance of the machine. Noteworthy is the segmented rotor construction and the development of what has come to be known as "Synduction Motor." By introducing barriers in the quadrature axis magnetic structure, the ratio of synchronous reactance in the direct axis to that in quadrature is increased, thereby increasing the value of pull out torque.

However, though this development has made the reluctance motor commercially applicable to the extent that several

companies are now offering this as their standard production item, poor power factor has been one of the main disadvantages of this construction. Some attention is now being given to improve the performance by now introducing magnetic anisotropy inherent in the magnetic materials, as in the case of grain oriented sheet steel, in addition to the physical barriers in the quadrature axis. These motors, hereafter referred to as "Axially Laminated Anisotropic Reluctance Motors" (for brevity called Anisotropic motor) have better power factors and specific output than the commercially available "Synduction Motors."

The detailed analysis in the following paper is confined to the two improved versions of the Reluctance motors, namely Synduction and Anisotropic motors.

Emphasis is particularly on bringing out the advantages of the Anisotropic motor. The constructional features calculated parameters, calculated performance and comparison of test values for both types form the topics for different chapters. For sake of comparison, identical stators are used in both motors, and rotors of identical diameters and lengths as well as pole span/pole pitch are chosen. This would enable the results to be interpreted more accurately and improvements attributed to the aspect of the intrinsic anisotropy of the Anisotropic design.

It is to be noted that the performance equations de-

rived in the following chapters hold good for any type of Reluctance machine whether Synduction or Anisotropic. It is to be emphasized that the difference in their performance is only due to the magnitudes of $\frac{Xd}{Xq}$ ratios in either case.

Therefore, except for the development of the theory of the two types where separate chapters are devoted, the rest of the material dealing with steady state of transient performance work out to be identical equations. However, as said above, in view of the enormous difference in the reactance values for the two machines, the magnitude of performances come out to be different. This is clearly seen from test results in Chapter 10.

Several Anisotropic motors were designed, constructed and tested. For purposes of comparison a commercially available Synduction motor was used. The performances are compared in Chapters 10 and 12. A computer program was developed for solution of the nonlinear differential equation of dynamic state. The results showing the variation of torque angle with time for a sudden application of load is included in Chapter 11.

Scope and Objectives

The thesis is undertaken mainly to elaborate on the new concept of incorporating intrinsic anisotropy into

reluctance motors. The following logical steps form the scope of the thesis:

(a) Theory and prediction of performance of the Synduction and Anisotropic motor.

(b) Design of the two types of motors of identical physical dimensions.

(c) Calculation of the direct and quadrature axes reactances, on which depend most of the steady state behavoir.

(d) To study the dynamic equivalent circuits and transient behavoir.

(e) Test results from the actual machines built as per above.

(f) Comparison of the performance to bring out the improvement of the performance of the Anisotropic motor over the Synduction motor.

It is to be noted, again, that the emphasis of this entire work is based on bringing out a new motor which is production worthy and commercially feasible. It would be of interest to people engaged in industries who always look for a large ratio of performance to cost and a wide range of applications.

It is realized that considerable work could be done in transient analysis. While this feature would undoubtedly be of enormous interest, most of the work done here deals

with the design and steady state analysis for the following reasons. However, two chapters are devoted to the dynamic behavoir and equivalent circuits.

Any involved work done using transient analysis would be meaningful in understanding its actual operation, only if the phenomenon of saturation is taken into full account. As can be seen from the oscillogram pictures of transient conditions at starting, (see Figure 8.1) and explained in Chapter 8, the current oscillations at speeds below synchronous are very large, due to the combination of asynchronous torque of induction motor plus synchronous torque of reluctance motor. Also from the test results in Chapter 10, it can be seen that while the d-axis is driven into deep saturation and thereby varying the direct axis reactance, the quadrature axis is in low saturation and the reactance associated is constant. Therefore any prediction of torque in transient condition, that is below synchronous speed involves calculation of true subtransient and transient direct and quadrature axes reactances. This again depends on the unequal saturations in the two axes due to the large current pulsations. The author feels that theoretical evaluation of transient conditions would have no meaningful practical significance unless the phenomenon of saturation is incorporated in full. Unfortunately, the present state of art in machines has still not produced any reliable factors or

methods of evaluating saturation. Since the use of Lagranges' equations is limited to only the unsaturated region, any use of these to predict dynamic behavoir may only produce results whose reliability is questionable in view of the lack of any practical form of predicting saturation particularly in the transient stages. Hence, the analysis is mainly confined to steady state behavoir. However an attempt was made to run the motor at certain slip as shown in the test results in Chapter 10. In view of the large pulsating torques, the machine was not stable and behavoir under those conditions is not of interest, except for determining stability and transient frequency response.

Since no discussion of a new machine is complete without some indication as to the approach of machine behavoir under dynamic conditions, a section of the work is devoted for same. Chapter 6 explains the magnitude and time response of the machine under dynamic condition. Mr. Kron's approach is used in Chapter 7 to develop equivalent circuits and transient equations using impedance matrices. The equation derived in Chapter 6 was solved using a computer. Chapter 11 deals with the program developed for solution of the Dynamic equation.

CHAPTER 2

CONSTRUCTION

Synduction Motor

Figure 2.1 shows the rotor construction of a Synduction motor. Laminations are punched out like regular induction motor stampings and stacked and die cast in aluminum. The aluminum filling up the voids in the barrier and interpolar region helps provide the starting torque for the motor. Once the motor pulls into synchronism, no current flows in the squirrel cage "bars" or end ring.

The direct axis and quadrature axis flux paths are shown in the figure. While the reluctance of the direct axis path is low, the reluctance in the interpolar space is high due to the cut out and the barriers. The sections of aluminum, or any other conductor material in the direct and quadrature axes, produce torque by linking the d-axis and q-axis fluxes in the asynchronous mode, i.e. at starting or at regions of hunting or any instantaneous disturbances like sudden application of load. The narrow bridges along the q-axis have been found to be helpful in improving the stability of the motor for sudden application of loads.

Anisotropic Rotor Motor

Figure 2.2 shows the cross-section of 4-pole rotor. The core is basically a toroid as shown in Figure 2.2 and cut into four segments and reassembled on a square stainless

(a) Synduction Rotor

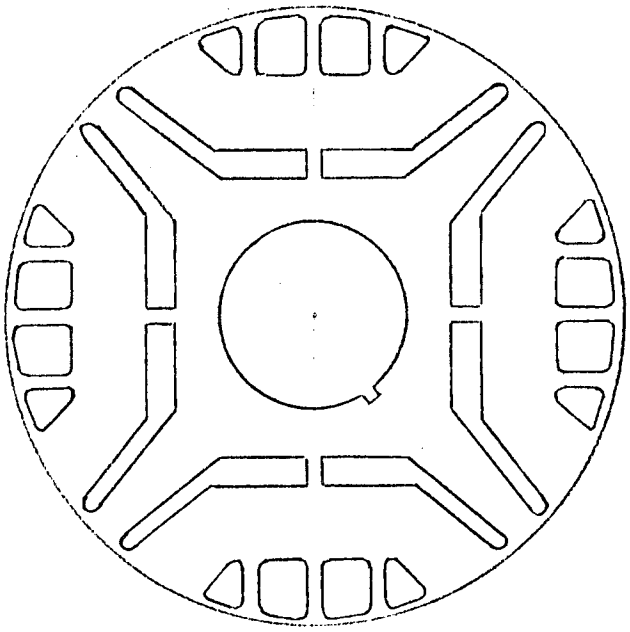

(b) Anisotropic Rotor

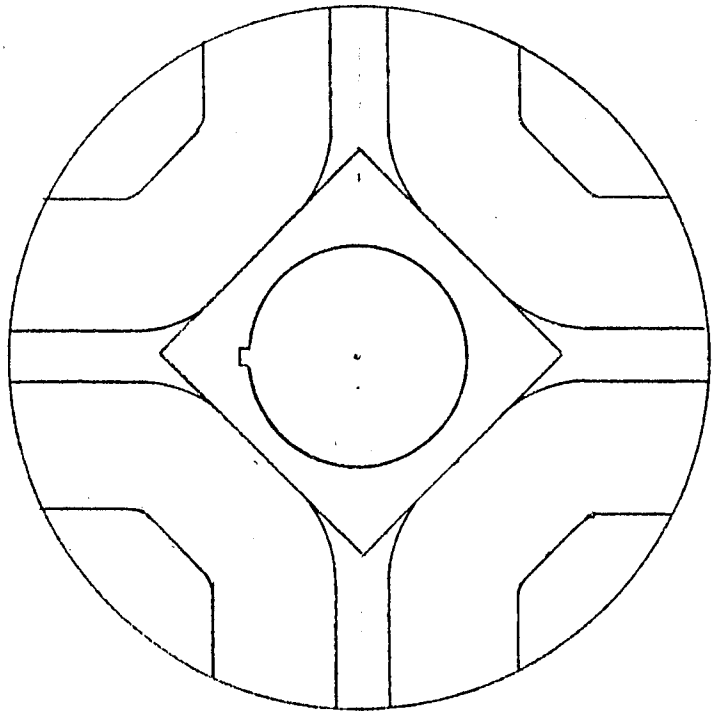

FIGURE 2.1 CROSS SECTION OF ROTOR SHOWING LAMINATIONS

steel hub as shown in Figure 2.2. The octagonal toroid could be replaced by a circular one, but the shape was chosen as it would provide more space for conductor material in the quadrature axis, as can be seen in Figure 2.2, thereby providing larger pull in torque. The core is tape wound from grain oriented silicon steel strips of a width equal to axial length of the motor. When cut and assembled, as shown in Figure 2.2, the reluctance in the direct axis is very low since flux lines flow along the direction of grain orientation. The quadrature axis provides high reluctance path for flux due to the cutouts, barriers, and also due to the low permeability perpendicular to the direction of rolling. In addition, the stacking factor also contributes to the reluctance. The poorer the stacking factor, the more the reluctance. One advantage of using this type of construction as against the Synduction motor type is the magnitude of intrinsic magnetic anisotropy. We can increase pole span/pole pitch ratio without unduly increasing the quadrature axis flux. Although for the purpose of comparing the performance of the two rotors, the pole span to pole pitch ratio has been kept substantially the same.

The four pole segments are assembled on the stainless steel hub through stainless steel bolts and the subassembly is die cast in aluminum. The final dimension of the rotor has been kept the same as in the case of Synduction motor.

FIGURE 2.2 CROSS SECTION OF ANISOTROPIC ROTOR

The cross section shown in Figure 2.2 shows four aluminum sections in q-axis and four in direct axis. The substantially increased condutor material in q-axis compared to Synduction motor is evidenced.

Complete assembly of test rotor. The above constructions were made for a 25 HP motor. For complete evaluation of the performance of the two types, the two rotors were assembled with stators identical in magnetic structure and electrical windings. The motor was coupled to a 15 KW generator which was used as an electrical dynamometer.

The complete assembly was intended to serve as a 400 Hz. power supply unit. A large flywheel of inertia of 140 ft.lbs. (10 x Normal WK^2) was assembled with it. This serves dual purpose of maintaining output voltage and frequency for a brief outage of input power as well as to conduct tests on the pull in capability of the two types of rotor for a 10 x rotor inertia load connected to the motor.

CHAPTER 3

THEORY AND REACTANCE CALCULATION FOR SYNDUCTION MOTOR

The Synduction motor shown in Figure 2.1 can be basically shown as in Figure 3.1. The symbols used in the following analysis are given in the following list.

The stator has a three phase winding, but the deviations are generalized by using m phases. The rotor cutout and the barrier configurations of Figure 2.1 are simulated by circular and radial lines. The flux lines are assumed to be perpendicular to the surfaces they enter into. Since the structure of grain orientation is of no concern, the permeability or iron is the same in the d-axis and q-axis.

The analysis of the three phase machine is done in terms of d and q axes parameters using the d-q frame fixed in the rotor as in Park's transformation. This results in the following assertions:

(1) The stator windings are now replaced by two windings along d-axis and q-axis and have no relative motion with respect to the rotor.

(2) Only fundamentals are considered as far as the phase or d and q axes currents are concerned.

(3) Saturation is neglected in the basic analysis. However, since the present state of art in the study of saturation permit "fudge factors" to be introduced, comments will be

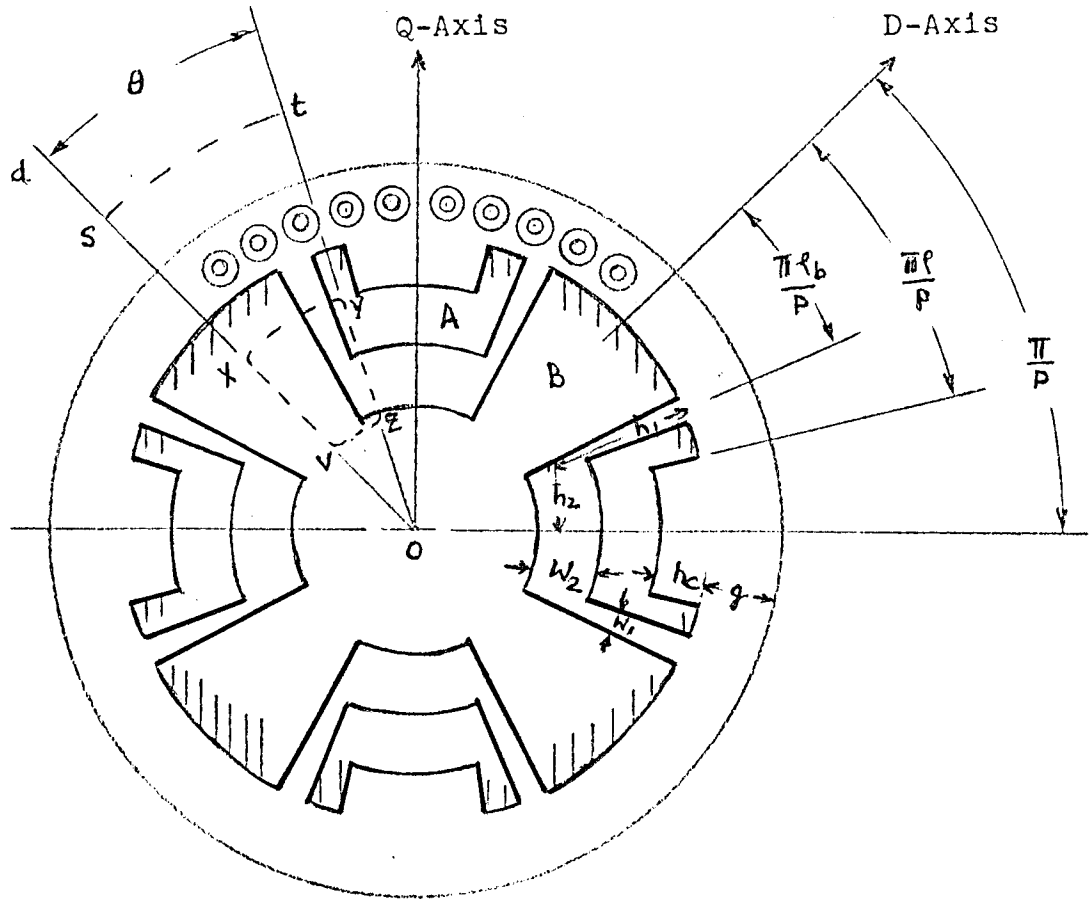

FIGURE 3.1 CROSS SECTIONAL REPRESENTATION OF ROTOR

included on the magnitude of saturation factors in the d-axis and q-axis later in the paper under "test results."

The magnitude of mmfs in the d and q axis is given by:

$$F_d = \frac{0.9\ mI_d\ NK_w}{P} \text{ Cos } \frac{P}{2}\ \theta \qquad \ldots\ldots\ldots 3.1$$

$$F_q = \frac{0.9\ mI_q\ NK_w}{P} \text{ Sin } \frac{P}{2}\ \theta \qquad \ldots\ldots\ldots 3.2$$

The magnitude of the stator mmfs are, for convenience, rewritten F_{dm} and F_{qm} each associated with a cosine and sine function respectively. As far as the rotor is concerned, since no current exists the mmf in the rotor is considered to be zero. It now remains to evaluate the flux densities in the cutouts, barriers, and air gap.

The magnitude of each line of force can be deduced in the barriers, gap and cutouts by taking line integrals around various closed paths.

$\oint Hsds = 0.4\ \pi\ (I)$, where I is the total current enclosed and it is the force intensity in the direction ds.

Direct Axis Flux Densities

The flux in the region of barriers and cutouts are all caused by quadrature axis mmf only. Referring to Figure 3.1 let W_2 be the radial and W_1 is the circumfer-

ential width of the barriers. Assuming fluxes crossing perpendicular to the surface of iron at the barriers, and B_2, B_1 being flux densities, the following derivations are made. As far as the direct axis is concerned, there is no flux in the cut out region and the flux flows along the laminations and the only reluctance in the path is due to air gap.

As only the flux in the region marked A and B are of importance, total flux density

$$B_{d(AB)} = \frac{0.4\,\pi\,Fdm}{g} \cos\frac{P}{2}\theta \quad \text{where } 0 \leq \theta \leq \frac{\pi}{p}; \qquad \ldots\ldots\ldots 3.3$$

Quadrature Axis Flux Densities

As far as the quadrature is concerned, the mmf is maximum at the center of cut out and decreases sinusiodally to zero at the center of the pole. The reluctance offered to the quadrature axis flux consists of cut out, barrier regions also.

The line integral around any path abcd must be zero, as $\oint Hs\ ds = 0$.

i.e. $B_1W_1 - B_2W_2 = 0$ where B_1, and B_2 are the flux densities across W_1 and W_2 respectively. 3.4

The line integrals into stator path along Otso enclose the mmf F_q equal to $F_{qm} \sin\frac{P}{2}\theta$. Here again the line integrals

have to be considered in the region.

(a) Pole center to barrier.

(b) Barrier to pole edge.

(c) Pole edge and cut out center.

i.e. (a) $Bq_1\ g = 0.4\pi F_{qm} \operatorname{Sin} \frac{P}{2}\ \theta;\ 0 \leq \theta \leq \frac{\pi \ell_b}{P}$;

(b) $Bq_2\ g + B_2\ W_2 = 0.4\pi F_{qm} \operatorname{Sin} \frac{P}{2}\ \theta;$

$$\text{for } \frac{\pi \ell_b}{P} \leq \theta \leq \frac{\pi \ell}{P} ;$$

(c) $Bg_3\ (g+h_c) + B_2\ W_2 = 0.4\pi F_{qm} \operatorname{Sin} \frac{P}{2}\ \theta;$

$$\text{for } \frac{\pi \ell}{P} \leq \theta \leq \frac{\pi}{P}$$

..... 3.5

All the flux entering the rotor or a segment must leave that segment with no gain or loss, since it is assumed to begin with that rotor potential in zero. Just considering the cut out region of Figure 4.1, flux entering and leaving are equal.

$$\int_{\frac{\pi \ell_b}{P}}^{\pi \ell/\rho} Bq_2\ r d\theta + \int_{\frac{\pi \ell}{P}}^{\frac{\pi}{P}} Bq_3\ (r-hc)\ d\theta = B_1 h_1 + B_2 h_2$$

..... 3.6

But since by 3.4, $B_1 = \frac{B_2 W_2}{W_1}$;

Carrying out the integration on (3.6)

$$B_2 W_2 = 0.4\pi F_{qm}\ \frac{f_{b2}}{\pi}$$

..... 3.7

where $f_b = \dfrac{\cos \pi \ell_b/2 - \cos \pi \ell/2 + C_1}{(B - \ell) - (\ell_b + C_2)}$ 3.8

$B = \dfrac{Pg}{\pi r}\left(\dfrac{2h1}{rW_1} + \dfrac{h2}{W_2}\right)$ 3.9

$C_1 = \dfrac{1-2hc}{2r} \quad \dfrac{g}{g+h_c} \quad \cos \dfrac{\pi \ell}{2}$ 3.10

$C_2 = \dfrac{1-2hc}{2r} \quad \dfrac{g}{g+h_c} \quad (1-\ell)$ 3.11

Substituting 3.4, 3.8 to 3.11 in 3.5, we can get values of:

$$Bq_2 = \frac{0.4\pi F_{qm}}{g} \sin \frac{P}{2}\theta; \quad 0 \leq \theta \leq \frac{\pi \ell_b}{P}$$

$$Bq_2 = \frac{0.4\pi F_{qm}}{g}\left(\sin \frac{P}{2}\theta - \frac{2}{\pi} f_b\right); \quad \frac{\pi \ell_b}{P} \leq \theta \leq \frac{\pi \ell}{P}$$

$$Bq_3 = \frac{0.4\pi F_{qm}}{g+h_c}\left(\sin \frac{P}{2}\theta - \frac{2}{\pi} f_b\right); \quad \frac{\pi \ell}{P} \leq \theta \leq \frac{\pi}{P}$$

..... 3.12

Also flux densities in the barrier region

$B_1 = \dfrac{0.4\pi F_{qm}}{W_1} \quad \dfrac{2}{r} \quad \dfrac{f_b^2}{\pi}$ 3.13

$B_2 = \dfrac{0.4\pi F_{qm}}{W_2} \quad \dfrac{f_b^2}{\pi}$ 3.14

Once the flux densities in each region is known, the generated voltage can be calculated.

Reactance Calculation

Quadrature axis reactance. The total flux per pole

$$\phi_q = L\int_0^{2\pi/p} B_q \; r \, d\theta = 2L \; \frac{D}{2}\int_0^{\pi/p} B_q \, d\theta \qquad \ldots\ldots\ldots 3.15$$

The flux linkages of all poles and inductances per phase are:

$$\lambda_{mq} = K_w N \phi_q \qquad \ldots\ldots\ldots 3.16$$

$$L_{mq} = \frac{\lambda_{mq}}{\sqrt{2}\, I_q} \; 10^{-8} \qquad \ldots\ldots\ldots 3.17$$

Substituting the values of flux densities in the three regions as given by equations 3.12, equation 3.15 can be rewritten as

$$\phi_q = LD \int_0^{\pi\ell_b/p} B_{q1} d\theta + \int_{\pi\ell_b/p}^{\pi\ell/p} B_{q2} d\theta + \int_{\frac{\pi\ell}{p}}^{\pi/p} B_{q3} d\theta \qquad \ldots\ldots\ldots 3.18$$

Substituting the values given by equations 3.12 and using equations 3.16 and 3.17, performing integration,

$$L_{mq} = \frac{1.6m\, LD}{g} \quad \frac{NK_w}{P}^2 \quad C_q \; 10^{-8} \qquad \ldots\ldots\ldots 3.19$$

where $C_q = 1 - \cos\frac{\pi\ell}{2} - (\ell - \ell_b)\, f_b + \alpha$

where $\alpha = \frac{g}{g+h_c}\left[\cos\frac{\pi\ell}{2} - f_b\,(1-\ell)\right]$;

Direct Axis Reactance

By a similar reasoning like above, the direct axis flux

$$\phi = DL \int_{0}^{\pi/p} B_d \, d\theta$$

Substituting for B_d from 3.3,

$$\phi d = \int_{0}^{\pi - \varphi/p} DL \quad B_{d(AB)} \, d\theta.$$

As in the case of quadrature axis reactance evaluation, using equations 3.16 and 17, and performing integration,

$$L_{md} = \frac{1.6mLD}{g} \left(\frac{NK_w}{P} \right)^2 C_d \times 10^{-8}$$

where $C_d = \frac{\text{Sin } \pi - \varphi}{2}$.

CHAPTER 4

THEORY AND REACTANCE CALCULATIONS FOR ANISOTROPIC MOTOR

Basic work on the Anisotropic rotor motors has been done by Messrs. J. F. Doughlas, Mathur, and Menzies, where starting from the segmented lamination type (as explained in Chapter 3), attention has been turned into reducing the magnetic flux in the q-axis by introducing internal anisotropy. Referring to Figure 4.1 which shows one quadrant of a two pole cylindrical rotor, a series of slits are introduced parallel to the d-axis. Thereby, any flux that has to travel along q-axis has to encounter several air gaps. The slits are interrupted by teeth, purely from the point of view of mechanical configuration of holding the laminations together. These teeth get saturated even at low values of quadrature axis flux. The internal anisotropy introduces a certain factor in the ratio $\frac{Bd}{Bq}$. In the above cylindrical rotor it is taken as k_i. In the absence of slits $\frac{Bd}{Bq}$ would be equal to 1. However, if pole span to pole pitch ratio is less than 1, then a further factor is introduced in the ratio of $\frac{Bd}{Bq}$. Let this be k_s.

The total ratio of the permeances in the d-axis and q-axis is the product of superficial anisotropy k_s due to the pole span to pole pitch ratio, multiplied by the factor due to internal anisotropy k_i.

$$k' = k_s k_i \qquad \ldots\ldots\ldots 4.1$$

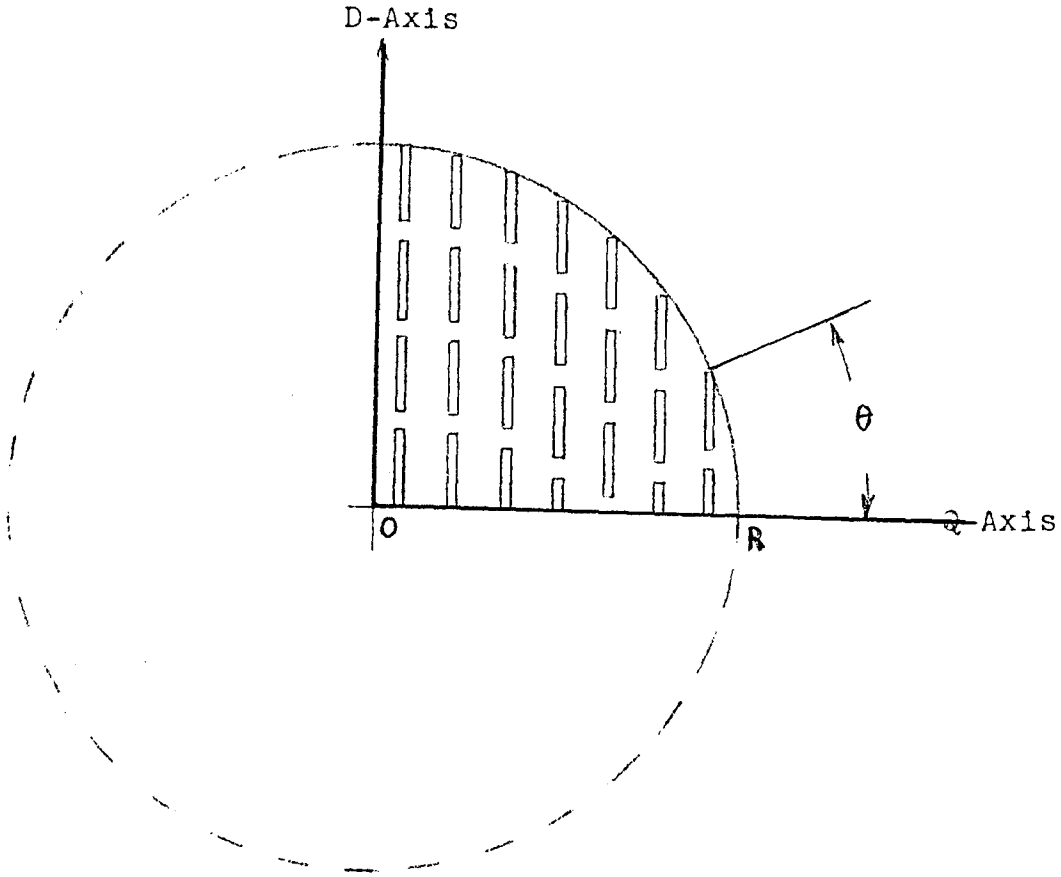

FIGURE 4.1 CROSS SECTION OF 2-POLE SLITTED LAMINATION ROTOR

To determine k_s, there are well established formulas for salient pole machines for different pole span/pole pitch ratio and air gap ratios in the two regions of pole and interpolar space.

However the internal anisotropy can also be obtained, instead of using slits, by using cores like in Figure 4.2 where there is grain orientation in the direction of d-axis. If "g" is the effective air gap introduced in the q-axis in the stack of laminations due to the stacking factor, and μ_a is the permeability in the direction of q-axis, i.e. perpendicular to the grain orientation, then k_i can be evaluated as follows:

The mmf drop in the air gap along q-axis

$$M_1 - M_2 = \frac{B}{\mu_a} g \cos \theta \qquad \ldots\ldots\ldots 4.2$$

where M_1 is the mmf of the stator and M_2 is the rotor mmf. Note $M_2 = 0$ if anisotropy is absent, then above equation is same as M_1.

For cylindrical rotor in the d-axis

$$M_2 = \frac{B}{\mu} R \cos \theta \qquad \ldots\ldots\ldots 4.3$$

Since air gap density is proportional to the density from 4.2 and 4.3,

$$k_i = \frac{M_1}{M_1 - M_2}$$

$$= 1 + \frac{M_2}{M_1 - M_2}$$

$$= 1 + \frac{(B/\mu)\ R\ \text{Cos}\ \theta}{(B/\mu_a)\ g\ \text{Cos}\ \theta}$$

$$= 1 + \frac{R}{g}\ \frac{\mu_a}{\mu}; \qquad \ldots\ldots\ldots\ 4.4$$

Equation 4.4 is the ratio B_2/B_1, where B_2 is the quadrature axis density in absence of internal anisotropy and B_1 is in presence of the internal anisotropy.

Now that the basis for accounting for structural and internal anisotropy is established, let us start with the analysis of the Anisotropic rotor under consideration.

Figure 4.2 shows the basic tape wound core which is then cut into four segments and reassembled on a stainless steel non-magnetic hub and secured with non-magnetic bolts (Figure 4.2). The tape wound core is wound with C-core technique using #29 gauge silicon steel strips. The grain

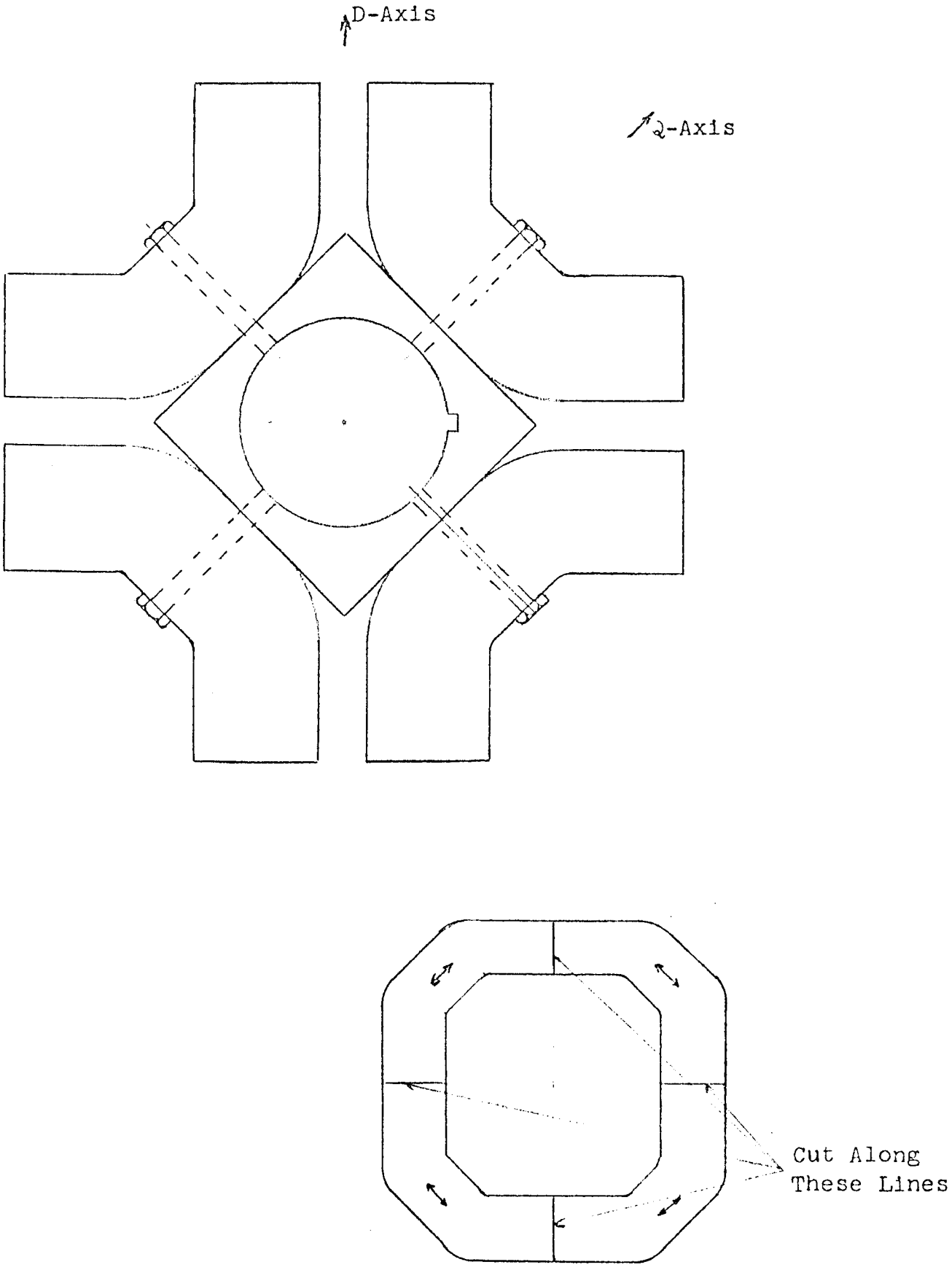

FIGURE 4.2 ASSEMBLY OF ANISOTROPIC ROTOR SEGMENTS

orientation is in the direction of winding. This ultimately results in a strongly d-axis grain oriented pole structure. As far as the q-axis is concerned, while the large interpolar air gap cuts down the major part of flux like in any other reluctance machine, the high reluctance of the magnetic material in the direction of q-axis and the interlaminer insulation help cut the quadrature flux thereby the quadrature axis reactance. The sub-assembly is now cast in aluminum and the resulting rotor looks very much like an ordinary squirrel cage rotor. The conductor material in the interpolar region and between two sets of cores in the d-axis form the squirrel cage bars. Complete with the two end rings, they form the squirrel cage winding for starting purposes.

In fact, the core could be shaped like a toroid as tried by Mr. Mathur and colleagues. However, as the present design is intended to start up a high inertial load (10 x Normal Wk^2) and also be able to pull in at full load on the motor, the octagonal shape was chosen, as this would provide more pull in torque. Also, the octagonal shaped segments are preferred from the point of view of easier mechanical assembly.

Another advantage of laminated structure is the prevention of flux reversals of quadrature axis flux on the

pole shoes, which is very common in the case of conventional reluctance motors. The reason is that individually every lamination assumes its own magnetic potential and the flux lines from the rotor travel radially across the air gap into the stator. In consequence not only is it difficult for quadrature axis flux loops to form from pole to pole, but even within the pole. This forms an additional feature in favor of the anisotropic rotor compared to Synduction motor.

In fact, with this construction it is possible to have a large pole span to pole pitch ratio without appreciably increasing the quadrature axis flux. However from the point of view of having a good starting and pull in performance, it was decided to have large conductor material and a pole span to pole pitch ratio of 0.5 just like in the Synduction motor which was chosen.

Analysis of Ideal Anisotropic Rotor

For the purpose of analysis a two pole rotor shown in Figure 4.3 is considered. The following assumptions are made:

(1) Saturation is neglected.

(2) The permeability of iron in the rolling direction is infinite and in the perpendicular direction the reluctance is infinite.

(3) Only fundamentals are considered.

(4) Flux lines cross the air gap radially.

The fundamental mmf of stator is:

$$F_s = F \cos (wt + \alpha - p\theta) \quad \ldots\ldots\ldots 4.5$$

$$\text{where } F = \frac{6NK_1 I}{\pi} \quad \ldots\ldots\ldots 4.6$$

$$\text{and } i_a = I \sin (wt + \alpha) \quad \ldots\ldots\ldots 4.7$$

Consider a lamination situated at an angle γ from the quadrature axis. Stator mmf opposite on end of lamination

$$F_s = F \cos (wt + \alpha - p\beta + P\gamma) \quad \ldots\ldots\ldots 4.8$$

and at the opposite end at distance - from the q-axis.

$$F_s = F \cos (wt + \alpha - p\beta - P\gamma) \quad \ldots\ldots\ldots 4.9$$

So the total potential across the two air gaps is given by the difference of equations 4.8 and 4.9

$$F_\gamma = F \cos (wt + \alpha - p\beta + P\gamma) - \cos (wt + \alpha - p\beta - P\gamma)$$

$$= 2F \sin (wt + \alpha - p\beta) \sin p\gamma \quad \ldots\ldots\ldots 4.10$$

The rotor lamination between these two stator points can be assumed to acquire an average potential as above. As the total air gap is 2g, the flux density

$$B_r = \frac{\mu_o}{g} F \text{ Sin } (wt + \alpha - p\beta) \text{ Sin } p\gamma \quad \ldots\ldots\ldots 4.11$$

The above is for one lamination, considering all laminations from $\ell \leq \gamma \leq \sigma$

$$\text{Sin } P\gamma = \sum_{n=1}^{\infty} bn \text{ Sin } np\gamma \quad \ldots\ldots\ldots 4.12$$

where $b_1 = \frac{1}{\pi} (2 p\theta - 2 p\ell - \text{Sin } 2 p\sigma + \text{Sin } 2 p\ell)$

and $b_n = \frac{2}{\pi} \left[\frac{\text{Sin } (n-1) P\sigma - \text{Sin } (n-1) P\ell}{n-1} - \frac{\text{Sin } (n+1) P\sigma - \text{Sin } (n+1) P}{n+1} \right]$ $\ldots\ldots\ldots 4.13$

for n being odd.

Since $\gamma = \theta - \beta$, the flux density can now be expressed in terms of θ and is obtained by substituting equation 4.12 in 4.11

$$B_\theta = \frac{\mu_o}{g} F \text{ Sin } (wt + \alpha - pb) \Sigma bn \text{ Sin } nP (\theta - \beta) \quad \ldots\ldots\ldots 4.14$$

If rotor rotates at synchronous speed, then the rotor angle is $P\beta$.

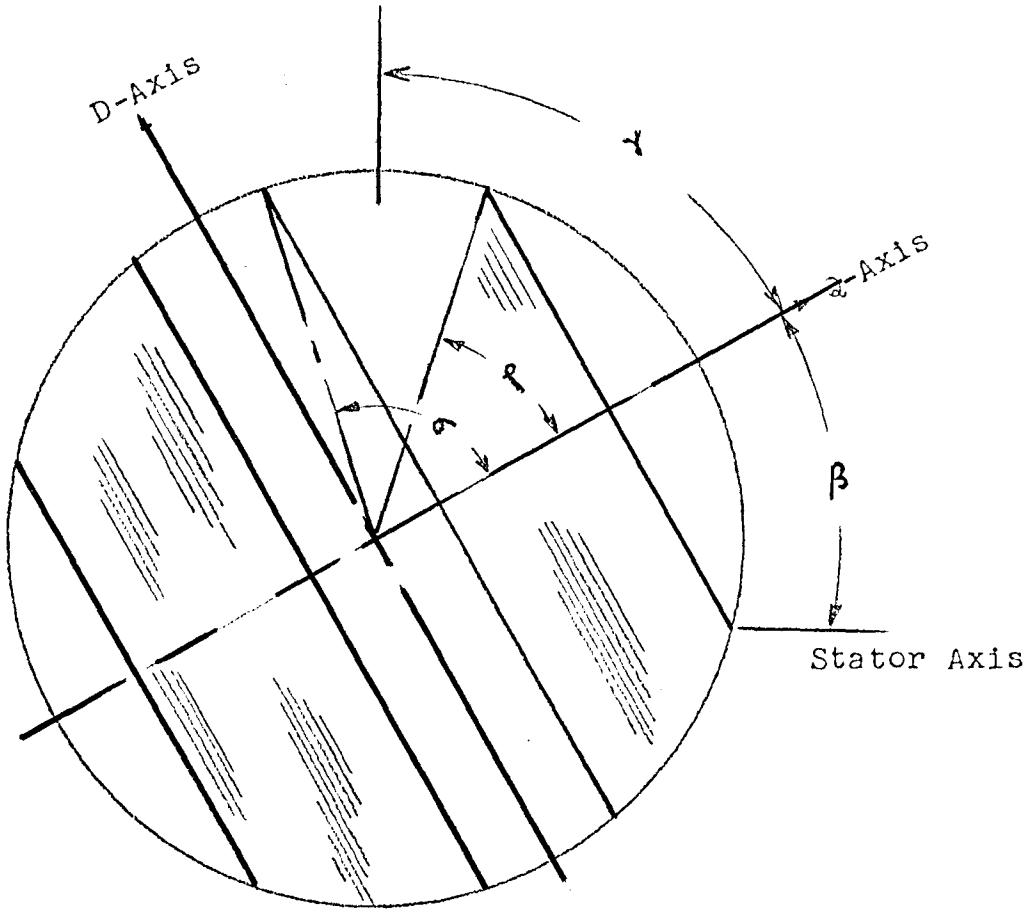

FIGURE 4.3 CROSS SECTIONAL REPRESENTATION OF 2-POLE ANISOTROPIC ROTOR

$P\beta = wt + p\beta o$, βo being the initial angle at $t = 0$.

Expanding the equation 4.14

$$B_\theta = \frac{\mu_o F}{2g}\left[b_1\left\{\cos(wt + \alpha - p\theta) - \cos(wt - \alpha - p\theta + 2p\beta_o)\right\}\right.$$

$$+ b_3\left\{\cos(3wt + \alpha - 3p\theta + 2p\beta o) - \cos(3wt - \alpha - 3p\theta + 4p\beta o)\right\}$$

$$\left. + b_5\ (\qquad\qquad)\ \right] \quad \ldots\ldots\ldots 4.15$$

The total flux over a pole is given by integrating $B_\theta lrd\theta$ where l = axial length and $rd\theta$ is that part of the rotor circumference facing the stator.

$$\text{Total flux} = \int_0^{\pi/p} B_\theta\ lrd\theta$$

$$\text{anf flux linkage } \lambda_a = PNK_w \int_0^{\pi/p} 2B_\theta\ lrd\theta \quad \ldots\ldots\ldots 4.16$$

where N = No. of turns,

K_w = winding factor,

P = No. of pairs of poles.

$$\text{i.e. } \lambda_a = 2NK_1 \frac{\mu_o}{g} Flrb_1 \left\{\sin(wt + \alpha) - \sin(wt - \alpha + 2p\beta o)\right\}$$

minimum is obtained by substituting the fundamental component only of equation 4.15 in 4.16 and carrying out the integration.

But since $F = \frac{6NK_1 I}{\pi}$ from equation 4.6

$$\lambda_a = 12 (NK_1)^2 \frac{\mu_o}{\pi} \frac{lrbl}{g} \left[\text{Sin } (wt + \alpha) - \text{Sin } (wt - \alpha + 2p\beta o) \right] I \quad \ldots\ldots\ldots 4.17$$

The induced voltage

$$E = \frac{d \lambda_a}{dt}$$

Carrying out the differentiation and expressing in phasor form

$$E = \left\{ j WL_m - j WL_m \text{ Cos } 2 (P\beta o - \alpha) \right\} I_m \quad \ldots\ldots\ldots 4.18$$

where $L_m = \frac{\mu_o}{\pi} 12 (NK_w)^2 \frac{lrb_1}{g}$, $\ldots\ldots\ldots 4.19$

Direct Axis Reactance

From the above equation one can deduce the direct and quadrature axis reactance.

When $= P\beta o \pm \pi/2$, i.e. when the rotor direct axis is in alignment with stator maximum mmf

$$E = j (L_m + L_m) I_m = j X_{md} I_m \quad \ldots\ldots\ldots 4.20$$

Here again, like in equation 4.19

$$X_{md} = \mu_o \frac{24 (NK_w)^2 \ lrb_1}{\pi \ g} \quad \ldots\ldots\ldots 4.21$$

Quadrature Axis Reactance

When $\alpha = p\beta o$ or $P\beta o + \pi$, the rotor quadrature axis alignment is reached and $E = j\omega(L_m - L_m) = 0$.

This again shows that for an ideal Anisotropic rotor the quadrature axis flux is zero and hence the reactance also is zero.

However, in a practical machine this is far from being true.

The direct and quadrature axis reactance can be expressed in forms of the cylindrical magnetizing reactance X_{mc} where $X_{mc} = \dfrac{\mu_o \, 24(NK_w)^2 \, l}{\pi \, g}$ 4.22

$$X_{md} = K_d \, X_{mc}; \; X_{mq} = K_q \, X_{mc}; \qquad \text{..... 4.23}$$

Now the leakage reactance X_l has to be accounted for. If X_l is expressed as $X_l = K_l \, X_{mc}$; 4.24

then the torque equation can be expressed in terms of the above. For purposes of simplification and neglecting the stator resistance, and where

$$X_d = X_{md} + X_l; \text{ and } X_q = X_{mq} + X_l \qquad \text{..... 4.25}$$

$$T = V^2 \left\{ \frac{1}{X_q} - \frac{1}{X_d} \right\} \text{Sin } 2\theta$$

whereby maximum torque

$$T_m = \frac{V^2}{2X_{mc}}\left(\frac{1}{K_q + K_1} - \frac{1}{K_d + K_1}\right) \quad \ldots\ldots\ldots 4.26$$

and maximum power factor

$$\cos\alpha_{max} = \frac{(X_d/X_q)-1}{(X_d/X_q)+1} \; ; \quad \ldots\ldots\ldots 4.27$$

The limitations in the actual motor where the assumptions made above for ideal conditions, decrease the maximum pull out torque as well as power factor. These limitations being the assumption of infinite premeability in the d-axis and infinite reluctance on the q-axis, as well as the saturation of iron etc. In Chapter 7 where some of the parameters are evaluated, a closer value of reactance to the final test figures is attempted.

However, a note with reference to equation 4.26 is worthwhile. As the quadrature axis magnetizing reactance becomes less and less, the importance of leakage reactance X_1, which is a constant additive factor to the total axis reactance becomes significant. In fact, when in the pull out region, torques may be significantly affected by the per unit value of leakage reactance compared to the X_{md} and Xmq. This is not the case in Synchronous machines or other reluctance motors, where leakage reactance is always

assumed to have insignificant, but detrimental effect on pull out torque.

The above analysis lays down the basis for proving the superiority of Anisotropic rotors over Reluctance rotors of conventional as well as segmental type. Further notes on this in Chapter 8 regarding starting performance will be made.

CHAPTER 5

EQUATIONS OF PERFORMANCE-STEADY STATE

The equivalent circuit for both the Synduction as well as the Anisotropic machine is the same. It is a general circuit for any reluctance machine.

The analytical derivation of the equivalent circuit is similar to Synchronous machines except for the absence of field windings. The applied voltage of the machine is used up in overcoming the stator leakage reactance and resistance, as well as to create and maintain a flux equal and opposite to the armature reaction. The armature reaction caused by the distributed conductors along the stator periphery is rotating at synchronous speed with respect to stator. Hence, its phase relationship with the synchronously rotating rotor is fixed. Since the rotor has high permeance in one axis along poles and high reluctance along the perpendicular q-axis, we can represent armature reaction using Park's transformation. Instead of a three phase rotating armature reaction, we can consider fixed d-axis and q-axis armature reactances. The two axes reactances together with the stator leakage reactance and resistance are shown in Figure 5.1.

In the d-axis, the field winding is replaced by one turn shorted damper winding, which is actually the conductor material (aluminum) surrounding the pole. Since there

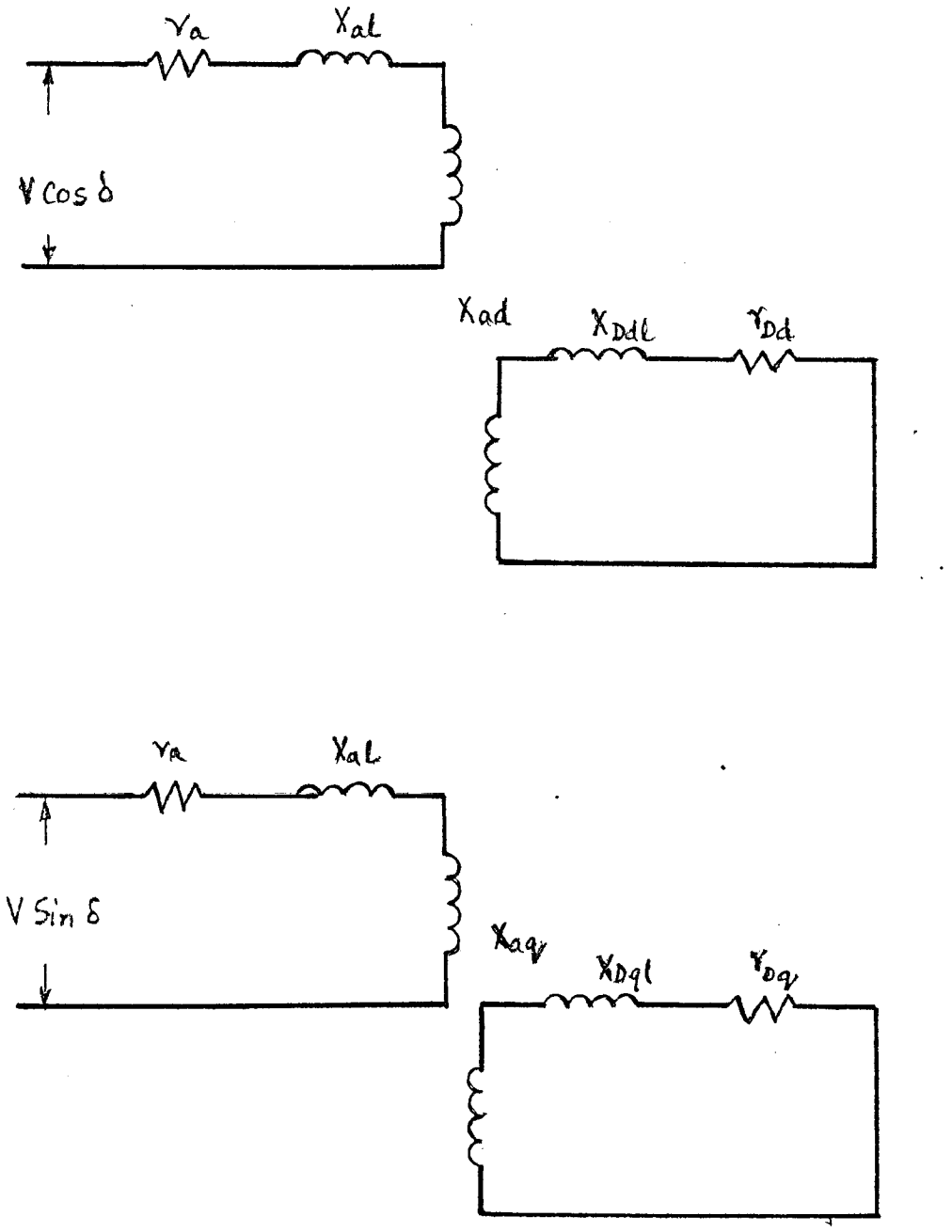

FIGURE 5.1 EQUIVALENT CIRCUITS OF RELUCTANCE MOTORS

is no external excitation, this winding may be assumed to be absent as far as steady state is concerned. However, its presence affects transient performance and this has been discussed in Chapters 6, 7, and 8.

So confining ourselves to steady state analysis in this Chapter, since there is no current flowing in the rotor during steady state, the field or damper windings can be eliminated altogether. So from the equivalent circuit we can now draw the vector diagram (Figure 5.2) where the load current I has been shown to be made up of two components I_d and I_q, 90° electrical degrees apart. I_q lags behind the voltage vector by torque angle.

From the vector diagram we can see that

$$V \cos\theta = I_d X_d + I_q r_a$$

$$V \sin\theta = I_q X_q - I_d r_a \qquad \ldots\ldots\ldots 5.1$$

Solving the above, $I_q = \dfrac{VZ_d}{(X_d X_q + r_a^2)} \cos(\phi_d - \theta)$ 5.2

$$I_d = \frac{VZ_q}{(X_d X_q + r_a^2)} \sin(\phi_q - \theta) \qquad \ldots\ldots\ldots 5.3$$

where $\phi_d = \tan^{-1} \dfrac{X_d}{r_a}$

$\phi_q = \tan^{-1} \dfrac{X_q}{r_a}$;

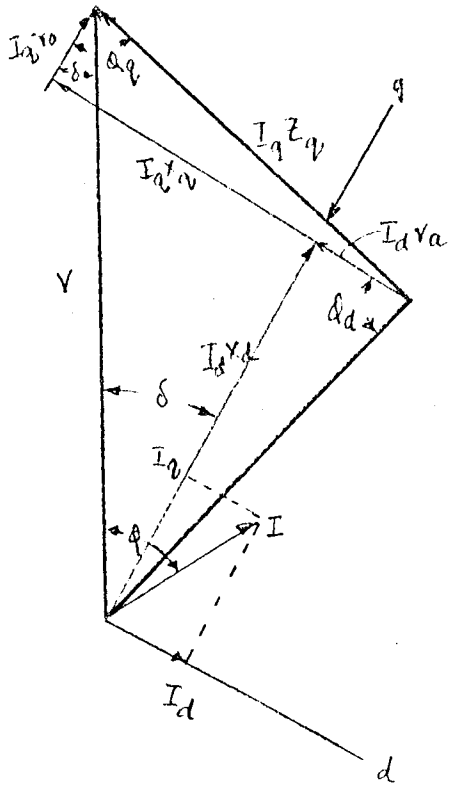

FIGURE 5.2 VECTOR DIAGRAM OF RELUCTANCE MOTOR

$$\text{Load current } I_L = \sqrt{I_d^2 + I_q^2} \qquad \ldots\ldots\ldots 5.4$$

Note that the effect of iron losses and friction which can be taken as a parallel branch to X_{ad}, is neglected in our analysis, in view of the order of magnitudes of X_{ad} and the factor due to losses. However, at a later stage in Chapter 10, while evaluating X_q, the iron and other losses are accounted for.

Equations of Performance

The phasor diagram of the reluctance motor under steady state can be drawn as in Figure 5.2.

From the diagram

$$V \cos \theta = I_d X_d + I_q r_a$$

$$V \sin \theta = I_q X_q - I_d r_a \qquad \ldots\ldots\ldots 5.1$$

Solving the above, $I_q = \dfrac{VZ_d}{X_d X_q + r_a^2} \cos (\phi_d - \theta)$ $\ldots\ldots\ldots 5.2$

$$I_d = \frac{VZ_q}{X_d X_q + r_a^2} \sin (\phi_q - \theta) \qquad \ldots\ldots\ldots 5.3$$

where $\phi_d = \tan^{-1} \dfrac{X_d}{r_a}$

$$\phi_q = \tan^{-1} \frac{X_q}{r_a}$$

The load current $I_L = \sqrt{I_d^2 + I_q^2}$ $\ldots\ldots\ldots 5.4$

Input Power

The input power is obtained by adding the direct axis and quadrature axis product of current and voltages in respective axes.

$$P_i = mV\ (I_q \cos\theta - I_d \sin\theta\ ) \qquad \ldots\ldots\ldots\ 5.5$$

using equations 5.1, the torque angle is eliminated.

$$P_i = mI_dI_q(X_d - X_q) + m\ I^2r_a \qquad \ldots\ldots\ldots\ 5.6$$

Since the stator loss = mI^2r_a, the developed electrical power

$$P_e = mI_dI_q(X_d - X_q); \qquad \ldots\ldots\ldots\ 5.7$$

Since there is no rotor loss involved, due to absence of any currents, the above also gives the shaft power available.

Shaft Torque

$$T_e = \frac{mP}{2\omega}\ I_dI_q\ (X_d - X_q) \qquad \ldots\ldots\ldots\ 5.8$$

$$= \frac{mP}{2}\ I_dI_q\ (L_d - L_q) \qquad \ldots\ldots\ldots\ 5.9$$

From equations 5.2 and 5.3

$$I_dI_q = \frac{V^2 f_{\omega o}}{\omega^2 L_d L_q} \sin\ (\phi_q - \theta\ )\ \cos\ (\phi_d - \theta\ ) \qquad \ldots\ldots\ldots\ 5.10$$

Where $$f_{\omega o} = \frac{\sqrt{1 + \left(\frac{r_a}{X_d}\right)^2}\sqrt{1 + \left(\frac{r_a}{X_q}\right)^2}}{\left[1 + \frac{r_a^2}{X_d X_q}\right]^2} \quad \ldots\ldots\ldots 5.11$$

Substituting 5.10 in 5.8

$$T_e = \frac{MPV^2}{2}\left(\frac{1}{X_q} - \frac{1}{X_d}\right) \quad \text{Sin } (\phi_q - \theta) \quad \text{Cos } (\phi_d - \theta) \quad \ldots\ldots\ldots 5.12$$

At no load, the machine is assumed to be drawing no real power from the line. However in actual condition, the friction and windage losses are supplied by the line resulting in a small torque angle. For the purposes of this analysis, ideal machine with no losses in considered.

Torque angle at no load. At no load the equation 5.12 reduces to a value of zero:

i.e. $(\phi_d - \theta) = 90°$

i.e. $$\theta_{NL} = (\phi_d - 90°) = \left[\tan^{-1}\left(\frac{X_d}{r_a}\right) - 90°\right] \quad \ldots\ldots\ldots 5.13$$

Torque at pull out. Pull out torque is obtained by differentiating equation 5.12 with respect to torque angle and equating to zero.

$\frac{dTe}{d\theta}$ = 0 results in the torque angle

$$\theta_{po} = \frac{\phi_d + \phi_q}{2} - 45° \qquad \ldots\ldots\ldots 5.14$$

So pull out torque of reluctance motor is less than 45°.

The pull out torque is given by 5.12 in which θ is replaced by 5.14, substituting

$$T_{po} = \frac{mV^2P}{4\omega^2 L_d}\left[\frac{L_d}{L_q} - 1\right] F_{po} \qquad \ldots\ldots\ldots 5.15$$

where
$$F_{po} = \frac{\sqrt{1 + \left(\frac{r_a}{X_d}\right)^2}\sqrt{1 + \left(\frac{r_a}{X_q}\right)^2} - \left(\frac{r_a}{X_d}\right)\left(\frac{X_d}{X_q} - 1\right)}{\left[1 + \left(\frac{r_a}{X_d}\right)^2 \left(\frac{X_d}{X_q}\right)^2\right]} \qquad \ldots\ldots\ldots 5.16$$

It is to be noted that for most machines except at low frequencies, the value of ϕ_d and ϕ_q are almost zero. This results in simplifying the torque equation 5.12 as follows:

$$T_e = \frac{mPV^2}{4\omega^2}\left[\frac{1}{L_q} - \frac{1}{L_d}\right] \text{ Sin } 2\theta \qquad \ldots\ldots\ldots 5.17$$

<u>No load current.</u> No load torque angle $\theta_{NL} = \phi_d - 90°$. Substituting this in equation 5.2 and 5.3 results in

$$I_q = 0$$

$$I_d = I_{NL} = \frac{V}{\sqrt{X_d^2 + r_a^2}} \quad ;$$

When r_a is small compared to X_d, $I_{NL} = \frac{V}{X_d}$ or $X_d = \frac{V}{I_{NL}}$ which gives an easy method of measuring the direct axis reactance. However X_d is again a function of saturation. Its dependence on the current can be easily found out by running the motor at different voltages at no load.

Development of equivalent circuit. From the phasor diagram, component of current in phase with voltage is I Cos ϕ where I Cos $\phi = I_q \text{ Cos } \theta - I_d \text{Sin } \theta$ 5.18

$$\text{But } I_q = \frac{V\ (X_d \text{ Sin } \theta + r_a \text{ Cos } \theta\ )}{X_d\ X_q + r_a^2} = V_{fq} \quad \text{..... 5.19}$$

$$I_d = \frac{V\ (X_q \text{ Cos } \theta - r_a \text{ Sin } \theta\ )}{X_d\ X_q + r_a^2} = V_{fd} \quad \text{..... 5.20}$$

Substituting 5.19 and 5.20 in 5.18,

$$\frac{I}{V} \text{ Cos } \phi = f_q \text{ Cos } \theta - f_d \text{ Sin } \theta$$

$$\frac{I}{V} \text{ Sin } \phi = f_q \text{ Sin } \theta + f_d \text{ Cos } \theta \quad \text{..... 5.21}$$

If machine admittance is Y, then

$$Y = \frac{I}{V} \text{ and since } Y = G - JB \qquad \ldots\ldots\ldots 5.22$$

$$\text{and } \cos \phi = \frac{G}{Y} ;$$

$$\text{We have } G = f_q \cos \theta - f_d \sin \theta \qquad \ldots\ldots\ldots 5.23$$

$$\text{Similarly since } \sin \phi = \frac{B}{Y}$$

$$\text{We have } B = f_q \sin \theta + f_d \cos \theta \qquad \ldots\ldots\ldots 5.24$$

Thus we get the machine parameters in terms of conductance and susceptance. To eliminate f_d and f_q from equations 5.23 and 5.24, substitute for f_d and f_q from equations 5.19 and 5.20.

$$\text{Result is } G = \frac{2r_a + (X_d - X_q) \sin 2\theta}{2 (X_d X_q + r_a^2)} \qquad \ldots\ldots\ldots 5.25$$

$$B = \frac{(X_d + X_q) - (X_d - X_q) \cos 2\theta}{2 (X_d X_q + r_a^2)} \qquad \ldots\ldots\ldots 5.26$$

Note the G and B also include the leakage reactance and resistance of primary circuit. The third branch of the equivalent circuit as shown in Figure 5.3 is now calculated as $g_o = \frac{W_o}{mV^2}$; this represents iron, friction and windage losses.

The above analysis holds good for any reluctance motor, whether Synduction or Anisotropic. Using the above method, performance of the two types is calculated and compared to show the differences between the two types in Chapters 10 and 12.

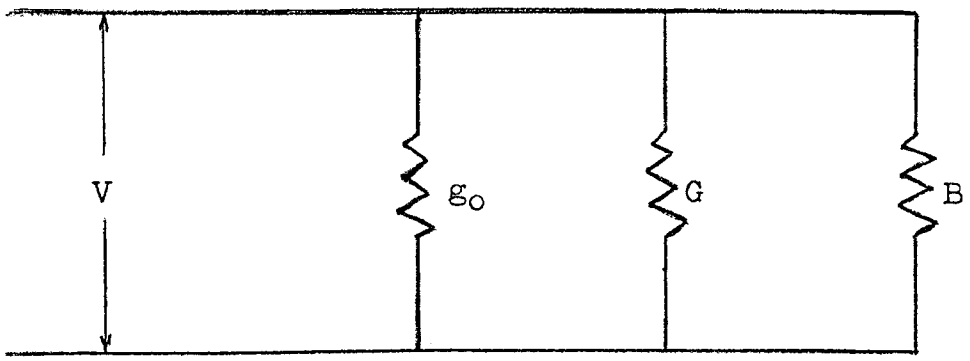

FIGURE 5.3 MODIFIED STEADY STATE EQUIVALENT CIRCUIT

CHAPTER 6

DYNAMIC BEHAVOIR OF RELUCTANCE MOTORS

The chapter is developed as follows: First the induced voltages produced during sudden loading are considered. Then the transient reluctance power developed is determined. To this is added the damper circuit developed power. These parameters all form a function of slip. The final dynamic equation involving variance of slip S and the torque angle Θ with respect to time is derived, with the knowledge of the transient total power developed, mechanical time constant of the machine and the load conditions prevailing at the time.

Induced Voltages During Sudden Loading

Unlike in a synchronous machine, there are no field windings. Hence whatever induced voltages are developed, will be only in the d-axis and q-axis damper circuits. A more rigorous approach than in synchronous machine is required, since we have to consider the effect of induced voltage in d and q axis separately. It is to be noted than unlike in synchronous machine, here there are only damper circuits where voltages are induced.

Induced Voltage In The d-axis

Equivalent circuit is shown below:

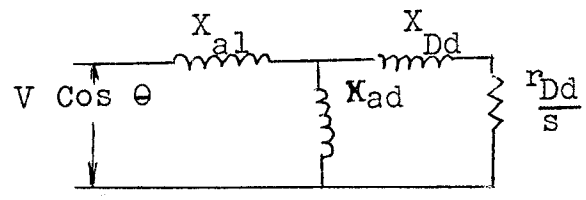

During steady state the torque angle is θ which changes to $(\theta + \Delta\theta)$ at the end of the interval. So the applied voltage across d-axis changes from V Cos θ to V Cos $(\theta + \Delta\theta)$; so the change in voltage

$$\begin{aligned} V &= V \cos(\theta + \Delta\theta) - V \cos\theta \\ &= V \cos\theta \cos\Delta\theta - V \sin\theta \sin\Delta\theta - V \cos\theta \\ &= -V \sin\theta (\Delta\theta) \end{aligned} \quad \ldots\ldots\ldots \quad 6.1$$

(Since $\Delta\theta$ is small, Cos $\Delta\theta = 1$.)

Additional armature current induced is equal to $\frac{V}{Z_{d(S)}}$

$$Z_{d(S)} = jX_{al} + \frac{\left(\frac{r_{Dd}}{S} + jK_{Dd}\right) jX_{ad}}{\frac{r_{\emptyset d}}{S} + j(X_{Dd} + X_{ad})} \quad \ldots\ldots\ldots \quad 6.2$$

By definitions of X_d, X_d'', and T_d'', we have

$$\frac{1}{Z_{d(S)}} = \frac{1}{jX_d''} + \left(\frac{1}{jX_d} - \frac{1}{jX_d}\right) \frac{jST_d''}{1 + jST_d''} \quad \ldots\ldots\ldots \quad 6.3$$

$$\Delta I_d = \frac{V \sin\theta \, d\theta}{jX_d} \left[\frac{1 + jST_{do}''}{1 + jST_d''}\right] \quad \ldots\ldots\ldots \quad 6.4$$

where $\frac{1}{Zd_{(S)}} = \frac{1}{jX_d} \left[\frac{1 + jST_{do}''}{1 + jST_d''}\right]$; $\quad \ldots\ldots\ldots \quad 6.5$

Out of the total current ΔI_d, the current following through the d-axis of rotor is

$$\Delta I_{Dd} = \Delta I_d \frac{jX_{ad}}{j(X_{ad} + X_{Dd}) + \frac{r_{Dd}}{S}} \quad \ldots\ldots\ldots 6.6$$

Substituting the value of ΔI_d, we have

$$\Delta i_{Dd} = - \frac{V \text{ Sin } \theta}{jX_d} \left(\frac{1 + jST''_{do}}{1 + jST''_d} \right) \frac{jX_{ad}}{\frac{r_{Dd}}{S} + j(X_{ad} + X_{Dd})} \cdot \Delta\theta$$

$$= - \frac{V \text{ Sin } \theta}{X_d} \cdot \frac{1 + jST''_{do}}{1 + jST''_d} \cdot \frac{S}{r_{Dd}} \frac{X_{ad}}{1 + jST''_{do}} \cdot \Delta\theta$$

$$= - V \text{ Sin } \theta \frac{X_{ad}}{X_d} \cdot \frac{X}{r_{Dd}} \cdot \frac{1}{(1 + jST''_d)} \Delta\theta \quad \ldots\ldots\ldots 6.7$$

Armature induced voltage $\Delta E_d = \Delta i_{Dd} X_{ad}$

$$\text{i.e. } \Delta E_d = - V \text{ Sin } \theta \frac{jX^2_{ad}}{X_d} \cdot \frac{S}{r_{Dd}} \cdot \frac{1}{1 + jST''_d} \Delta\theta$$

Also since $X^2_{ad} = (X_d - X''_d)(X_{Dd} + X_{ad})$

we have

$$\Delta E_d = - V \text{ Sin } \theta \frac{j(X_d - X''_d)}{X_d} \frac{S(X_{el} + X_{ad})}{r_{Dd}} \frac{1}{1 + jST''_d}$$

$$= - V \text{ Sin } \theta \frac{X_d - X''_d}{X_d} \frac{jST''_{do}}{1 + jST'_d} \Delta\theta.$$

$$= - V \text{ Sin } \theta \frac{X_d - X''_d}{X_d} \cdot \frac{jST''_d}{1 + jST''_d} \Delta\theta. \quad \ldots\ldots\ldots 6.8$$

The total induced voltage for change of angle θ to θ_o at Slip S is given by integrating the above equation,

$$E_{d\ add} = \int_{\theta_o}^{\theta} \Delta E_d$$

$$= \int_{\theta_o}^{\theta} -V \sin\theta \frac{X_d - X_d''}{X_d''} \frac{jST_d''}{1 + jST_d''} \Delta\theta$$

$$= - V \frac{X_d - X_d''}{X_d''} \cdot \frac{jST_d''}{1 + jST_d''} (\cos\theta_o - \cos\theta) \quad \ldots\ldots\ldots 6.9$$

The above is the general expression for the additional induced voltages in the d-axis. If load conditions change suddenly, we can consider $S \longrightarrow \infty$ as then $\frac{r_{Dd}}{S} \longrightarrow 0$. Therefore, for the rotor flux to remain constant, we have

$$E_{d\ add} = - V \frac{X_d - X_d''}{X_d} (\cos\theta_o - \cos\theta) \quad \ldots\ldots\ldots 6.10$$

as $\frac{jST_d''}{1 + jST_d''}$ becomes 1 for $S \rightarrow \infty$.

It should be noted that the above is the additional induced emf during transient in the d-axis.

Induced Voltages In The q-axis

The q-axis circuit is given below.

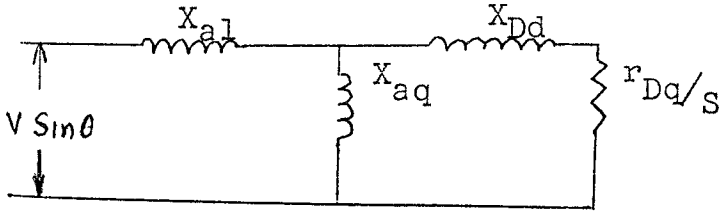

Unlike in a synchronous machine, since we are interested in finding out in the final analysis the total reluctance torque in the transient state, both due to d-axis and due to q-axis, it would be only correct if the contribution due to q-axis circuit is also evaluated.

Since by inspection the q-axis circuit is similar to the d-axis circuit described earlier and only the reactances X_{Dq}, X_{aq}, and resistances r_{Dd} and time constant T''_q and T''_{qo} are encountered in place of their d-axis counterparts, it would be quite proper to write down the final equations just by inspecting those derived for the d-axis.

To start with, the change in voltage at the terminals of q-axis, ΔV is equal to $V \sin(\theta + \Delta\theta) - V \sin\theta =$ $V \sin\theta \cos\Delta\theta + \cos\theta \sin\Delta\theta - \sin\theta$.

Since $\Delta\theta$ is small $\cos\Delta\theta = 1$ and $\sin\Delta\theta = \Delta\theta$

$$\Delta V = V. \cos\theta. \Delta\theta.$$

From here onwards the rest of the derivations are identical with the previously derived d-axis equations, but for substitution of subscript q in place of d.

So in the final analysis,

$$E_{q\ add} = V \cos\theta \frac{X_q - X''_q}{X_q} \frac{jST''_q}{1 + jST''_q} \Delta\theta. \quad \ldots\ldots\ldots 6.11$$

Further integration results in

$$E_{q\text{-add}} = V \frac{X_q - X_q''}{X_q} (\text{Sin } \theta - \text{Sin } \theta_o) \quad \ldots\ldots\ldots 6.12$$

As the term $\frac{jST_q''}{1 + jST_q''} = 1$ as $S \rightarrow \infty$.

The above equation gives the induced emf added during transient stage in the q-axis.

Transient Power Equation

Now that we know the induced additional voltages, it is possible to evaluate the transient reluctance power developed. Here again, unlike in a synchronous machine, we have to consider both the d-axis and q-axis separately.

Transient power in d-axis. Let us consider the steady state equation for reluctance motor:

$$N_p = \frac{V^2}{2} \left(\frac{1}{X_q} - \frac{1}{X_d} \right) \text{Sin } 2\theta$$

$$= V \text{ Cos } \theta \left(\frac{V}{X_q} \right) \cdot \text{Sin } \theta - V \text{ Sin } \theta \cdot \left(\frac{V}{X_d} \right) \cdot \text{Cos } \theta$$

$$= V \frac{V \text{ Sin } \theta}{X_q} \cdot \text{Sin } (\theta + \pi/2) - V \cdot \frac{V \text{ Cos } \theta}{X_d} \cdot \text{Sin } \theta$$

$$= V \cdot \frac{V_q}{X_q} \cdot \text{Sin } (\theta + \pi/2) - V \frac{V_d}{X_d} \cdot \text{Sin } \theta .$$

$$= N_{pq} - N_{pd} \quad \ldots\ldots\ldots 6.13$$

Where N_{pq} and N_{pd} are the torques produced due to quadrature and direct axes.

Now consider $N_{pd} = V \cdot \frac{V_d}{X_d} \cdot \text{Sin } \theta$.

This is similar to the torque equation for synchronous machine where $N_s = V \cdot \frac{E}{X_d} \cdot \text{Sin } \theta$.

..... 6.14

By comparison of the equations for N_{pd} and N_s, we can say that the term V_d is substituted for induced voltage E of the synchronous machine.

Now, bringing equation 6.10 into the picture where

$$E_{d\text{-add}} = - V \cdot \frac{X_d - X_d''}{X_d} \cdot (\text{Cos } \theta_o - \text{Cos } \theta);$$

We can say that total induced voltage in d-axis

$$E_d' = V_d + E_{d\text{-add}}.$$

$$= V_d - V \cdot \frac{X_d - X_d''}{X_d} \cdot (\text{Cos } \theta_o - \text{Cos } \theta)$$

Hence the power developed in d-axis from equation 6.14

$$N_{pd}' = V \left[\frac{V_d}{X_d} - \frac{X_d - X_d''}{X_d X_d''} V(\text{Cos } \theta_o - \text{Cos } \theta) \right] \text{Sin } \theta$$

$$= V \left[\frac{V_d}{X_d''} - \left(\frac{1}{X_d''} - \frac{1}{X_d} \right) V \text{ Cos } \theta_o \right] \cdot \text{Sin } \theta$$

..... 6.15

Transient power in q-axis. By similar process of deduction the induced voltage on the q-axis is:

$$E'_q = V_q + E_{q\text{-add}}$$

$$= V_q + \frac{X_q - X''_q}{X''_q} \cdot (\text{Sin } \theta - \text{Sin } \theta_o)$$

Hence the power developed in q-axis is given by using equation 6.14.

$$N'_{pq} = V\left[\frac{V_q}{X_q} + \frac{X_q - X''_q}{X_q X''_q} V.(\text{Sin } \theta - \text{Sin } \theta_o)\right] \text{ Cos } \theta$$

$$= V\left[\frac{V_q}{X''_q} - \left(\frac{1}{X''_q} - \frac{1}{X_q}\right) V \text{ Sin } \theta_o\right] \text{ Cos } \theta \quad \ldots\ldots\ldots 6.16$$

Further simplification of equations 6.15 and 6.16 can be done by substituting $V_d = V \text{ Cos } \theta$ and $V_q = V \text{ Sin } \theta$,

Total power developed in the two axes are

$$N'_{pd} = V^2\left[\frac{\text{Cos } \theta}{X''_d} - \left(\frac{1}{X''_d} - \frac{1}{X_d}\right) \text{ Cos } \theta_o\right] \text{ Sin } \theta$$

and

$$N'_{pq} = V^2\left[\frac{\text{Sin } \theta}{X''_q} - \left(\frac{1}{X''_q} - \frac{1}{X_q}\right) \text{Sin } \theta_o\right] \text{ Cos } \theta$$

and the resultant transient power,

$$N'_p = N'_{pd} - N'_{pq}$$

$$\text{i.e. } N'_p = V^2 \left[\left(\frac{1}{X''_d} - \frac{1}{X''_q} \right) \text{Sin } \theta \text{ Cos } \theta - \left(\frac{1}{X''_d} - \frac{1}{X_d} \right) \text{Sin } \theta \text{ Cos } \theta + \left(\frac{1}{X''_q} - \frac{1}{X_q} \right) \text{Sin } \theta_o \text{ Cos } \theta \right] \quad \ldots\ldots\ldots 6.17$$

From this we can verify that under steady state condition when $X''_d = X_d$ and $X''_q = X_q$, we get back the steady state equation

$$N_p = V^2 \left(\frac{1}{X_d} - \frac{1}{X_q} \right) . \text{ Sin } \theta \text{ Cos } \theta \quad \ldots\ldots\ldots 6.18$$

Damping Power Developed By The Rotor

Damping power in the d-axis. The equivalent circuit for d-axis is given below:

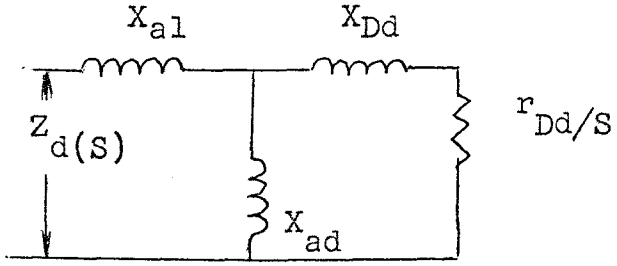

The analogy of the derivation is similar to the synchronous machine except for the absence of field winding.

$$Z_{d(S)} = jX_{al} + \frac{jX_{ad} \left(r_{Dd/S} + jX_{Dd} \right)}{\left(\frac{r_{Dd}}{S} + j X_{ad} + jX_{Dd} \right)}$$

therefore the current

$$I_{d(S)} = \frac{V_d}{Z_{d(S)}} = V_d \cdot \frac{r_{Dd}/S + j\,(X_{ad} + X_{Dd})}{jX_d\,\frac{r_{Dd}}{S} + j^2\,(X_{a1}X_{ad} + X_{a1}X_{Dd} + X_{ad}X_{Dd})} \quad \ldots\ldots\ldots 6.19$$

The portion of the current flowing through the rotor portion of the motor is

$$i_{Dd(S)} = I_{d(S)}\ \frac{jX_{ad}}{\frac{r_{Dd}}{S} + j\,(X_{ad} + X_{Dd})}$$

Substituting the value of $I_{d(S)}$ derived above

$$i_{Dd(S)} = V_d \cdot \frac{jX_{ad}}{j\,X_d\,\frac{r_{Dd}}{S} + j^2\,(X_{a1}X_{ad} + X_{a1}X_{Dd} + X_{ad}X_{Dd})} \quad \ldots\ldots\ldots 6.20$$

Let us define T_d'' as the transient short circuit time constant of the rotor direct axis.

$$T_d'' = \frac{X_{Dd1} + \left(\frac{X_{ad}\ X_{a1}}{X_{ad} + X_{a1}}\right)}{r_{Dd}}$$

Using this definition

$$i_{Dd(S)} = V_d \cdot \frac{X_{ad}}{X_d\,(1 + jST_d'')} \cdot \frac{1}{r_{Dd}/S} \quad \ldots\ldots\ldots 6.21$$

The damping power of the d-axis winding

$$N_{Dd} = i^2_{Dd(S)} \frac{r_{Dd}}{S} (1-S)$$

$$= i^2_{Dd(S)} \cdot \frac{r_{Dq}}{S} \quad \text{for } S \longrightarrow \infty$$

i.e. $$N_{Dd} = V_d^2 \frac{X_{ad}^2}{X_d^2 (1 + S^2 T_d''^2)} \frac{1}{(r_{Dd}/S)^2} \frac{r_{Dd}}{S}$$

Also we know that $\frac{X_{ad}^2}{X_d^2} \cdot \frac{1}{(r_{Dd}/S)} = \left(\frac{1}{X_d''} - \frac{1}{X_d} \right) S T_d''$

$$N_{Dd} = V_d^2 \left(\frac{1}{X_d''} - \frac{1}{X_d} \right) \frac{ST_d''}{1 + S^2 T_d''^2} \quad \ldots\ldots\ldots 6.22$$

Since S is very small, $S^2 T_d''^2 \ll 1$

So $N_{Dd} = V_d^2 \left[\frac{1}{X_d''} - \frac{1}{X_d} \right] ST_d''$;

Let $V_d = V \sin \theta$ in the direct axis.

$$N_{Dd} = V^2 \sin^2\theta \left[\frac{1}{X_d''} - \frac{1}{X_d} \right] ST_d''; \quad \ldots\ldots\ldots 6.23$$

Damping power in the q-axis. It is to be noted in the following derivation of the damping power in the q-axis, the derivation would be similar to the synchronous machine since the equivalent circuit in q-axis is the same as for a synchronous machine.

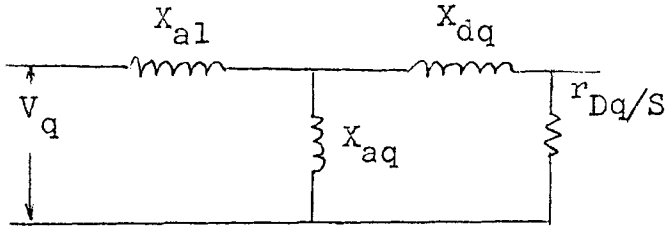

Effective impedance

$$Z_{q(S)} = j X_{al} + \frac{j X_{aq}\left(\frac{r_{Dq}}{S} + j X_{Dq}\right)}{\frac{r_{Dq}}{S} + j (X_{aq} + X_{Dq})} \quad \ldots\ldots\ldots 6.24$$

The armature current I_q flowing in the q-axis at any Slip S

$$i_q (S) = \frac{V_q}{Z_{q(S)}} = V_q \frac{\frac{r_{Dq}}{S} + j (X_{aq} + X_{dq})}{jX_q\frac{r_{Dq}}{S} + j^2(X_{al}X_{aq}+X_{al}X_{Dq}+X_{aq}X_{Dq})} \quad \ldots\ldots\ldots 6.25$$

The position of armature current flowing through the rotor

$$i_{Dq} (S) = I_{q(S)} \cdot \frac{j X_{aq}}{\frac{r_{Dq}}{S} + j (X_{aq} + X_{dq})}$$

Substituting the value for $I_{q(S)}$ from previous equation:

$$I_{Dq(S)} = V_q \frac{j X_{aq}}{j X_q\frac{r_{Dd}}{S} + j^2 (X_{al}X_{aq}+X_{al}X_{Dq}+X_{aq}X_{Dq})} \quad \ldots\ldots\ldots 6.26$$

Definition of T_q'' is the same as in a synchronous machine being:

$$T_q'' = \frac{X_{Dq}X_{aq} + X_{Dq}X_{al} + X_{aq}X_{al}}{(X_{aq} + X_{al})\ r_{Dq}} \qquad \ldots\ldots\ldots 6.26$$

Using this we have:

$$i_{Dq(S)} = V_q \cdot \frac{X_{aq}}{X_q\ (1 + jST_q'')} \cdot \frac{1}{r_{Dq}/S}$$

The damping power in the q-axis is given by the loss in damper bars times (1-S)/S.

$$\text{i.e. } N_{Dq} = i^2_{Dq(S)} \frac{r_{Dq}}{S}(1-S) = i^2_{Dq(S)} \frac{r_{Dq}}{S} \text{ as } S \longrightarrow 0$$

$$= V_q^2 \frac{X^2_{aq}}{X_q^2\ (1 + S\ T_q''^2)} \frac{}{\left(\frac{r_{Dq}}{S}\right)^2} \frac{r_{Dq}}{S}$$

$$\text{Also we have } \frac{X^2_{aq}}{X_q^2} \cdot \frac{1}{\frac{r_{Dq}}{S}} = \left(\frac{1}{X_q''} - \frac{1}{X_q}\right) ST_q'' \qquad \ldots\ldots\ldots 6.27$$

$$\text{So } N_{Dq} = V_q^2 \left(\frac{1}{X_q''} - \frac{1}{X_q}\right) \frac{ST_q''}{1 + S^2T_q''^2} \qquad \ldots\ldots\ldots 6.28$$

Since S is small, $S^2T_q'' \ll 1$ and can be neglected

$$N_{Dq} = V_q^2 \left(\frac{1}{X_q''} - \frac{1}{X_q}\right) ST_q''. \qquad \ldots\ldots\ldots 6.29$$

Since the voltage across q-axis is by definition, $V_q = V \cos\theta$, we have

$$N_{Dq} = V^2 \cos^2\theta \left(\frac{1}{X''_q} - \frac{1}{X_q} \right) ST''_q$$

Total damping power in the two axes. The total available power from the damping circuit is given by $N_D = N_{Dd} + N_{Dq}$

$$\text{i.e. } N_D = V^2 \sin^2\theta \left(\frac{1}{X''_d} - \frac{1}{X_d} \right) ST''_d + V^2 \cos^2\theta \left(\frac{1}{X''_q} - \frac{1}{X_q} \right) ST''_q. \quad \ldots\ldots\ldots 6.30$$

Behavoir Of Reluctance Machine Under Sudden Real Loading

The factors that influence the behavoir under real loading are:

(a) The inertial time constant of the machine.

(b) The actual load the machine is seeing.

(c) The damper and transient power available for acceleration or retardation of the machine.

In the above (c) has been discussed. Let us now derive equations for the inertial time constant T_m, of the motor.

(a) Inertial time constant (T_m). During steady state the electrical power delivered to the machine is equal to the mechanical power delivered by the motor to the shaft.

However, during transient condition, the balance does not hold good and the difference between the two powers helps accelerate or retard the motor. The equation for accelerating or decelerating power is $N_a = N_p \backsim N_L$ 6.31

where N_p = electrical power input, N_L = load connected, and N_a = accelerating/retarding power.

We know that torque $T = I \frac{d\omega}{dt}$ where I = inertia. The total power required to accelerate the rotor from standstill to synchronous is

$$\Delta P = \int_0^{\omega_s} \frac{I\omega}{t} \, d\omega$$

i.e. $$P = \frac{I\omega_s^2}{t} \quad \text{where } I = \frac{WR^2}{g};$$

$$t = \frac{I\omega_s^2}{P} = \frac{WR^2}{g} \frac{\omega_s^2}{P} \qquad \text{..... 6.32}$$

Where, if P = rated KVA, ω_s = rated speed, then the inertial time constant of the machine t seconds is required to accelerate the inertia WR^2 from standstill to rated speed. Expressing WR^2 in pounds-feet^2 and T_m the mechanical time constant in seconds, speed in RPM then

$$T_m = \frac{WR^2 (RPM)^2}{2.168 \ (KVA)} \ 10^{-6} \text{ seconds}$$

Having derived the expression for the mechanical time constant, we can now express the accelerating power.

$$N_a = \frac{T_m}{\omega_s} \frac{d^2\theta}{dt^2}$$

We have from equation 6.31, $N_a = N_L - N_p$..... 6.33

For a gradual load change the electrical real power

$$N_p = \frac{V^2}{2} \frac{X_d - X_q}{X_d X_q} \text{ Sin } 2\theta, \text{ therefore}$$

$$N_a = N_L - \frac{V^2}{2} \cdot \frac{X_d - X_q}{X_d X_q} \cdot \text{Sin } 2\theta.$$

For gradual load changes N_L changes slowly and there is no resultant value of N_a. However for sudden change in load, we have to consider the inertia and the constancy of flux linkage. In other words, the transient power N_p' is to be used in place of N_p.

From equation 6.17 we know that

$$N_p' = V^2\left[\left(\frac{1}{X_d''} - \frac{1}{X_q''}\right) \text{Sin } \theta \text{ Cos } \theta - \left(\frac{1}{X_d''} - \frac{1}{X_d}\right) \text{Sin } \theta \text{ Cos } \theta_o + \left(\frac{1}{X_q''} - \frac{1}{X_q}\right) \text{Cos } \theta \text{ Sin } \theta_o\right] \quad \text{..... 6.34}$$

At $\theta = \theta_o$, corresponding to the initial condition of loading, we have from the preceding equation

$$N'_{po} = V^2 \left[\left(\frac{1}{X''_d} - \frac{1}{X''_q} \right) - \left(\frac{1}{X''_d} - \frac{1}{X_d} \right) + \left(\frac{1}{X''_q} - \frac{1}{X_q} \right) \right] \text{Sin } \theta_o \text{ Cos } \theta_o \quad \ldots\ldots\ldots 6.35$$

Now we have a situation where the transient torque and load torque are not balanced. This results in an acceleration or deceleration torque N_a, and rotor slips from synchronism. This develops a new torque which is the asynchronous torque due to damper circuits of d and q axis.

Total electrical power $Np = N'_p + ND$. From equation 6.33 the acceleration torque

$$N_a = N_L - N_p$$
$$= N_L - (N'_p + N_D)$$

Substitute for N'_p from equation 6.17 and for N_D from equation 6.30, we have

$$N_a = N_L - V^2 \left[\left(\frac{1}{X''_d} - \frac{1}{X_q} \right) \text{Sin } \theta \text{ Cos } \theta - \left(\frac{1}{X''_d} - \frac{1}{X_d} \right) \text{Sin } \theta \text{ Cos } \theta_o \right.$$
$$+ \left(\frac{1}{X''_q} - \frac{1}{X_q} \right) \text{Sin } \theta_o \text{ Cos } \theta$$
$$\left. + S \left\{ \left(\frac{1}{X''_d} - \frac{1}{X_d} \right) \text{Sin}^2\theta \; T''_d + \left(\frac{1}{X''_q} - \frac{1}{X_q} \right) T''_q \text{ Cos}^2\theta \right\} \right] \quad \ldots\ldots\ldots 6.36$$

We have already shown previously that

$$N_a = \frac{T_m}{\omega_s} \frac{d^2\theta}{dt^2}$$

and $S = \frac{1}{\omega} \frac{d\theta}{dt}$

Making the above substitutions in equation 6.36, we have

$$\frac{T_m}{\omega_s} \frac{d^2\theta}{dt^2} = N_L - V^2 \left[\left(\frac{1}{X_d''} - \frac{1}{X_q''} \right) \text{Sin } \theta \text{Cos} \theta - \left(\frac{1}{X_d''} - \frac{1}{X_d} \right) \text{Sin} \theta \text{Cos} \theta + \left(\frac{1}{X_q''} - \frac{1}{X_q} \right) \text{Sin} \theta_o \text{Cos} \theta \right.$$
$$\left. + \frac{1}{\omega} \left\{ \left(\frac{1}{X_d''} - \frac{1}{X_d} \right) T_d'' \text{Sin}^2 \theta + \left(\frac{1}{X_q''} - \frac{1}{X_q} \right) T_q'' \text{Cos}^2 \theta \right\} \frac{d\theta}{dt} \right] \quad \ldots\ldots\ldots 6.37$$

The above equation 6.37 is the dynamical equation for sudden and real loading. This equation describes the time dependence of torque θ upon sudden application of load. As can be seen above, the left hand side of equation has a term $\frac{d^2\theta}{dt^2}$ and the right hand side has a term $\frac{d\theta}{dt}$. This second order differential equation is nonlinear and can be solved using analogue computer or by numerical integration. However, even with numerical integration great errors may arise because of the fact that the time interval cannot be made infinitesimally small. Also the contribution damper torques to the equation cannot be exactly predicted since the sub-

transient reactances X''_d, X''_q and time constants T''_d and T''_q depend to a great degree on saturation, However on an analogue computer, continuous time varying $\frac{d\theta}{dt}$ and $\frac{d^2\theta}{dt^2}$ can be overcome. In the final analysis, the rotor angle keeps oscillating about a mean position with gradually decreasing amplitude and subsequent decreasing damping torque, until the accelerating or retarding torque becomes zero and the torque angle will correspond to the new load torque.

CHAPTER 7

EQUIVALENT CIRCUITS AND DYNAMICAL EQUATIONS

Development of equivalent circuits and the dynamical equations for any general class of machines with n windings in stator, and m windings in rotor, have been developed extensively by Mr. Gabriel Kron in his treatise on the subject. In the following, an attempt is made to confine the development of the circuit to the reluctance motor in question under balanced input conditions. In fact, the analysis would closely resemble synchronous machine except for absence of field winding and, of course, the existance of saliency of the rotor.

The Circuits For Revolving Field and Cross Field

First the general case is taken up for unbalance voltage conditions. Figure 7-1 shows the revolving field and cross field circuits for forward rotating field. Figure 7-2 is developed with backward rotating emf, both the revolving field and cross field circuits. Note subscript a refers to armature and subscript D refers to damper circuit.

The reluctance motor being excited only on the armature stationary axes by an emf rotating at unit speed in the direction of rotor speed v . In the d-q reference frame, this emf appears to rotate forward with slip frequency $s = f - v$ during start-up. Hence f in the primitive

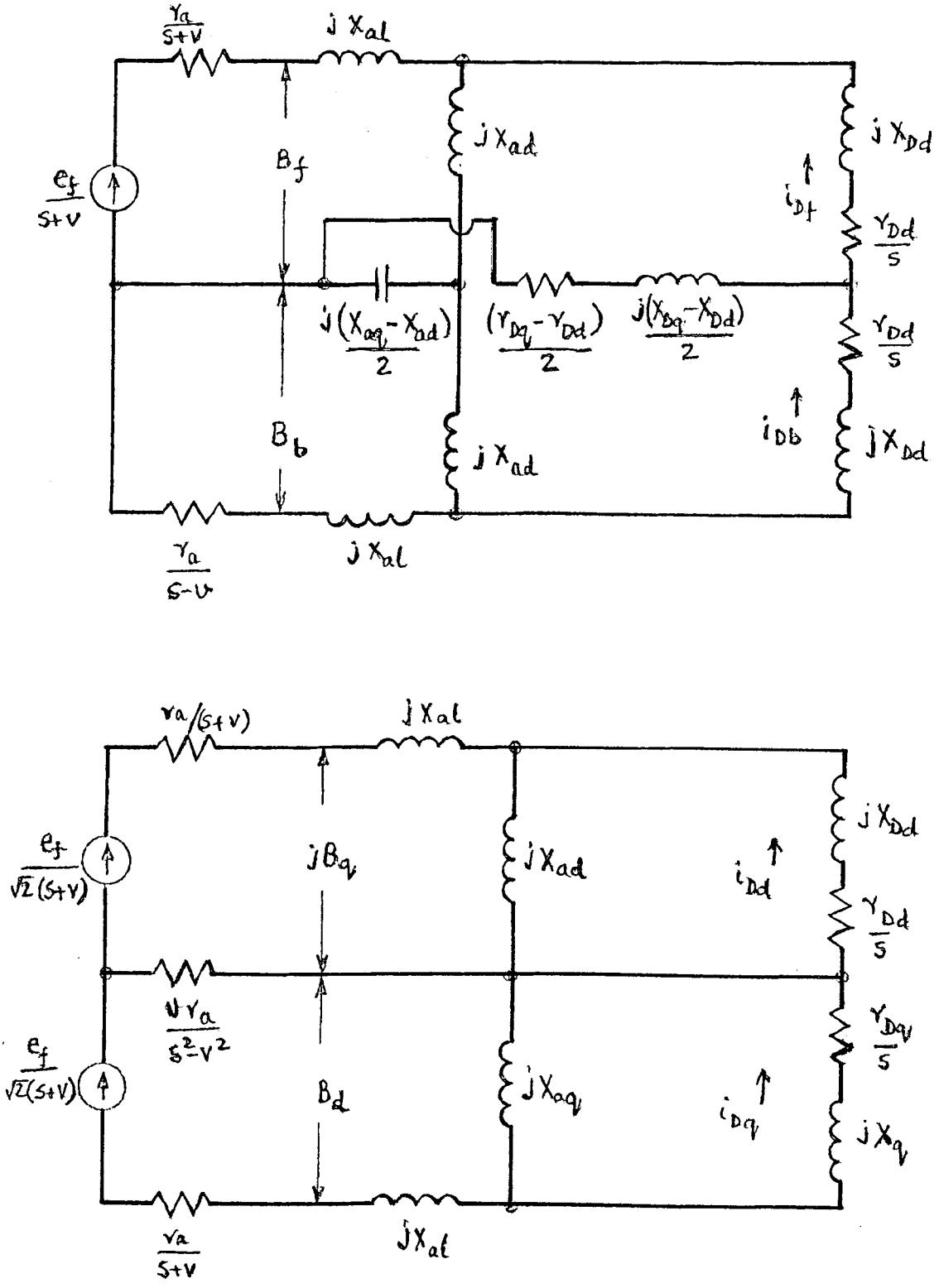

FIGURE 7.1 REVOLVING AND CROSS FIELD EQUIVALENT CIRCUITS WITH FORWARD ROTATING EMF APPLIED

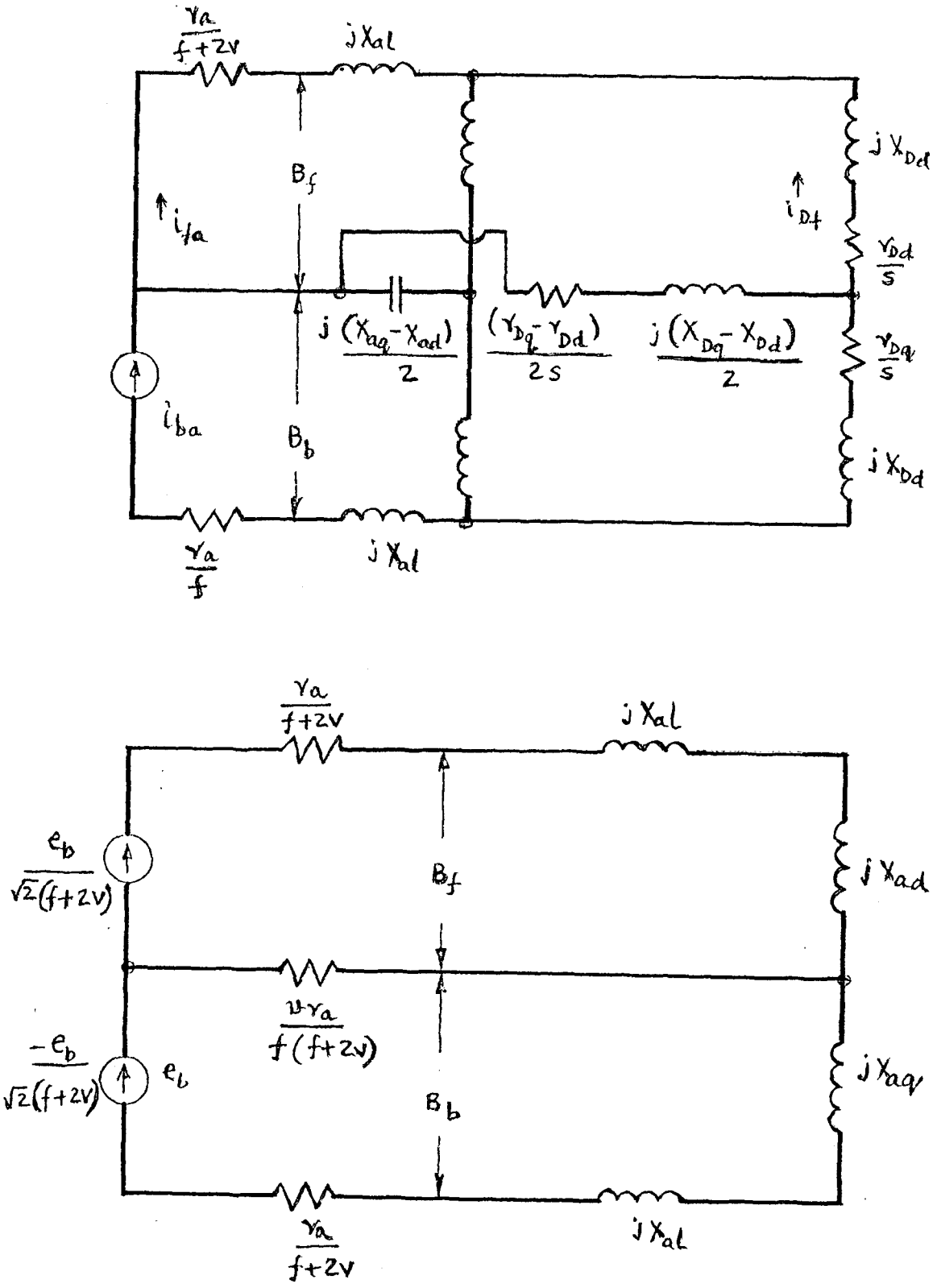

FIGURE 7.2 REVOLVING AND CROSS FIELD EQUIVALENT CIRCUITS WITH BACKWARD ROTATING EMF APPLIED

machine becomes s. Here the backward rotating emf e_b is assumed to be zero. (Figure 7-1.)

When only the backward rotating emf is applied, the f in the primitive machine becomes $(f + v)$ where V is the forward speed of rotor. Here forward applied voltage is assumed zero. (Figure 7-2.)

During the course of run-up from standstill the motor is subjected to both the accelerating and alternating torque. At half speed at slip $s = v$, i.e. $s - v = o$.

The characteristics of equivalent circuit changes and the new equivalent circuit can be depicted as in Figure 7-3. Further increase in speed takes the rotor into pull in region and provides the inertia of the motor rotor and connected load is within the region of pull in torque, the motor pulls into synchronism and runs at rotor speed $v = f$ due to reluctance torque developed. The equivalent circuit for this condition of running can be shown as in Figure 7-4.

It should be noted that Figures 7-1, 7-3, and 7-4 depict conditions of the existance of balanced voltages only. This is usually the case. However, in case of unbalanced voltages existing in the incoming lines, the situation may be taken care of by modifying the equivalent circuits of Figure 7-2 and 7-4 for backward rotating emf e_b and in which f is replaced by $(f + v)$.

(a) Revolving Field

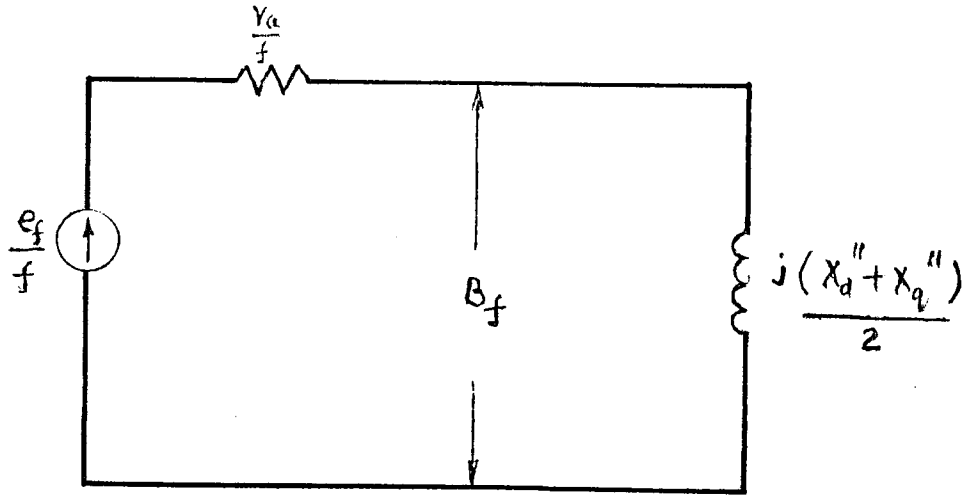

(b) Cross Field

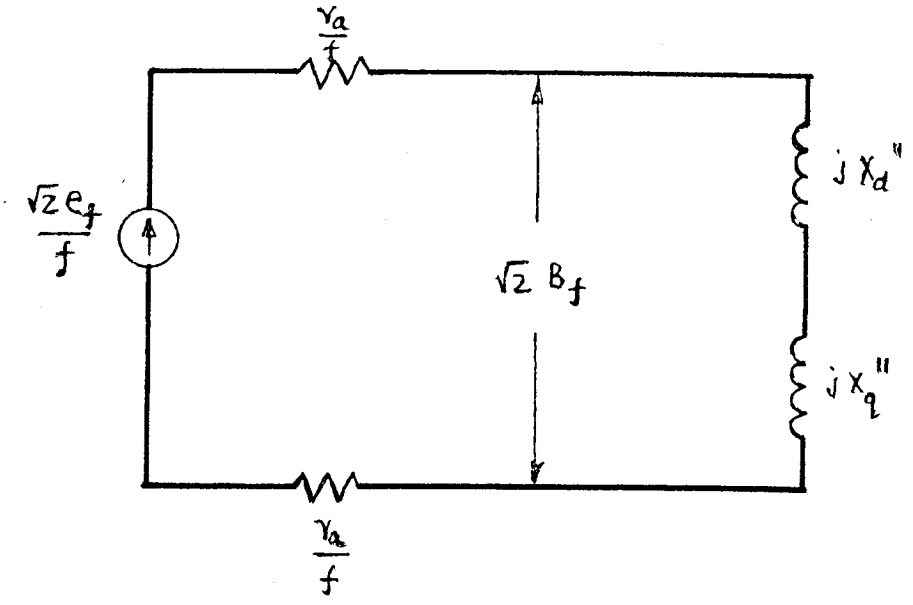

FIGURE 7.3 EQUIVALENT CIRCUIT AT HALF SPEED WITH FORWARD EXCITATION ONLY ON ARMATURE

(a) Revolving Field

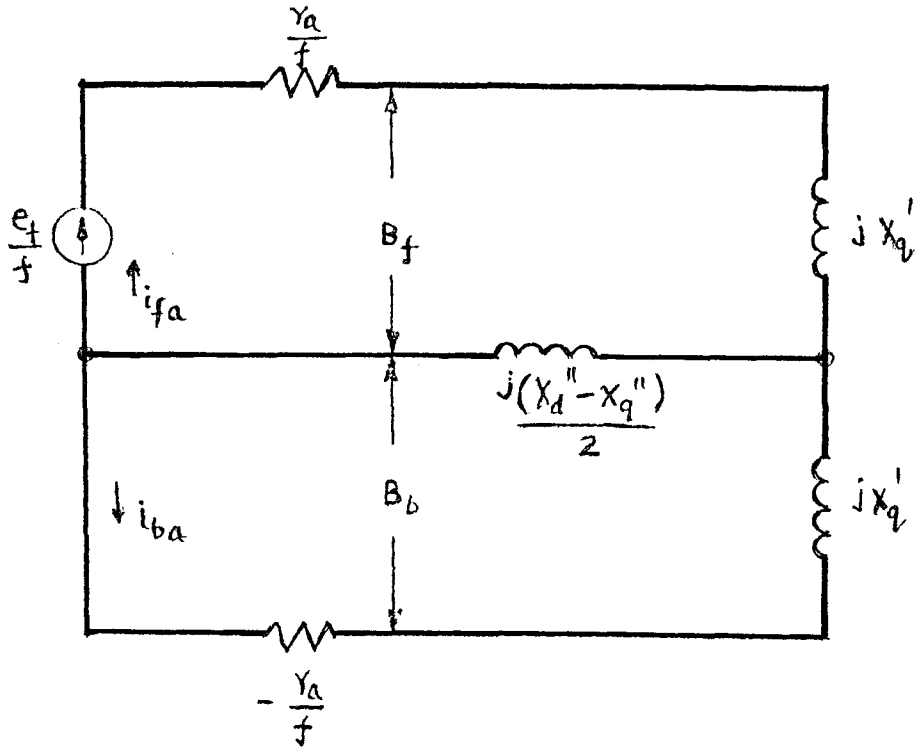

(b) Cross Field

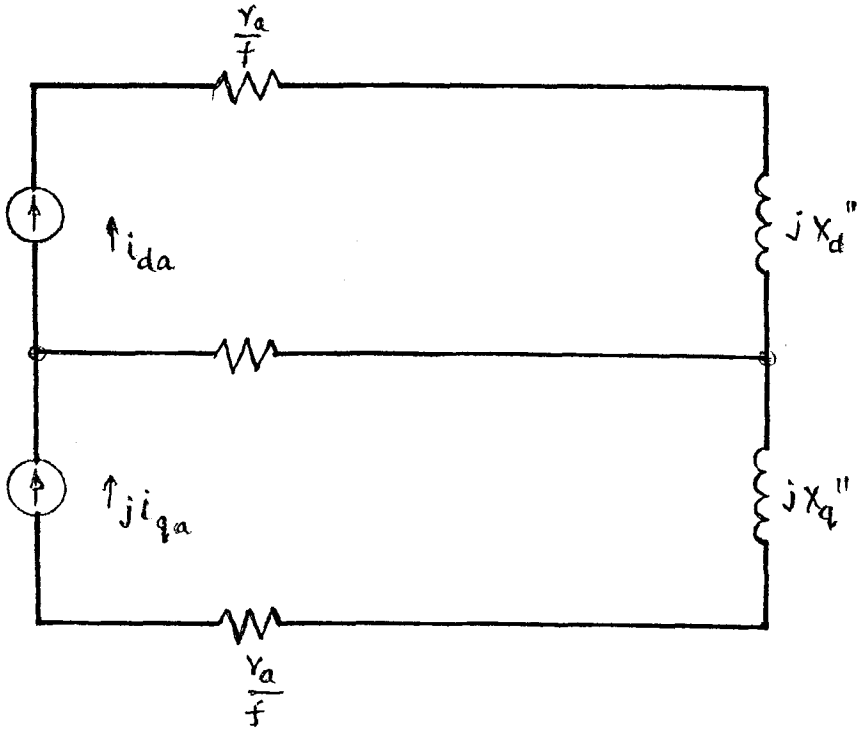

FIGURE 7.4 EQUIVALENT CIRCUIT AT FULL SPEED WITH FORWARD EXCITATION ONLY ON THE ARMATURE

Combined Equivalent Circuit

The Figures 7-1 and 7-2 depicting the forward and backward applied voltages can, in fact, be combined into one with the following difference. The frequency of the positive sequence voltage e_{sf} is f and the negative sequence voltage e_{sb} is f where as in Figure 7-1 and 7-2 they were f - v and f + v respectively. It should be noted that now the armature reference axes are rigidly connected to the armature. This is shown in Figure 7-5.

Having expressed the equivalent circuit for reluctance motors under various conditions of impressed voltages, we can now attempt to establish transient dynamical equations, as follows.

Dynamical Equations From Equivalent Circuits

Instead of attempting to write the transient equivalent circuit directly, it is easier to start with a steady state equivalent circuit containing variable frequency f feature. From this the transient equation is easily found by replacing f by $\frac{P}{j} = \left[\left(\frac{d}{dt}\right)/j\right]$.

Figure 7-6 (a) shows the variable frequency network from which is derived Figure 7-6 (b) showing transient network. These equivalent circuits are derived for condition of $v < f$. Since $f = S$, we can replace f by jp, S by - jp and v by $P\Theta$.

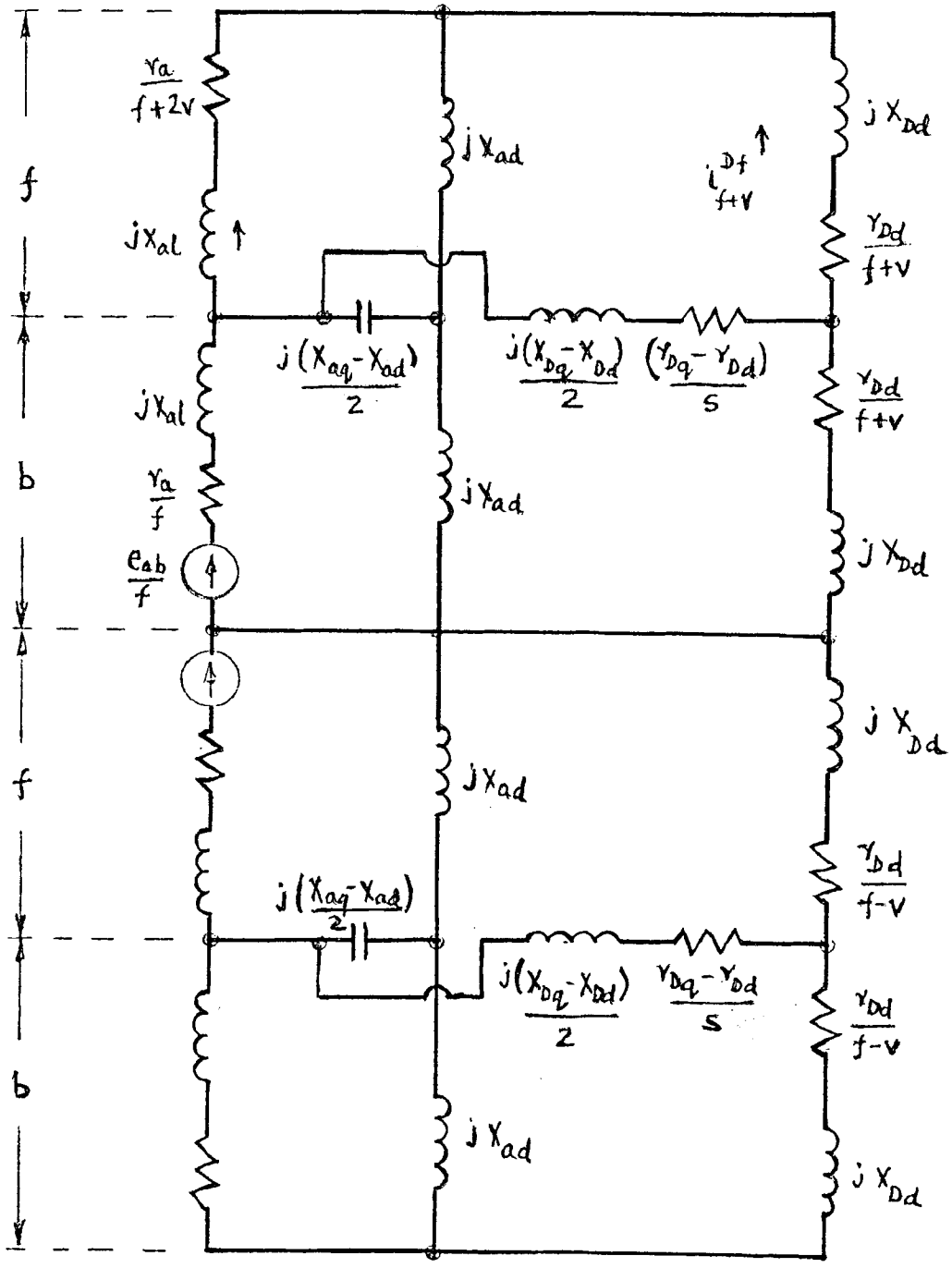

FIGURE 7.5 COMBINED EQUIVALENT CIRCUIT WITH BALANCED AMATURE

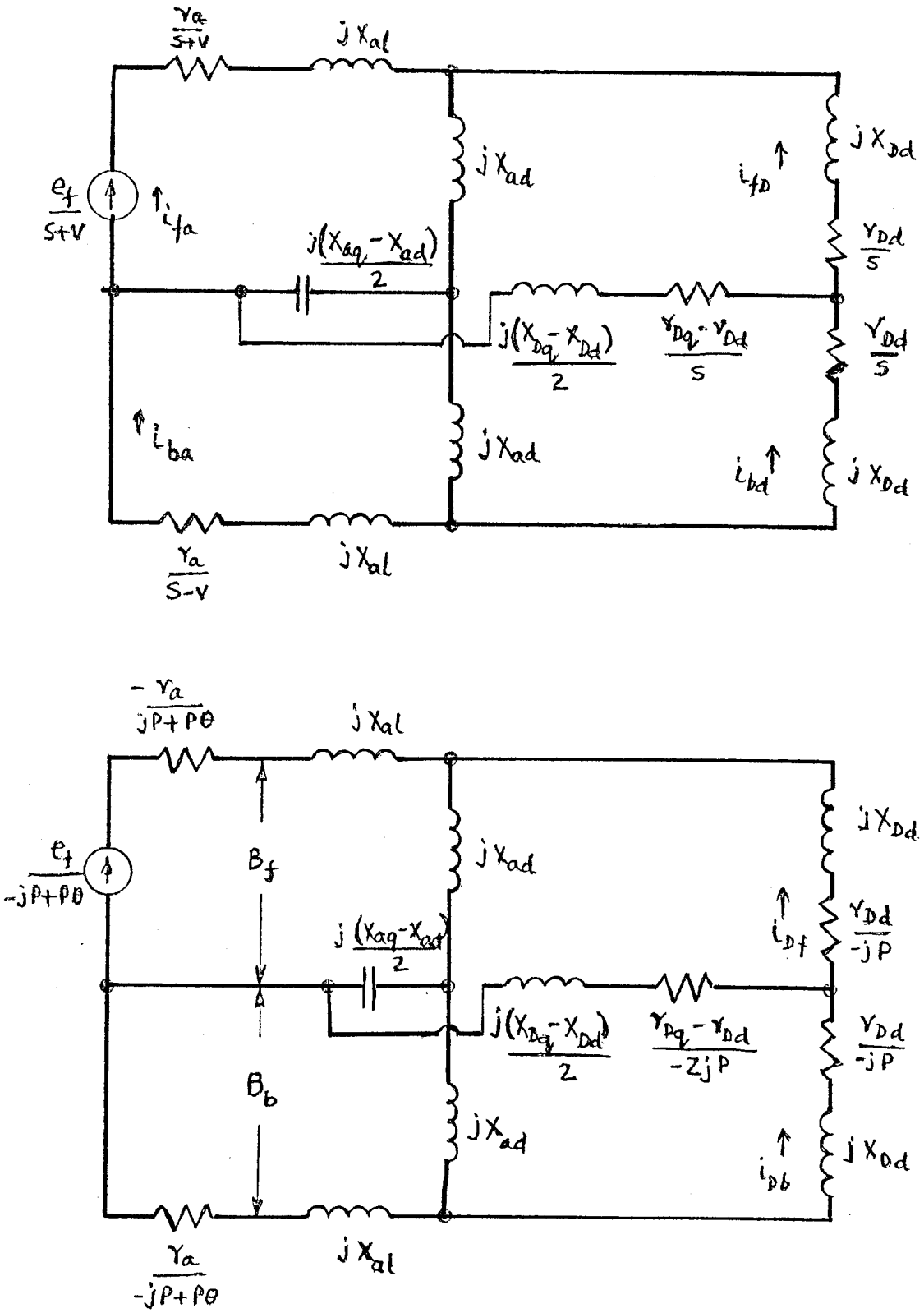

FIGURE 7.6 TRANSIENT EQUIVALENT CIRCUIT

Self Impedances of Reluctance Motor

Let us write down the voltage equations e = Zi for the four meshes in the circuit of Figure 7-6 (a).

These networks contain the only reactances X_{ad}, X_{aq}, X_{Dd}, X_{Dq}, and X_{al} and their combinations. Let us define the following self impedances:

$$\begin{aligned} x_d &= x_{ad} + x_{al}, \\ x_q &= x_{aq} + x_{al}, \\ X_{Dd} &= x_{ad} + x_{Dd}, \\ X_{Dq} &= x_{aq} + x_{Dq}. \end{aligned} \qquad \text{..... 7.1}$$

In addition to these, we have resistances and reactances as combinations of these. Let us define these impedances with terms using subscripts s for sums and D for differences of the above.

$$\begin{aligned} r_{Ds} &= \frac{r_{Dd} + r_{Dq}}{2} \\ r_{DD} &= \frac{r_{Dd} - r_{Dq}}{2} \\ X_{Ds} &= \frac{X_{Dd} + X_{Dq}}{2} \\ X_{DD} &= \frac{X_{Dd} - X_{Dq}}{2} \end{aligned} \qquad \text{..... 7.2}$$

Also,

$$X_s = \frac{x_d + x_q}{2}$$

$$X_D = \frac{x_d - x_q}{2}$$

$$X_{as} = \frac{x_{ad} + x_{aq}}{2}$$

$$X_{aD} = \frac{x_{ad} - x_{aq}}{2} \qquad \ldots\ldots\ldots \quad 7.3$$

Equations of Equivalent Circuit

Voltage equations of all the four meshes can be written as $e_1 = Z_1 i_1$ where e_1, Z_1, i_1 are all tensors.

$Z_1 =$

	f_D	b_D	f_a	b_a
f_D	$\frac{r_{Ds}}{s} + j X_{Ds}$	$\frac{r_{DD}}{s} + j X_{DD}$	$j X_{as}$	$j X_{aD}$
b_D	$\frac{r_{DD}}{s} + j X_{DD}$	$\frac{r_{Ds}}{s} + j X_{Ds}$	$j X_{aD}$	$j X_{as}$
f_a	$j X_{as}$	$j X_{aD}$	$\frac{r_a}{s+v} + j X_s$	$j X_D$
b_a	$j X_{aD}$	$j X_{as}$	$j X_D$	$\frac{r_a}{s-v} + j X_s$

$\ldots\ldots\ldots \quad 7.4$

The current vector i_1 is deduced.

$i_1 =$

f_D	b_D	f_a	b_a
i_{fD}	i_{bD}	i_{fa}	i_{ba}

$\ldots\ldots\ldots \quad 7.5$

Regarding the voltage vector, the only voltage under consideration is the forward impressed voltage:

$$e_1 = \begin{array}{|c|c|c|c|} \hline f_D & b_D & f_a & b_a \\ \hline & & \dfrac{e_{fa}}{s+v} & \\ \hline \end{array}$$

..... 7.6

It is noted from above that the impedance matrix is symmetrical. The differences of potentials B_f and B_b are found as products of reactances and currents. The torque sensor G_1 to account for differences of potential B is expressed as follows:

$$G_1 = \begin{array}{c|c|c|c|c} & f_D & b_D & f_a & b_a \\ \hline f_a & j\,X_{as} & j\,X_{aD} & j\,X_s & j\,X_D \\ b_a & j\,X_{aD} & -j\,X_{as} & -j\,X_D & -j\,X_s \\ \hline \end{array}$$

..... 7.7

The torque developed by the motor is given by

$$T = i_1^* G_1 i_1$$

..... 7.8

Steady-State Sequence Equation

Let n be the absolute frequency tensor. By multiplying the impedance terms of Z matrix, by the tensor n, is obtained the steady state impedance tensor Z_2. For this conversion of Z_1, it would be necessary to multiply by the damper impedances by s, and the forward circuit impedances by s + v and the backward circuit impedances by x - v.

So the absolute frequency or the speed tensor can be defined as

$n =$

	f_D	b_D	f_a	b_a
f_D	s			
b_D		s		
f_a			s + v	
b_a				s - v

..... 7.9

The resultant impedance tensor Z_2 is

$Z_2 =$

	f_D	b_D	f_a	b_a
f_D	$r_{Ds} + jSX_{Ds}$	$r_{DD} + jSX_{DD}$	jSX_{as}	jSX_{aD}
b_D	$r_{DD} + jSX_{DD}$	$r_{Ds} + jSX_{Ds}$	jSX_{aD}	jSX_{as}
f_a	$j\ (s+v)\ X_{as}$	$j\ (s+v)\ X_{aD}$	$r_a + j(s+v)X_s$	$j\ (s+v)\ X_D$
b_a	$j\ (s-v)\ X_{aD}$	$j\ (s-v)\ X_{as}$	$j\ (s-v)\ X_D$	$r_a + j(s-v)X_s$

..... 7.10

The voltage vector however has only one term

$e_2 =$

f_D	b_D	f_a	b_a
		e_f	

..... 7.11

Transient Sequence Equations

As earlier explained, the transient solution is obtained by inspection of steady state equations and replacing

(a) $\frac{P}{j}$ by $-jP$

(b) v by $P\theta$

(c) x by L.

So the transient impedance tensor becomes

$Z_3 =$

	f_D	b_D	f_a	b_a
f_D	$r_{Ds} + L_{Ds} P$	$r_{DD} + L_{DD} P$	$L_{as} P$	$L_{aD} P$
b_D	$r_{DD} + L_{DD} P$	$r_{Ds} + L_{Ds} P$	$L_{aD} P$	$L_{aD} P$
f_a	$(P+jP\theta) L_{as}$	$(P+jP\theta) L_{aD}$	$r_a+(P+jP\theta)L_s$	$(P+jP\theta)L_D$
b_a	$(P-jP\theta) L_{aD}$	$(P-jP\theta) L_{as}$	$(P-jP\theta) L_D$	$r_a+(P-jP\theta)L_s$

..... 7.12

The transient voltage equations are then $e_1 = Z_3 i_1$.

Torque is still by the formula $T = i_1^* G_1 i_1$

Transient Equations Along Physical D-Q Axes

To avoid running into imaginary terms containing j in the above tensorial equations, physical reference frame is introduced. Let the sequence currents i_2 be replaced by Ci_4 where the transformation tensor

$$C = \frac{1}{\sqrt{2}}$$

	d_D	q_D	d_a	q_a
f_D	1	j		
b_D	1	-j		
f_a			1	j
b_a			1	-j

..... 7.13

Then we have the new impedance tensor $Z_4 = C_t^* Z_3 C$,

	d_D	q_D	d_a	q_a
d_D	$r_{Dd} + L_{Dd}\ P$		$L_{ad}\ P$	
q_D		$r_{Dq} + L_{Dq}\ P$		$L_{aq}\ P$
d_a	$L_{ad}\ P$	$-L_{ad}\ P\theta$	$r_a + L_d\ P$	$-L_q\ P\theta$
q_a	$L_{ad}\ P\theta$	$L_{aq}\ P$	$L_d\ P\theta$	$r_a + L_q\ P$

..... 7.14

(Note the L's correspond to the combinations of self inductances similar to the X's previously defined.)

The new e_3 becomes $e_3 = C_t^* e_2$

i.e. $e_3 =$

d_D	q_D	d_a	q_a
		$ef/\sqrt{2}$	$-jef/\sqrt{2}$

..... 7.15

The current vector i_2

$i_2 =$

d_D	q_D	d_a	q_a
i^{Dd}	i^{Dq}	i^{ad}	i^{aq}

..... 7.16

The torque tensor G_2 becomes

$G_2 =$

	d_D	q_D	d_a	q_a
d_a		$-L_{aq}$		L_q
q_a	L_{ad}		L_d	

..... 7.17

With the help of above tensors, we can obtain the transient equations along the physical reference frame

Voltage $e_3 = Z_4 i_2$

Torque $T = i_2 G_2 i_2$

During acceleration $T = i_2 G_2 i_2 - IP^2\theta$

During steady state $P = jf = js.$

..... 7.18

CHAPTER 8

STARTING AND PULL IN PERFORMANCE

For reluctance motors starting performance has always been a great set back for commercial applications. Till now where motors have to be connected to high inertia loads, and as is quite often, the motor has to be started with full load connected to the shaft, synchronous motors have been preferred in spite of the problems associated with synchronizing.

The following discussion on starting performance relates to any reluctance motor with an additional squirrel cage winding. Before going into the mechanism of pulling in, a note regarding the difference between Synduction rotor and Anisotropic rotor as to the starting performance is relevant.

In Anisotropic rotor, as shown in Figure 2.2, the four aluminum bars in the quadrature axis and the barrier regions on d-axis together with the end sections act as squirrel cage. While the section of iron relates the synchronizing torque developed at the pull in region, the space left out for conductor material decides the speed to which the motor will accelerate due to asynchronous torque; so a compromise between the synchronous and asynchronous characteristics, which are exclusive to each other, has to be arrived. This might seriously affect the load inertia that can be tolerated on any machine

In the case of Anisotropic rotor, though the basic principles as above, of the conflicting requirements of design parameters still holds good, the problem is greatly eased by the fact that rotor material has intrinsic anisotropy. Because of the increased anisotropy, the pole span to pole pitch ratio can be reduced for the same synchronous capability as for corresponding Synduction motor. This leaves more room for conductor material with consequent reduction of slip and the increased final speed due to asynchronous torque. Further, the pulling into step is made easier with the larger synchronous torque available. In addition, the special shape of the core chosen for the design described in this paper, allows more room for conductor material, apart from making mechanical assembly more rigid, than any other shape of core that has been tried so far, as far as this author is aware of.

The following analysis broadly explains the criteria for pull in performance. The squirrel cage effect of the rotor contributes to the asynchronous torque, which accelerates the inertia to a slip S_L with some load condition T_L. A reluctance torque is also produced at the same time. This reluctance torque which is of pulsating nature in view of continuously changing of torque angle from -180° to 180°, averages out during the start up. The pulsating torque is at 60 Hz. to start with and also has large magnitude due to

low reactances that are inevitable due to saturation by current. As the motor speeds up, the frequency and magnitude of pulsating torque decreases. After the rotor has reached a maximum speed corresponding to slip S_L, arrived at by psuedo-constant speed solution, the pull in is possible provided the reluctance developed is sufficient to accelerate the rotor to the nearest pole. In synchronous machines the salient pole has to choose the pole due to stator mmf of same polarity. On the other hand, in the case of reluctance motors there are twice as many alternative positions for rotor to lock into synchronism. On the other hand, since

$$T_s = T_{smax} \text{ Sin } 2\theta. \qquad \ldots\ldots\ldots 8.1$$

The salient pole has to be lagging within an angle of $\pi/2$ of the stator mmf wave in the direction of rotation.

Let T_a = Asynchronous Torque at Slip S_L

T_s = Synchronous Torque = T_{smax} Sin 2 θ

T_L = Load Torque connected

T_M = Torque of rotating masses

So $T_a + T_s = T_L + T_M \qquad \ldots\ldots\ldots 8.2$

The above condition must hold good during transition stage from asynchronous speed at slip S_L to synchronous speed at S = 0.

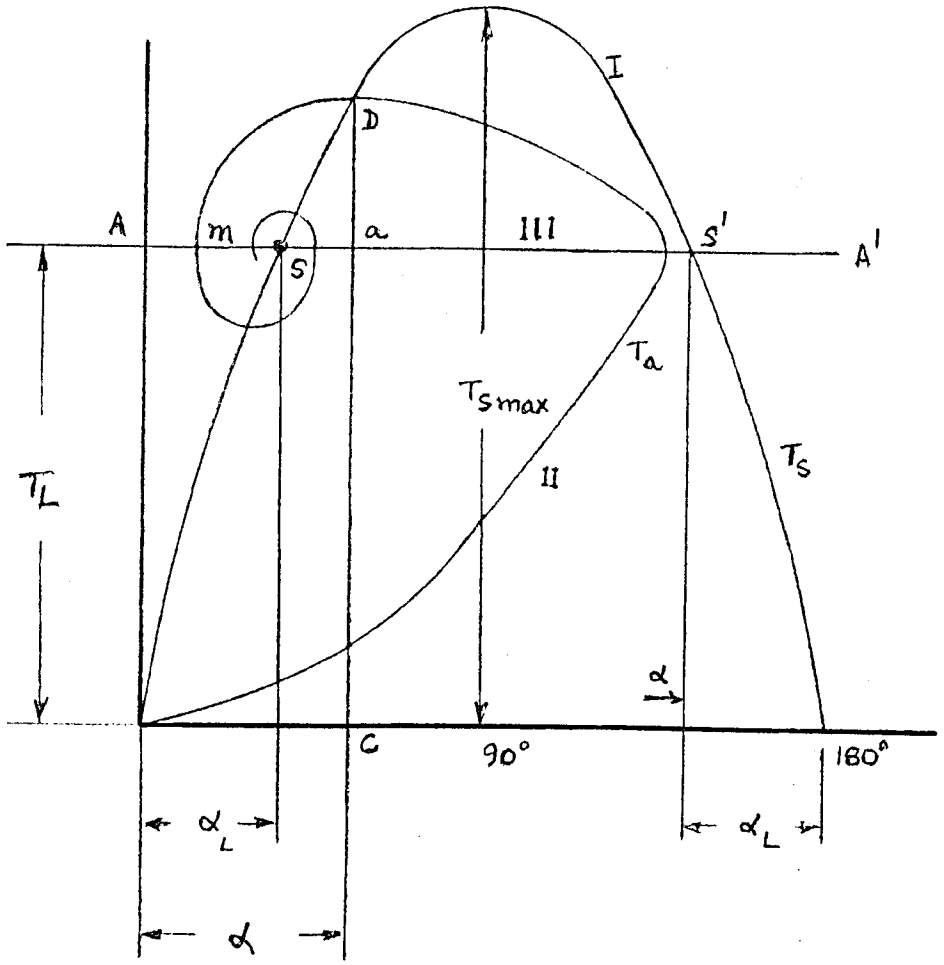

FIGURE 8.1 DIAGRAM SHOWING FOR PULL IN CRITERIA

Since for small values of slip, the torque speed characteristic is linear, the asynchronous torque at any slip S is given by $T_a = \frac{T_L}{S_L} S$, where T_L and S_L correspond to steady state asynchronous condition. If ω_r is mechanical angular velocity, then $\omega_r = (1-S)\ (\omega_s)/(P/2)$ 8.3

Let J be the moment of inertia of the rotating mass, then $T_M = \frac{J d\omega}{dt} = \frac{-J\omega_s}{(P/2)} \cdot \frac{ds}{dt}$ 8.4

Substituting (8.1) and (8.4) in (8.2), which describes the condition for pull in,

$$\frac{T_L}{T_L} S + T_{smax} \text{ Sin } 2\theta = T_L - J \frac{\omega_s}{(P/2)} \frac{ds}{dt} \quad \ldots\ldots\ldots 8.5$$

where θ is the angle at which rotor is lagging behind stator mmf in a fixed reference axis frame.

Also $S\omega_s = \frac{ds}{dt}$ 8.6

Substituting (8.6) in (8.5)

$$\frac{J}{(P/2)} \frac{d^2\theta}{dt^2} + \frac{T_L}{S_L \omega_s} \frac{d\alpha}{dt} + T_{smax} \text{ Sin } 2\theta = T_L \quad \ldots\ldots\ldots 8.7$$

The solution to this equation 8.7 will give the maximum value of load torque T_L for which the motor will pull in.

Now to establish the maximum speed or the value of S the motor has to reach for pull in, it is necessary to consider the work required to accelerate the mass from speed at slip $S = S_L$ to $S = 0$, which has to accomplish during rotor travel $\theta = \pi/2$ to $\theta = \theta_L$, which is final torque angle.

From equation (8.4) and (8.6) work done is

$$T_M \, d\alpha = \frac{-J \omega_s}{(P/2)} \frac{ds}{dt} \, S \, \omega_s \, dt$$

$$= \frac{-J \omega_s^2}{(P/2)} \, S \, ds \qquad \ldots\ldots\ldots 8.8$$

This expression when integrated from $S = S_L$ to $S = 0$, yields the total work done during this acceleration.

$$W = \frac{1}{2} J \cdot \left(\frac{\omega}{P/2} \right)^2 S_L^2 \qquad \ldots\ldots\ldots 8.9$$

This work is represented by area between curves I and II between limits $\alpha = 0$ and $\alpha_L = A_1$

Let $\frac{T_{smax}}{T_{rated}} = C;$

$$\frac{T_L}{T_{smax}} = K; \qquad \ldots\ldots\ldots 8.10$$

Where C = per unit pull out torque and K = per unit load applied, the area between curves I and II, between limits $\theta = 0$ and $\frac{\pi}{2} - \theta_L$

$$W_{acc} = T_{smax} \int_0^{\frac{\pi}{2}-\theta_L} \text{Sin } 2\theta \, d\theta - \frac{T_L}{3}\left(\frac{\pi}{2} - \theta_L\right)$$

$$= \frac{T_{smax}\,(1 + \text{Cos } 2\theta)}{2} - \frac{T_L}{3}\left(\frac{\pi}{2} - \theta_L\right) \qquad \ldots\ldots\ldots 8.11$$

Since $T_L = T_{smax} \text{ Sin } 2\theta_L$

$$\text{Sin } 2\theta_L = \frac{T_L}{T_{smax}} = K,$$

$$\text{Cos } 2\theta = \sqrt{1 - K^2}$$

$\ldots\ldots\ldots 8.12$

Introducing 8.12 in 8.11, we have

$$W_{acc} = \frac{T_{smax}\,(1 + \sqrt{1-K^2})}{2} - \frac{T_L}{3}\left(\frac{\pi}{2} - \frac{\text{Sin}^{-1}K}{2}\right)$$

i.e.

$$W_{acc} = T_L\left[\frac{1 + \sqrt{1-K^2}}{2K} - \frac{1}{3}\left(\frac{\pi}{2} - \frac{\text{Sin}^{-1}K}{2}\right)\right]$$

Let us designate

$$\left[\frac{1 + \sqrt{1-K^2}}{2K} - \frac{1}{3}\left(\frac{\pi}{2} - \frac{\text{Sin}^{-1}K}{2}\right)\right] = \psi$$

$\ldots\ldots\ldots 8.13$

Then the work done to accelerate from $S = S_L$ to $S = 0$,

i.e. $W_{acc} = T_L \psi$, ... 8.14

is given by area between curves I and II, from equation 8.9,

$$W = \frac{1}{2} J \frac{\omega_s^2}{\left(\frac{P}{2}\right)} S_L^2 \; ; \qquad \text{..... 8.15}$$

W_{acc} must be $\geqslant \omega$

i.e. $$T_L \psi \geqslant \frac{1}{2} J \frac{\omega_s^2 S_L^2}{\left(\frac{P}{2}\right)} \; ; \qquad \text{..... 8.16}$$

i.e. $$S_L \leqslant \omega_s \sqrt{\frac{T_L \psi P}{J}} \qquad \text{..... 8.17}$$

Since $\frac{T_L}{T_{smax}} = K$ and $\frac{T_{smax}}{T_{rated}} = C$;

$$T_L = K.C. T_{rated}$$

$$S_L \leqslant \omega_s \sqrt{\frac{KC \psi T_{rated}}{J}} \; ;$$

Where S_L = slip at steady state asynchronous condition at load T_L

ω_s = Synchronous speed rad/sec

J = Inertia in #ft. sec^2

T_{rated} = Rated torque #ft.

KC = Per unit load applied

The above is the criteria for pull in of the motor to synchronous speed.

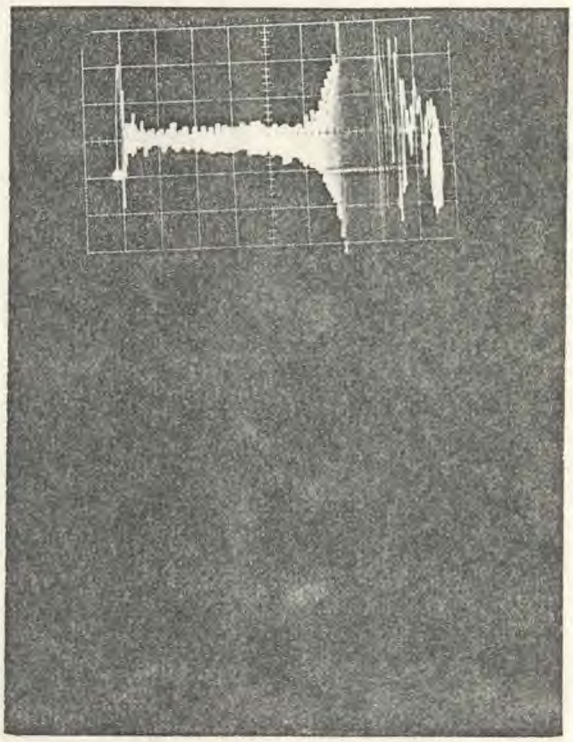

FIGURE 8.2 TYPICAL SPEED TORQUE CURVE DURING STARTING OF ANISOTROPIC MOTOR

CHAPTER 9

DESIGN PARAMETERS

The stator used for both the Anisotropic and the "Synduction" version is the same. The rotor configurations, however, are different.

The following deals with design parameters of reactances based on formulas by Mr. Kilgore and Mr. Alger.

Stator

D_o = Outside Diameter

D = Inside Diameter

L = Length of Core

g = Air Gap

No. of Slots

Skew - 1 Slot

Turns/Coil

Wire Size

Connection - 1-Y

Rating

The rating of machine can be either based on the pull out (the maximum) power developed or by the temperature rise of the machine at any load. Since the thermal rating of a machine is dependent on the cooling methods and capacity of fan attached, it is difficult to establish what can be called a standard rating. So the pull out power rating has

come to be recognized as a reliable standard. The full load rating is taken as 2/3 pull out rating.

The Synduction motor is rated for 25 hp. It is interesting to note from test results that the Anisotropic motor in the same stator size, develops a much better pull out power. The machine can easily be re-rated as 40 hp, exhibiting the superiority of the Anisotropic design. However, since it is intended to bring out comparison of two types, the same rating of 25 hp is taken as standard rating.

Rating: 25 Hp, 575V, 3 Phase, 60 Hz., 180 RPM

Stator Leakage Reactance

A sketch of stator slot is shown in Figure 9.1. The leakage reactance is given by the formula

$$x_{as} = \frac{2f\ell mN^2}{10^7 S_S}\left[K_s\left(\frac{d_1}{3w_1}+\frac{d_2}{2}\right)+\frac{.3(3P-1)DS_s}{P^2\ell}+\frac{.266DK_pK_d^2}{S_s\,\delta K}\right] \quad \ldots\ldots\ldots 9.1$$

Where f = frequency

ℓ = length of core

N = No. of conductors

S_S = No. of slots

K_s = Correction factor because of chording

δ = Air gap

K = Carter coefficient

D = Diameter

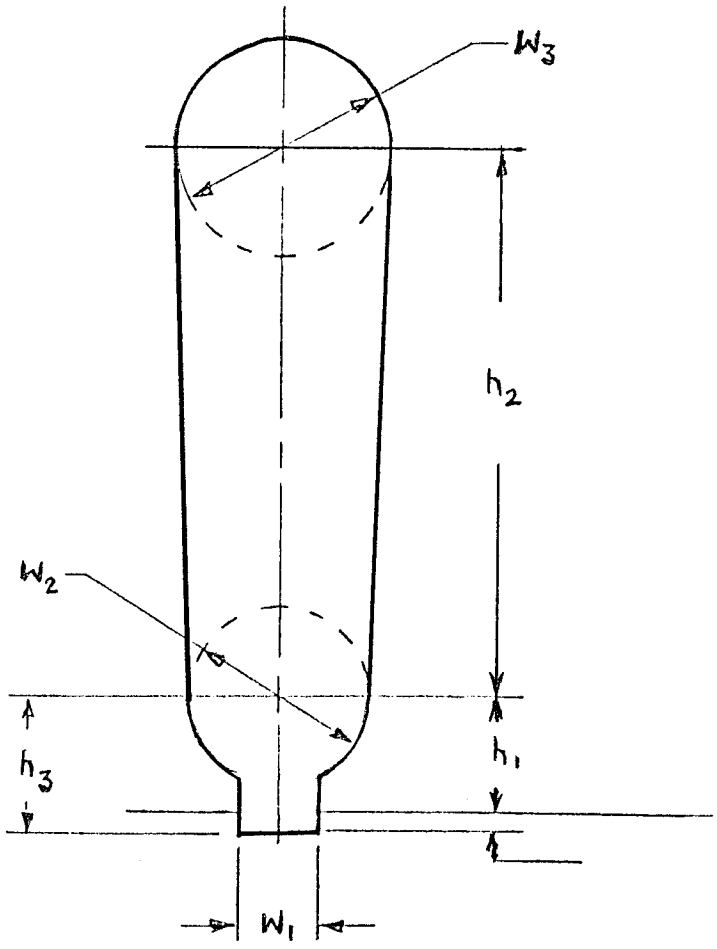

FIGURE 9.1 STATOR SLOT

K_p = Pitch Factor

K_d = Distribution factor

d_1, d_2, w_1, w_2 = Slot dimensions (See Figure 9.1)

P = No. of poles

Substituting actual values in equation 9.1 we obtain x_{as} = 0.35 ohms.

Rotor Slot Leakage Reactance

By a similar formula we can calculate the motor slot reactance also. Since the analysis pertains to synchronous operation only, where the rotor currents are zero, the reactance is neglected.

Zig Zag Leakage

The zig zag leakage reactance for stator is given by

$$x_{zs} = \frac{5}{6} X_m \left(\frac{P}{S_s}\right)^2 \qquad \ldots\ldots\ldots 9.2$$

Substituting dimensions, x_{zs} = 0.118 ohms.

For the rotor the zig zag reactance is assumed to be zero for synchronous operation.

Therefore, the standstill reactance of stator winding is given by adding equations 9.1 and 9.2.

i.e. total stator leakage reactance = 0.468 ohms

x_{al} = 0.468 ohms

Magnetizing Reactance

The magnetizing reactance of the two motors, viz the Synduction and the Anisotropic in the d and q axis are different, in view of the difference in permeability.

However, for the sake of obtaining performances of comparable values, the pole span to pole pitch ratios were kept the same in the two machines.

As far as the Anisotropic rotor is concerned, the exact calculation of the saliency factor involves using permeance matrix and ladder network of permeances along the d-axis of grain orientation and reluctances in the q-axis across the stack and orientation. By going into Fourier analysis and use of computers a more approximate solution can be obtained.

However, since an estimate of the order of reactance with a view to compare the two machines is aimed at in this Chapter, the following approach is resorted to. Accurate values are obtained from test in Chapter 10.

First the cylindrical magnetizing reactance is calculated. Account for saliency is made in the two cases later on.

Cylindrical Magnetizing Reactance

For a smooth rotor with uniform air gap, the magnetizing reactance is given by

$$X_m = \frac{6.38\ f l m N^2 K_p^2 K_d^2}{P^2\ \delta\ K\ 10^8} \qquad \ldots\ldots\ldots\ 9.3$$

Where all the symbols are already explained before, i.e. $x_m = 31.9$ ohms.

Direct and Quadrature Axis Reactance

The fundamental wave of stator mmf can be split up into a Sine and Cosine function each associated with the q-axis and d-axis respectively.

The axes reactances can be expressed as

$$x_{ad} = C_d x_m$$

and $$x_{aq} = C_q x_m$$

Where C_d and C_q are the reduction factors as defined below, and x_m is the magnetizing reactance for cylindrical rotor uniform gap.

A conventional salient pole machine,

$$C_d = \frac{\varphi\pi + \text{Sin}}{4\ \text{Sin}\ \varphi\pi/2} \quad \text{where } \varphi = \frac{\text{Pole arc}}{\text{Pole Pitch}} = 0.5$$

$$C_d = 0.925 \qquad \ldots\ldots\ldots\ 9.4$$

For quadrature axis

$$C_q = \frac{\varphi\pi - \text{Sin}\ \varphi\pi + \frac{1}{2}\ \text{Cos}\ \frac{\varphi\pi}{2}}{4\ \text{Sin}\ (\varphi\pi)/2}$$

$$C_q = 0.291 \qquad \ldots\ldots\ldots\ 9.5$$

The preceding value of C_q is for a conventional pole machine with a pole arc to pole ratio of 0.5.

However for a reluctance machine with two barriers, the parameter

$$C_q = 1 - \frac{\cos \pi \rho}{2} - (\rho - \rho_b) f_b + \alpha \quad \ldots\ldots\ldots 9.6$$

where $$= \frac{g}{g+h_c} \left[\cos \frac{\pi \rho}{2} - f_b (1 - \rho) \right] \quad \ldots\ldots\ldots 9.7$$

$$f_b = \frac{\cos \frac{\pi \rho_b}{2} - \cos \frac{\pi \rho}{2} + C_1}{\beta + \rho - \rho_b + C_2}; \quad \ldots\ldots\ldots 9.8$$

$$\beta = \frac{2Pg}{D} \left[\frac{2h_1}{rw_1} + \frac{h_2}{w_2} \right]; \quad \ldots\ldots\ldots 9.9$$

$$C_1 = \frac{(1 - 2h_c)}{D} \cdot \frac{g}{g+h_c} \cos \frac{\pi \rho}{2}; \quad \ldots\ldots\ldots 9.10$$

$$C_2 = \frac{(1 - 2h_c)}{D} \frac{g}{g+h_c} (1 - \rho); \quad \ldots\ldots\ldots 9.11$$

Substituting the physical parameters into the above equations, the following values are obtained:

$f_b = 0.6$

$C_1 = -0.0172$

$C_2 = -.0122$

$\beta = 0.0635$

$\alpha = 0.01$

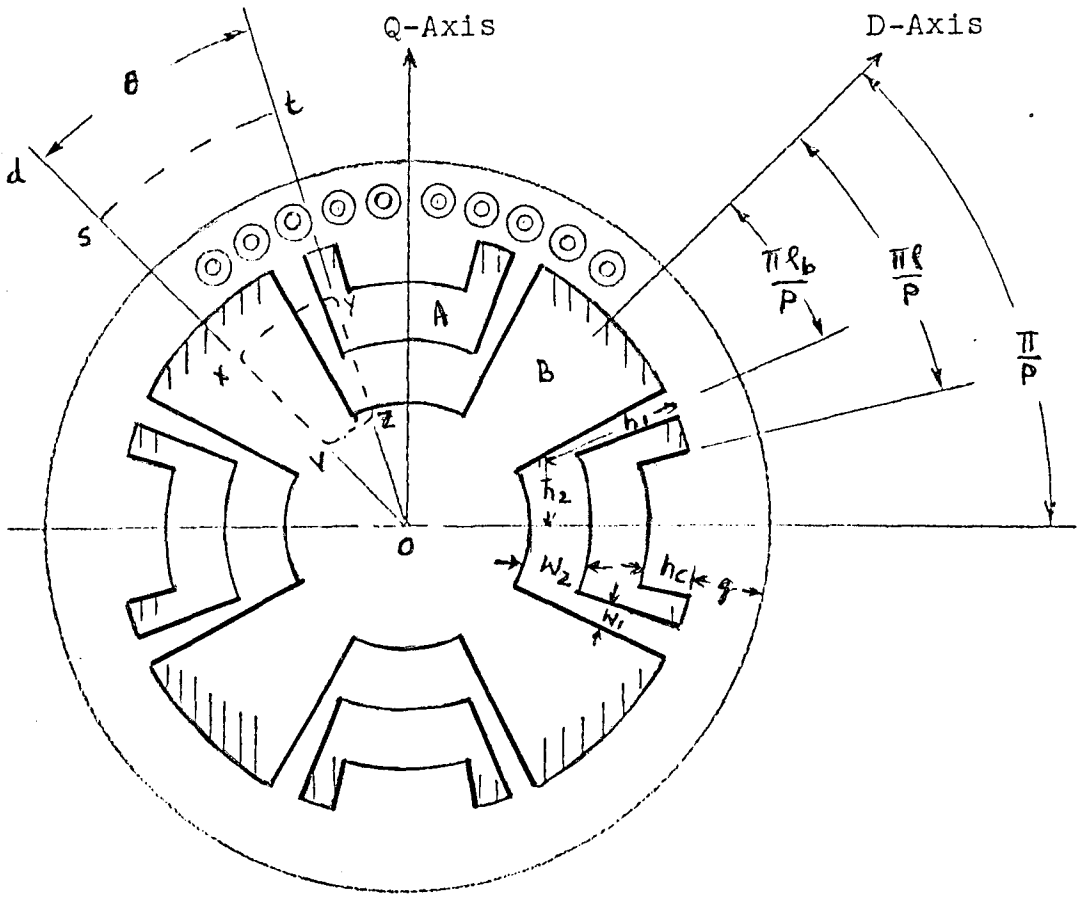

FIGURE 9.2 CROSS SECTIONAL REPRESENTATION OF ROTOR

Substituting these in equation 9.6

$$C_q = 0.183 \qquad \ldots\ldots\ldots 9.12$$

As can be seen, the value of C_q obtained above is considerably less than for a conventional machine of same pole arc to pole pitch ratio given by equation 9.5. This results in higher ratio of x_d to x_q resulting in greater torque than normal reluctance machines.

The unsaturated reactances for the two barrier pole construction of Synduction motor are given as:

$$x_{ad} = C_d x_m = .925\ (31.9)$$
$$= 29.5 \text{ ohms} \qquad \ldots\ldots\ldots 9.13$$

$$x_{aq} = .183\ (31.9)$$
$$= 5.95 \text{ ohms} \qquad \ldots\ldots\ldots 9.14$$

To this should be added the leakage reactance 0.468 ohms derived earlier.

$$x_d = 29.5 + .468 = 30.018 \text{ ohms}$$
$$= 30 \text{ ohms} \qquad \ldots\ldots\ldots 9.15$$

$$x_q = 5.95 + .468 = 6.418$$
$$= 6.42 \text{ ohms} \qquad \ldots\ldots\ldots 9.16$$

It should be noted at this point that the values derived above are unsaturated values. The value of x_d goes down as the stator current is increased and the value of x_q

remains substantially the same, as the quadrature axis flux density is far below saturation. This can be observed from the test results in Chapter 10.

Anisotropic Rotor

In the case of Anisotropic rotor, the two barriers of Synduction motor are replaced by many barriers caused by the interlaminar insulation. Also the permeability of the material for quadrature axis flux is very low resulting in an effective air gap. The most accurate way of dealing with the situation happens to be, as pointed out earlier, by adopting solution for a ladder network consisting of permeances along the grain (d-axis) and reluctances across. This computation involves use of computers and still results are only as accurate as the present state of art of understanding saturation permits. However, an attempt here is made in the following to obtain a more ready solution with limitations as stated before. Verification of these with the test results bears out the validity of method used.

Direct Axis

As far as the direct axis is concerned, the equations derived earlier for Synduction motor still hold good. Since the flux pattern or magnitude is unaffected, by equation 9.15

$$x_d = 30 \text{ ohms}$$

Quadrature Axis Reactance

Instead of one barrier, the number of barriers each constituting the thickness of the interlaminar insulation, is equal to the number of laminations in the Stack.

Pole width = Depth of Stack

Let thickness of each lamination = w_1

No. of laminations = r

Stacking factor = 0.95

The interlaminar insulation = w_1 (.05) = w

Going back to equation 9.9 where

r = No. of barriers

w_1 = Width of barriers,

we can substitute for r and w_1. Another term, $\frac{h_3}{w_3}$, has to be added since there are again barriers the same as above along the radius. In fact h_1 and h_3 constitute the lengths of path radial and circumferential. In fact, the two terms can be added together if we take a value of h_1 = mean length of the iron from pole center to pole center and w_1 = interlaminar insulation.

However, one more term in equation 9.9 has to be added to represent the gap that exists in the center of the pole. The factor is $\frac{h_4}{w_4}$, therefore, the final form of modified equation 9.9 is

$$= \frac{2\ Pg}{D} \left[\frac{h_1}{rw_1} + \frac{h_2}{w_2} + \frac{h_4}{w_4}\right]$$

$$= .00337 \quad (20.1 + 1.6 + 10.7)$$

$$= 0.109$$

All the other factors remain the same as in equations 9.10 and 9.11, since values of g, h_c and all others remain as before for the Synduction motor. For calculation of f_b, an equivalent barrier is assumed at the center of Stack.

Therefore from equation 9.8,

$$f_b = \frac{\text{Cos } \frac{\pi}{2} (.334) - \text{Cos } \frac{\pi}{2} (0.0172)}{0.109 + .5 - .335 + .0122}$$

$$= \frac{.862 - .707 - .0172}{0.2872}$$

$$= \frac{.1722}{.2872} = 0.5995$$

From equation 9.7,

$$= \frac{0.025}{1.025} \left[.707 - .5995\ (1 - .5)\right]$$

$$= .0099328$$

From equation 9.6,

$$= 1 - 0.707 - (.5)\ (.334) = .00904$$

$C_q = 0.116$

$x_{aq} = .116\ (31.5) = 3.654$

To this should be added the leakage reactance

$x_q = 3.654 + .468$

$= 4.122$ ohms

This value of x_q is lower than in case of Synduction motor.

However the actual value of x_q in this case will be lower even because of the fact that permeability in the q-axis of the laminations, i.e. across the grain orientation, is much higher than d-axis.

From the preceding the reactances of the two types of reluctance machines are calculated.

Resistance (r_a). Stator resistance calculation is quite simple since the mean length and wire size and number of terms are known.

It works out to be 0.25 ohms per phase.

Torque calculations. Knowing the value of x_d, x_q, r_a torque produced for any given voltage and torque angle can be calculated from the formula

$$T_e = \frac{m V^2}{2} \left(\frac{x_d}{x_q} - 1 \right) \text{Sin } 2\theta$$

CHAPTER 10

TEST AND COMPARISON OF RESULTS

The tests conducted on the two experimental designs viz Synduction and Anisotropic consist of the no load and load tests at various voltages. The direct and quadrature axes reactances are computed both from the no load and load tests for different levels of saturation as well as by the well known "Slip" test method at low levels of saturation.

For different load conditions, the power factors, currents and efficiencies at different voltage levels are compared for the two types of rotor construction.

A test was done under transient conditions of starting and running up to synchronous speed. With the help of oscillograph recording of the speed through a tach generator attached to motor shaft, speed time characteristic was drawn. Since torque is proportional to derivative of speed, a test circuit was designed to get a signal proportional to derivative speed. An X-Y plotter was used to plot this signal which is proportional to torque against speed input signal. Calculations for calibrating the chart for torque in ft.lbs. and speed in rpm are included.

The test rig consists of a motor being coupled to a single phase a.c. generator, which is connected to a load bank. A separate excitation was provided by a variable

d.c. power supply. A large flywheel (10 x normal WK^2) was attached to the shaft.

Measurements of output power of generator, input power into motor and input voltage and current were done using recently calibrated laboratory type of instruments.

Measurements of torque angle were done by attaching a calibrated marker strip on the rim of the flywheel connected and looking at it by a stroboflash synchronized with the input line frequency.

No Load Test

Synduction. Table 10.1 shows the readings taken with no load on the generator for Synduction motor. The only losses being supplied to the motor were friction, windage, and core and hysterisis losses. Knowing input KVA and the watts, the magnetizing current was derived and a curve of the terminal volts against magnetizing current is drawn in Figure 10.1.

Anisotropic. Table 10.2 lists the readings taken for reluctance motor. Note that identical stators were used in the Synduction and Anisotropic versions. Calculations of magnetizing current were made like in the Synduction motor test. The no load saturation curve is plotted as shown in Figure 10.2.

TABLE 10.1

NO LOAD TEST

Input Volts (V)	Input Amps (I)	Input Watts (W)	Power Factor (Cos Ø)	I Sin Ø Amps (I_m)
400	8.5	1250	0.212	8.31
450	9.7	1250	0.165	9.57
500	10.7	1250	0.134	10.64
550	12.8	1250	0.102	12.76
575	14.4	1500	0.104	14.32
600	16.3	1500	0.088	15.8
650	21.6	1750	0.072	21.52
700	29.3	2000	0.059	29.25
730	35.6	2500	0.055	35.90

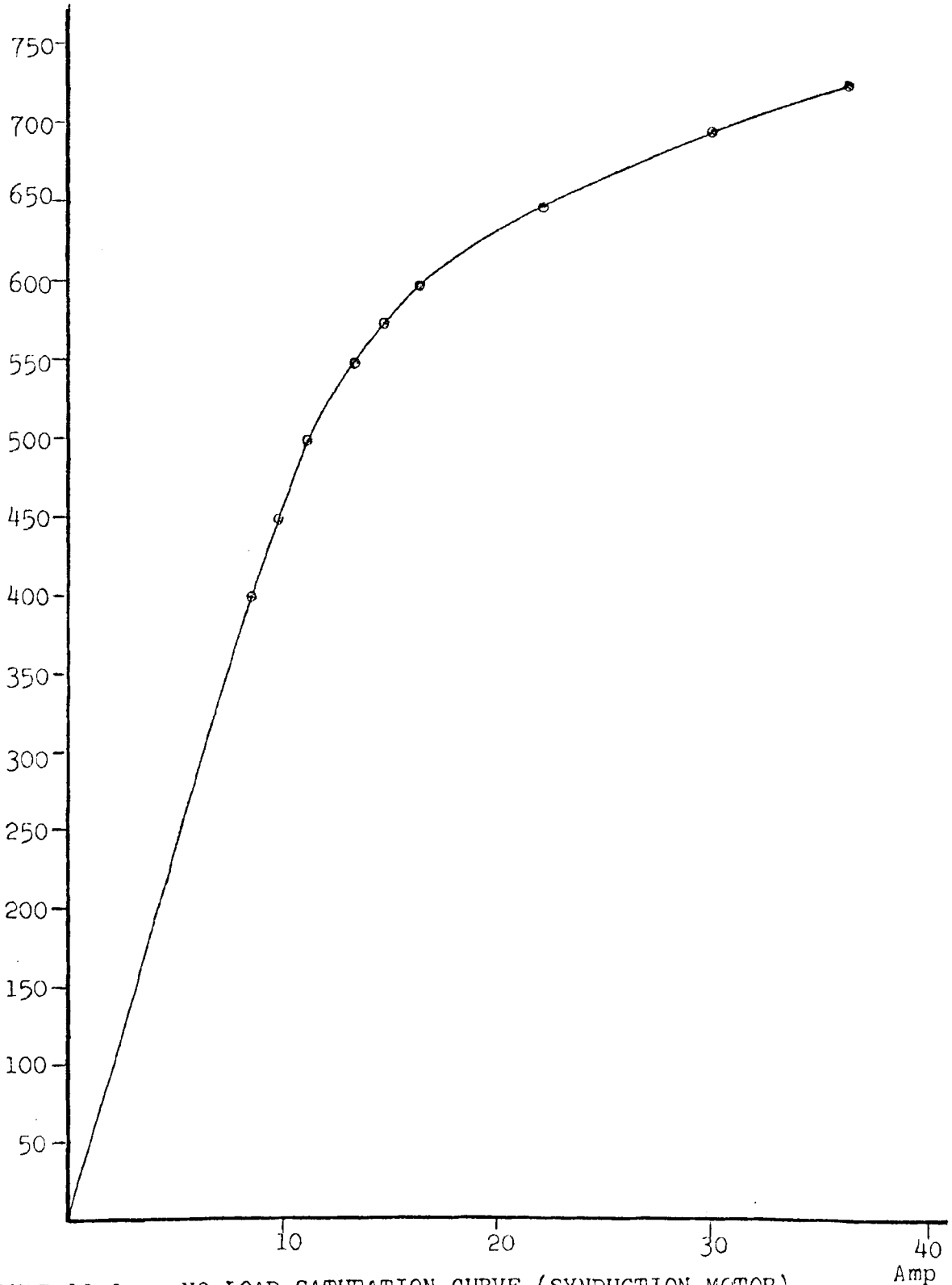

FIGURE 10.1 NO LOAD SATURATION CURVE (SYNDUCTION MOTOR)

TABLE 10.2

NO LOAD TEST

Input Volts (V)	Input Amps (I)	Input Watts (W)	Power Factor (Cos Ø)	I Sin Ø Amps (I_m)
400	9.96	1600	0.232	9.68
450	11.76	1900	0.207	11.50
500	13.40	2000	0.172	13.23
550	15.90	2500	0.165	15.68
575	17.4	2500	0.145	17.2
600	19.5	2500	0.123	19.3
650	24.23	3250	0.119	24.1
700	31.23	3900	0.103	31.1
740	34	5000	0.114	33.79

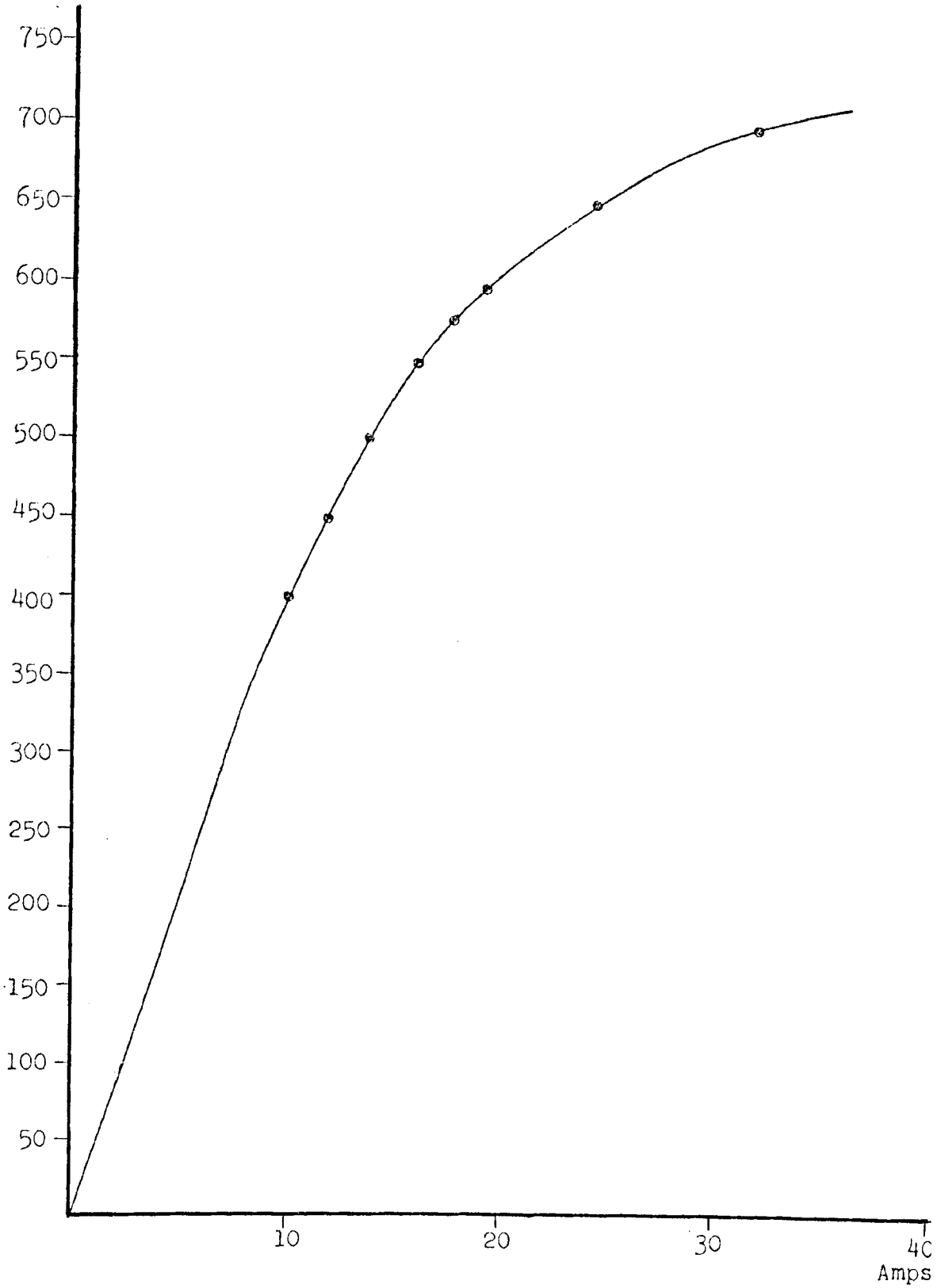

FIGURE 10.2 NO LOAD SATURATION CURVE (ANISOTROPIC MOTOR)

Load Tests

Synduction. Input voltage to motor was varied from 400 to 700 volts and at each voltage level the loads applied to the generator were 7.5 KW, 15 KW, and 22.5 KW. The mechanical output torque was based on the average of watts input to the motor and watts output of the generator, on the assumption of the efficiencies of motor and the generator being the same, which is true for this particular test set.

Torque in ft.lbs. is calculated from

$$T = \frac{\text{Watts} \times 7.04}{N_S}; \text{ where} \qquad \ldots\ldots\ldots 10.1$$

N_S = synchronous speed = 1800 RPM

Table 10.3 lists the readings taken. Table 10.4 is constructed using the calculated torque, average input current, and the calculated input power factor.

Figure 10.3 describes the current-torque relationship for different voltages. Figure 10.5 describes the torque power factor relationship at various input voltages.

TABLE 10.3

LOAD TEST DATA

Input Volts (V)	Input Amps (I)	Input Watts (W)	Output Watts (W)	Remarks
480	10.5	1250	0	
480	21.5	9750	7500	
480	38	16500	12500	Pull out
575	14.4	1500	0	
575	21.5	9750	7500	
575	33	18250	15000	
700	29.3	2000	0	
700	33	10750	7500	
700	38.5	19000	15000	

TABLE 10.4

LOAD TEST CALCULATIONS

Input Volts (V)	Input Amps (I)	Torque Developed (Ft.lbs.)	Power Factor (Cos Ø)
480	10.5	2.44	.1431962
480	21.5	33.73	.5454777
480	38	56.71	.5222894
575	14.4	2.933	.1045955
575	21.5	33.73	.4553533
575	33	65.022	.5553379
700	29.3	3.9111	.056301
700	33	35.788	.2686882
700	38.5	66.4887	.4070492

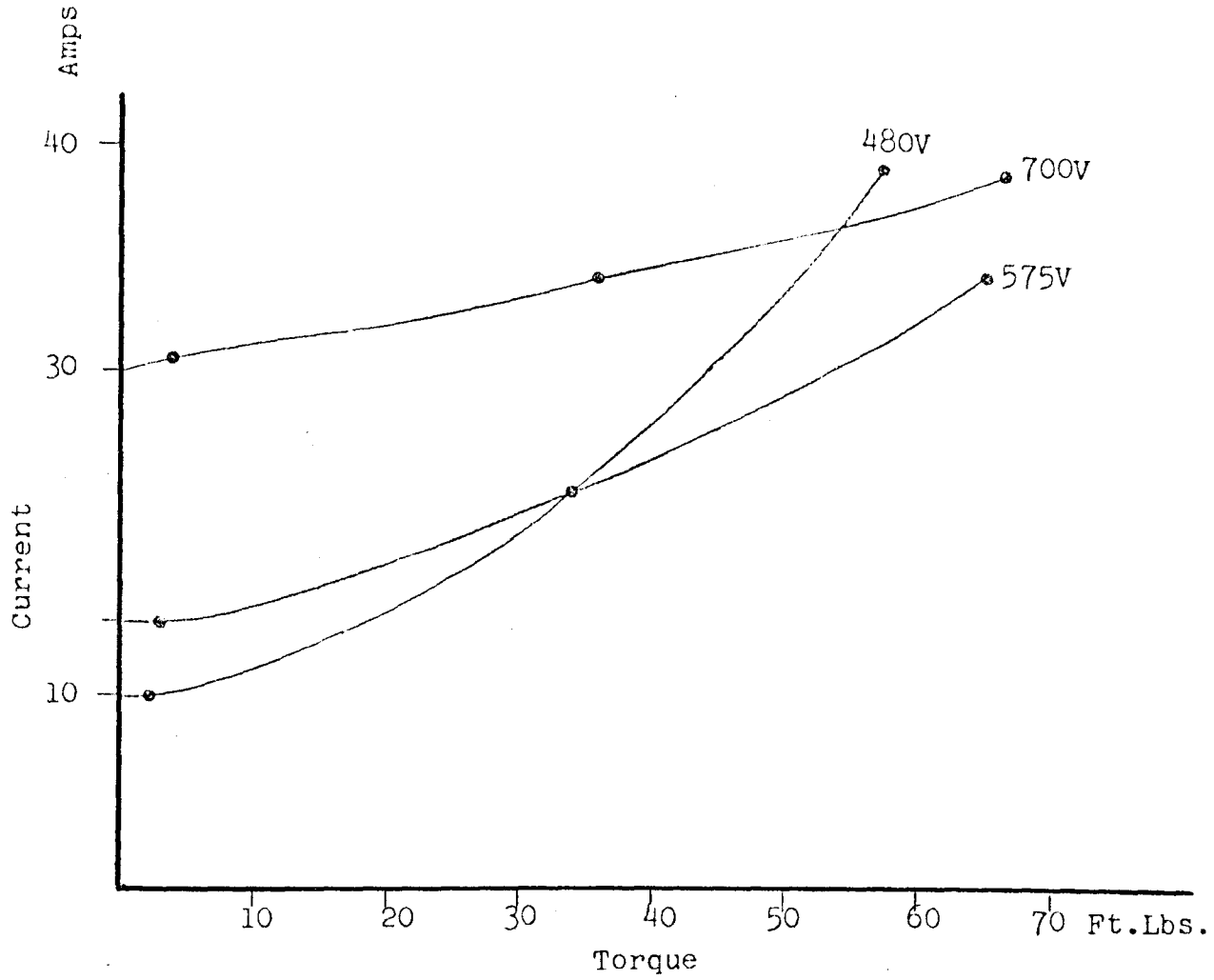

FIGURE 10.3 CURRENT-TORQUE CURVE (SYNDUCTION)

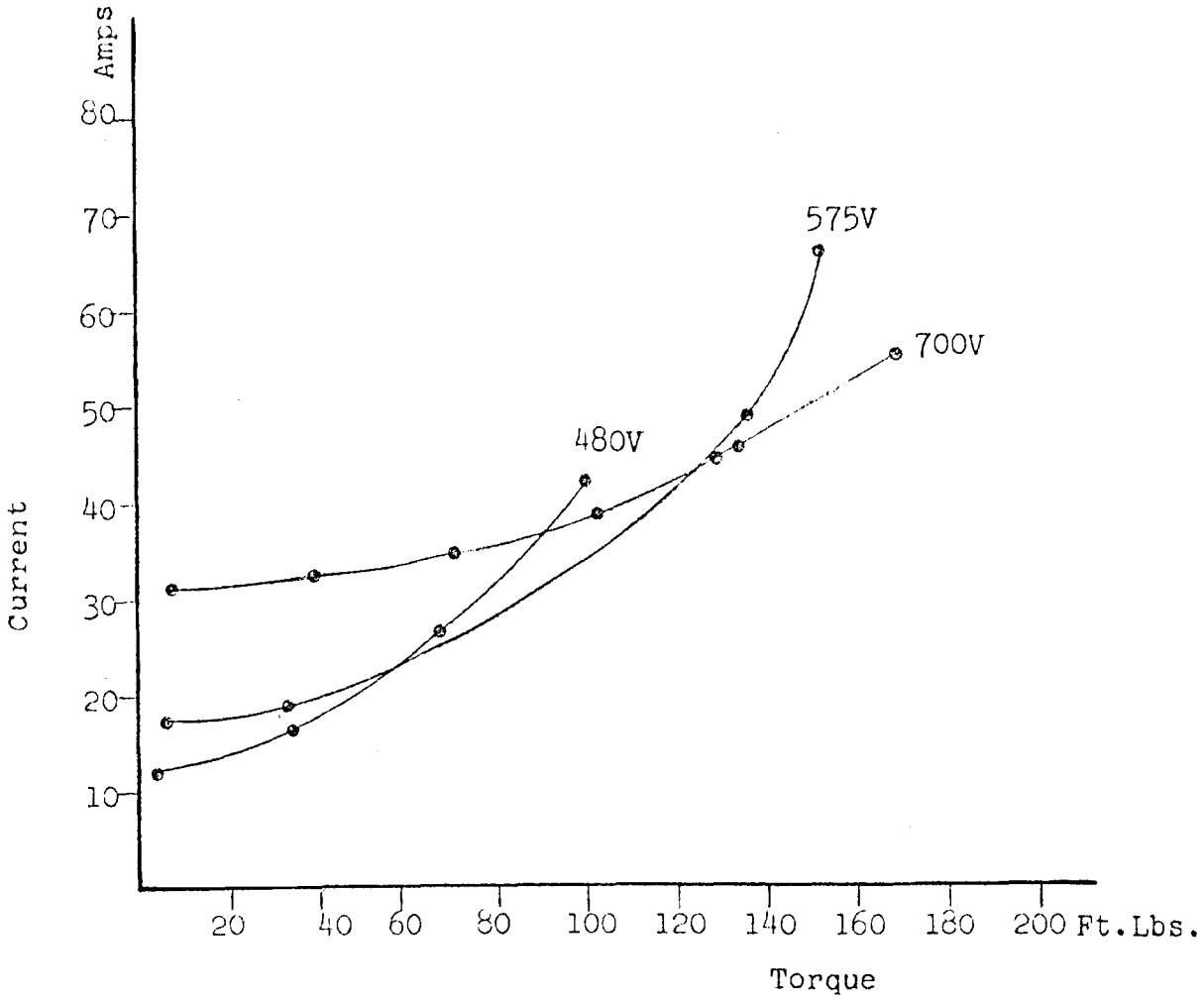

FIGURE 10.4 CURRENT-TORQUE CURVE (ANISOTROPIC)

Anisotropic. On a basis similar to the preceding, readings of the input power and current were taken for input various voltages and output power. Note that a greater load condition could be obtained in the case of Anisotropic compared to the preceding, in view of the fact that the motor could develop substantially larger pull out torques than Synduction motor for same input voltages.

Table 10.5 lists the readings taken and Table 10.6 lists the torque, current and power factor calculations derived from the above.

Figure 10.4 describes current-torque relationships and Figure 10.6 describes the torque power factor relationships for different input voltages.

TABLE 10.5

LOAD TEST DATA

Input Volts (V)	Input Amps (I)	Input Watts (W)	Output Watts (W)	Remarks
450	11.76	1900	0	
450	17.4	10000	7500	
450	30	18500	15000	
450	49	29000	22500	Pull out at 23 KW
480	12.5	1950	0	
480	17.0	10000	7500	
475	29	19000	15000	
475	42.4	28000	22500	Pull out at 27.5 KW
500	13.4	2000	0	
500	17	10000	7500	
500	27	19500	15000	
500	41	28000	22500	
500	64	40000	29500	Pull out at 30 KW
575	17.4	2500	0	
575	19.0	10500	7500	
575	26.0	19000	15000	
575	36.0	28000	22500	
575	49	39500	30000	
575	66	43500	35000	Pull out at 37.5 KW

Table 10.5 continued

Load Test Data

Input Volts (V)	Input Amps (I)	Input Watts (W)	Output Watts (W)	Remarks
650	24.2	3250	0	
650	25.0	11500	7500	
650	28.4	19500	15000	
650	36	29000	22500	
650	43.4	37000	30000	
650	56	48000	37500	
700	31.25	3900	0	
700	33	12500	7500	
700	35	20500	15000	
700	39	29500	22500	
700	46	38500	30000	
700	55	49000	37500	

TABLE 10.6

LOAD TEST CALCULATIONS

Input Volts (V)	Input Amps (I)	Torque Developed (Ft.lbs.)	Power Factor (Cos Ø)
450	11.76	3.715	.207
450	17.4	34.22	.737
450	30	65.51	.791
450	24.5	100.71	.759
480	12.5	3.813	.187
480	17	34.22	.707
475	29	65.51	.796
475	42.4	98.75	.8026
500	13.4	3.91	.172
500	17	34.22	.679
500	27	67.46	.834
500	41	98.75	.788
500	64	136.04	.7217
575	17.4	4.88	.144
575	19	35.2	.531
575	26	66.48	.733
575	36	98.75	.781
575	49	135.9	.809
575	66	153.51	.666

Table 10.6 continued

Load Test Calculations

Input Volts (V)	Input Amps (I)	Torque Developed (Ft.lbs.)	Power Factor (Cos Ø)
650	24.2	6.35	.119
650	25	37.15	.408
650	28.4	67.46	.6101
650	36	100.71	.7155
650	43.4	131.02	.757
650	56	167.19	.761
700	31.25	7.626	.103
700	33	39.111	.3125
700	35	69.42	.4831
700	39	101.688	.6238
700	46	133.955	.694
700	55	169.155	.735

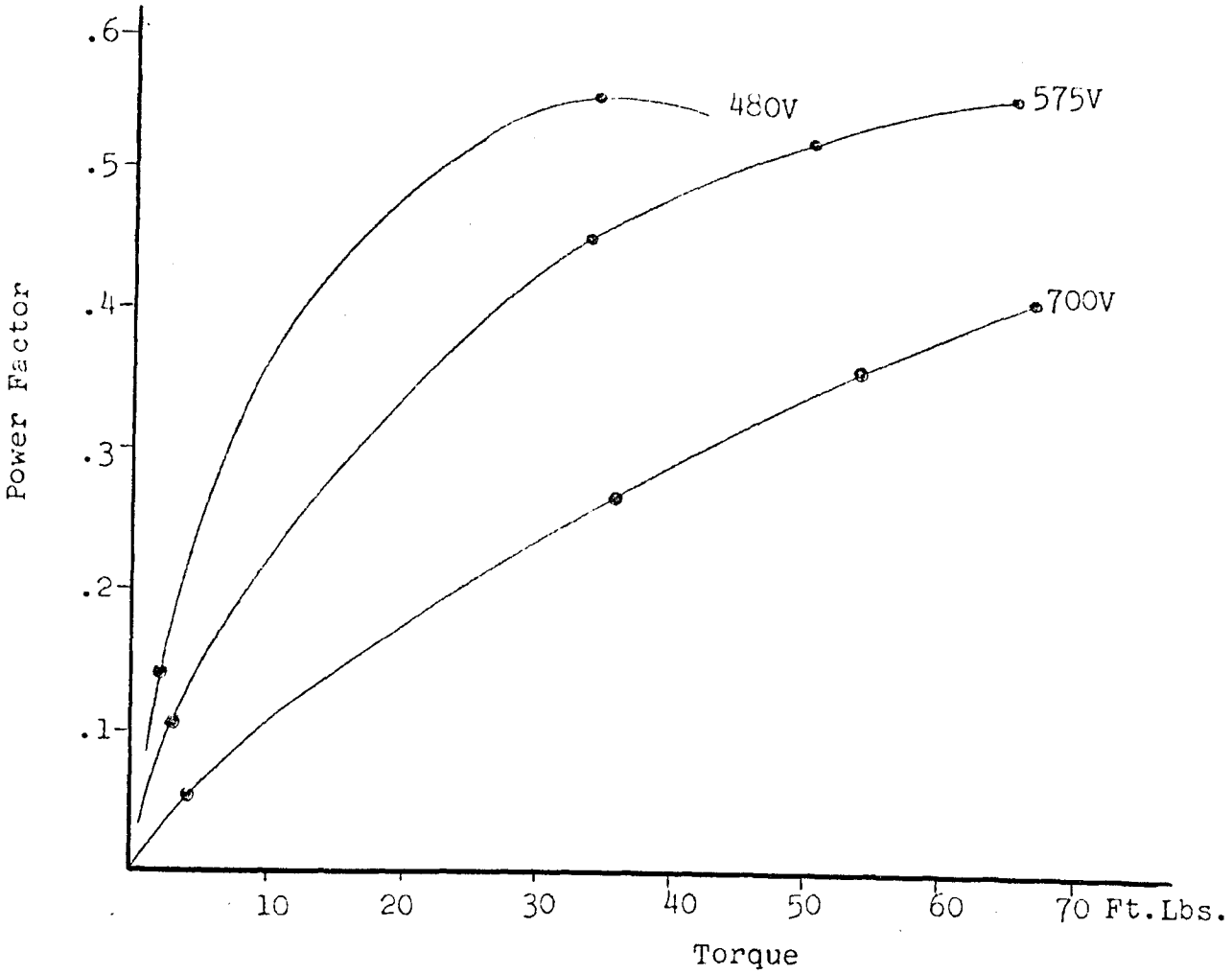

FIGURE 10.5 POWER FACTOR-TORQUE CURVE (SYNDUCTION)

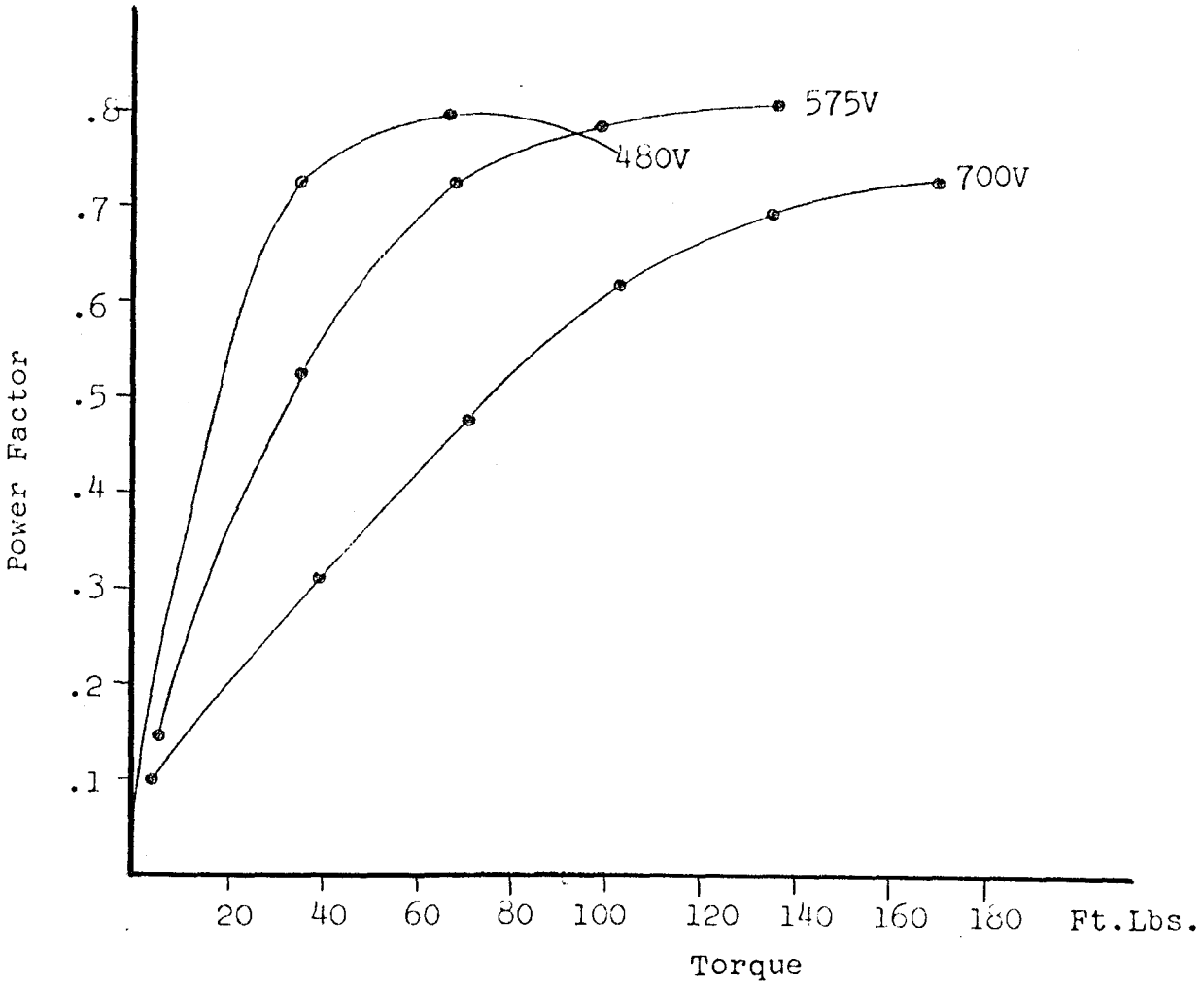

FIGURE 10.6 POWER FACTOR-TORQUE CURVE (ANISOTROPIC)

Reactance By Slip Test

It is usual practice in the case of synchronous machines to refer to the direct axis and quadrature axis reactances by their unsaturated values. One of the methods to obtain the same by test, as recommended by Mr. Liwschitz, is the "slip" method.

This method is basically intended for the synchronous motor. With appropriate modification the method was used here for the Anisotropic motor as follows: The motor was connected to a 480V power supply through a double throw switch and run at no load at synchronous speed. When steady state is reached, the switch is suddenly opened allowing the motor to slip by a few rpm's. The switch was immediately closed on to the other side connecting the motor to a low voltage (about 20-25% of nominal) source of the same phase sequence. An oscillograph of the voltage and current were taken.

As the slip is only a few rpm's, the rotor pole slips past the constant frequency stator mmf. Since the stator mmf has to link with the rotor inductances, which exhibits variation from direct axis to quadrature axis, the input current modulates at the slip frequency.

Figure 10.7 shows the oscillogram display.

The current will be minimum when the reluctance is minimum, i.e. when the d-axis lines up with the stator mmf and it is maximum as the q-axis lines up with the rotating mmf. The voltage wave also exhibits a certain modulation in view of the different values of induced voltage.

The d-axis and q-axis reactances are given by the ratio of voltage to current at the respective positions as shown in the oscillogram.

Calculation of x_d and x_q. From "Slip Test":

From the oscillogram,

$$V_{max} = \frac{115}{19.7}(17) = 99.238$$

$$V_{min} = \frac{115}{19.7}(17) = 99.238$$

$$I_{max} = \frac{11}{19}(28) = 16.21$$

$$I_{min} = \frac{11}{19}(7.5) = 4.34$$

Unsaturated value of,

$$x_d = \frac{V_{max}}{I_{min}} = \frac{99.238}{4.34} = 22.87 \text{ ohms}$$

Unsaturated value of,

$$x_q = \frac{V_{min}}{I_{max}} = \frac{99.238}{16.21} = 6.122 \text{ ohms}$$

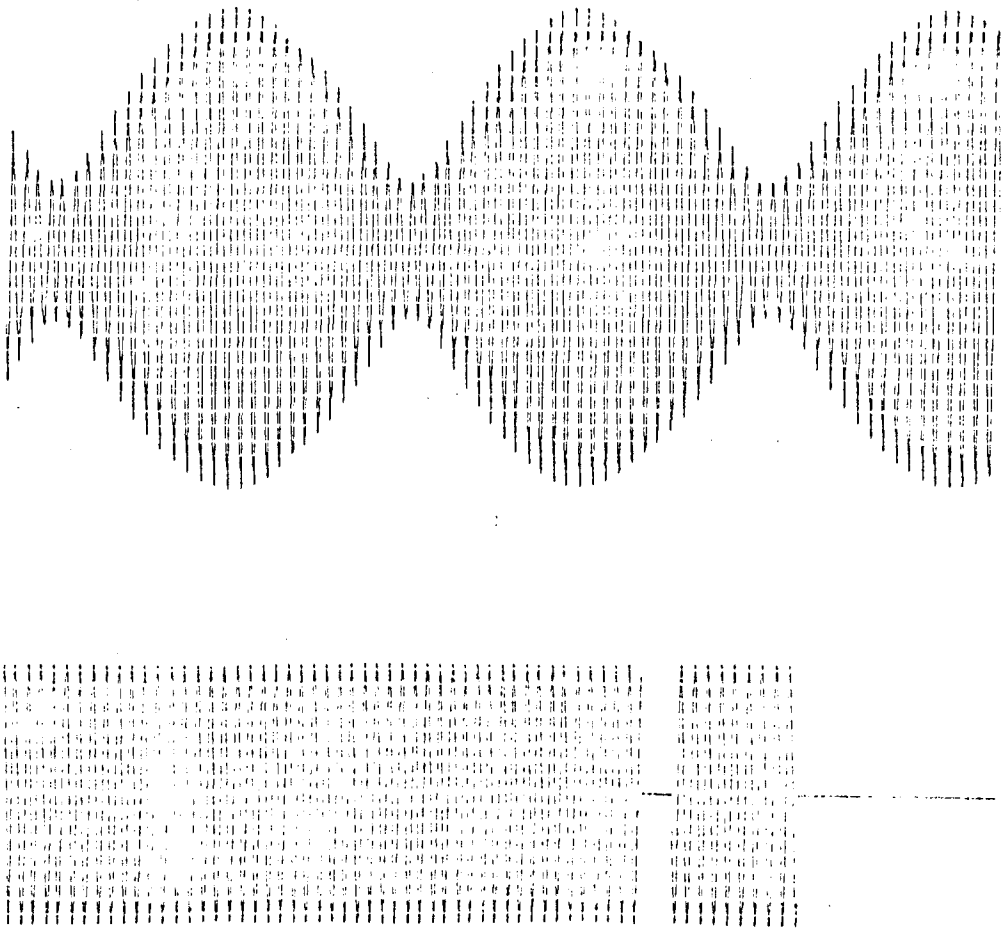

FIGURE 10.7 OSCILLOGRAM OF SLIP TEST (ANISOTROPIC)

These are reactances obtained for the particular values of current. It is interesting to compare results obtained by this method to the results obtained by computing from load tests for various degrees of saturation.

Reactance By No Load and Load Tests

Direct axis. The method described in the above section gives the unsaturated values only, which are of lesser significance in practical applications where load performances are to be predicted.

The following method is often used to determine the x_d and x_q at various levels, thereby accounting for saturation also.

At no load the torque angle is very small and is often neglected for calculation of x_d. However, accounting for the rotational and eddy current and hysterisis losses, the magnetizing current is already calculated in Table 10.1 and 10.2.

$$\text{At no load } I_d = I_{mag} = \frac{V}{\sqrt{X_d^2 + r_a^2}};$$

$$x_d = \sqrt{\left(\frac{V}{I_d}\right)^2 - r_a^2} \qquad \ldots\ldots\ldots \text{ 10.2}$$

Using the preceding formula, Table 10.7 is prepared calculating x_d at various levels of saturation. Figure 10.8 and 10.9 shows the variation of x_d with current.

Quadrature axis. An attempt is made below to exactly calculate the value of x_q. In Chapter 5 the machine admittance components were shown in equation 5.25 and 5.26 as:

$$G = \frac{2r_a + (x_d - x_q) \text{ Sin } 2\theta}{2 (x_d x_q + r_a^2)}; \qquad \ldots\ldots\ldots 10.3$$

$$B = \frac{(x_d + x_q) - (x_d - x_q) \text{ Cos } 2\theta}{2 (x_d x_q + r_a^2)}; \qquad \ldots\ldots\ldots 10.4$$

These can be expressed as

$$G = \frac{r_a + \alpha \text{ Sin } 2\theta}{D}$$

$$B = \frac{\beta - \alpha \text{ Cos } 2\theta}{D}$$

where $\alpha = \frac{x_d - x_q}{2}$; $\beta = \frac{x_d + x_q}{2}$; $D = x_d x_q + r_a^2$; $\qquad \ldots\ldots\ldots 10.5$

i.e. $GD - r_a = \alpha \text{ Sin } 2\theta \qquad \ldots\ldots\ldots 10.6$

$$BD - \beta = - \alpha \text{ Cos } 2\theta \qquad \ldots\ldots\ldots 10.7$$

Squaring and adding the preceding

$$(G^2 + B^2)\, D^2 - 2(Gr_a^2 + B\beta)\, D + \beta^2 + r_a^2 - \alpha^2 = 0 \qquad \ldots\ldots\ldots 10.8$$

But $G^2 + B^2 = Y^2$; where Y = machine admittance,

$\beta^2 - \alpha^2 + r_a^2 = D$; from equation 10.8,

therefore, $Y^2D^2 - 2(Gr_a + B\beta)\, D + D = 0$

or $Y^2D - 2(Gr_a + B\beta) + 1 = 0;$ $\ldots\ldots\ldots 10.9$

Using resistances, reactances, and impedances in place of their reciprocals,

$$Y = \frac{1}{Z};\ G = \frac{R}{Z^2};\ B = \frac{X}{Z^2};$$

Substituting for the above as well as for β and D in equation 10.9, we have

$$x_d x_q + r_a^2 - 2Rr_a - X\,(x_d + x_q) + R^2 + X^2 = 0.$$

or $(x_d - X)\, x_q + (R - r_a)^2 - X\,(x_d - X) = 0.$

Therefore, $x_q = X - \dfrac{(R - r_a)^2}{(x_d - X)}$ $\ldots\ldots\ldots 10.10$

Here $Z = \dfrac{V}{I},$ $\ldots\ldots\ldots 10.11$

$R = Z \cos \phi,$ $\ldots\ldots\ldots 10.12$

$$X = Z \sin \phi \qquad \ldots\ldots\ldots 10.13$$

Knowing the input voltage, current, power factor, and the stator resistance r_a as well as the value of x_d as previously calculated in the preceding section, the values of x_q can be calculated over the entire range of current. Although it is true that x_q is constant over the entire range since the saturation does not affect q-axis as much as the d-axis, however, it is preferable to use the values for V and I, near the pull out conditions, as these are found to yield more reliable values.

Correction for iron and rotational losses. While the iron and frictional losses have negligable affect on the value of x_d, these will appreciably affect the value of x_q. If these are to be included, then the admittance value Y, G, B will change to Y_1, G_1, and B_1 as follows:

Let W_o = losses due to iron and friction, windage, etc. then g_o, the conductance when the parameters are expressed as parallel branches as shown in Chapter 5 (see Figure 5.3).

$$g_o = \frac{W_o}{mV^2} \quad \text{where } W_o = W_{NL} - mI_{NL}^2 r_a$$

$$G_1 = G + g_o \qquad \ldots\ldots\ldots 10.14$$

$$B_1 = B \qquad \ldots\ldots\ldots 10.15$$

$$Y_1 = G_1 - jB_1 \qquad \ldots\ldots\ldots 10.16$$

Substituting for $G = G_1 - g_o$ in equation 10.6 and then carrying out the same procedure as described in the preceding for calculation of x_q, the following expression is arrived at:

$$x_q = \frac{X\,(x_d - X) - (R - r_a^2) - g_o\left[(Zg_o^2 - 2R)\,r_a^2 + 2r_a Z^2\right]}{1 + g_o\,(g_o\,Z^2 - 2R)\,x_d - X} \qquad \ldots\ldots\ldots 10.17$$

$$x_q = \frac{X\,(x_d - X) - (R - r_a)^2}{\left[1 + g_o\,(g_o Z^2 - 2R)\,x_d - X\right]} \qquad \ldots\ldots\ldots 10.18$$

Using the above formula, and by the load test data from Tables 10.5 and 10.6, using the values of current and other readings corresponding to near pull out region, the value of x_q is computed. The computed results of x_d and x_q are tabulated in Tables 10.7 and 10.8. The reactance values are plotted in Figure 10.9 along with the x_d values for different currents for Anisotropic motors.

Similarly the reactance calculations are done for the Synduction motor from load test data from Tables 10.3 and 10.4. The x_d and x_q are tabulated in Tables 10.9 and 10.10. The values are plotted in Figure 10.8.

TABLE 10.7

DIRECT AXIS REACTANCE (ANISOTROPIC)

V	I	$x_d = \sqrt{\frac{V}{I_d^2} - r_a^2}$
400	9.68	23.86
450	11.50	22.6
500	13.23	21.8
550	15.68	20.25
575	17.2	19.30
600	19.3	17.95
650	24.1	15.57
700	31.1	13
740	33.8	12.65

TABLE 10.8

QUADRATURE AXIS REACTANCE (ANISOTROPIC)

V = 575 Volts (L-L); x_d = 21 ohms; r_a = 0.25; g_o = 0.01 ;

I	Z	Cos ∅	Sin ∅	R (ZCos∅)	X (ZSin∅)	x_q
19	17.47	0.531	.8406	9.27	14.7	2.67
26	12.73	0.733	.6704	9.33	8.53	2.69
36	9.2	0.751	.6211	7.185	5.714	3.1
49	6.77	0.809	.5736	5.477	3.88	2.7
66	5.03	0.668	.7466	3.35	3.75	3.2

$$x_q = \frac{X\,(x_d - X) - (R - r_a)^2}{\left[1 + g_o\,(g_o Z^2 - 2R)\,x_d - X\right]}$$

TABLE 10.9

DIRECT AXIS REACTANCE (SYNDUCTION)

V_{L-L}	I_d	$x_d = \sqrt{\frac{V}{(I_d)^2} - r_a^2}$
400	8.31	27.79
450	9.57	27.15
500	10.64	27.13
550	12.76	25
575	14.32	23.2
600	15.8	22
650	21.52	17.43
700	29.25	13.8
730	35.90	11.75

TABLE 10.10

QUADRATURE AXIS REACTANCE (SYNDUCTION)

x_d = 23.2; r_a = .25; g_o = .005;

Volts	I	Z	Cos Ø	Sin Ø	R (ZCosØ)	X (ZSinØ)	x_q
575	33	10.06	.555	.835	5.533	8.4	7
700	38.5	10.5	.407	.913	4.2725	9.6	6.7

$$x_q = \frac{X\,(x_d - X) - (R - r_a)^2}{\left[1 + g_o\,(g_o Z^2 - 2R)\;\; x_d - X\right]}$$

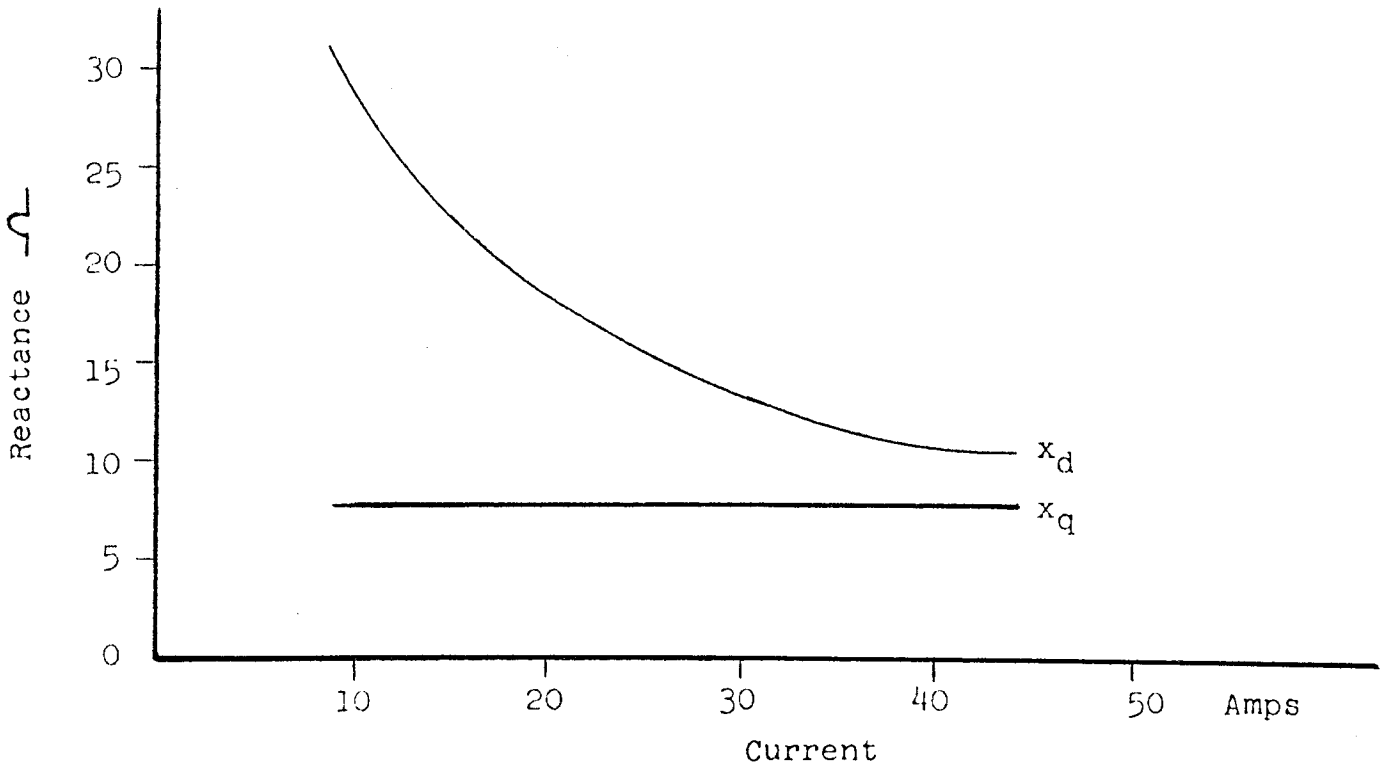

FIGURE 10.8 D-AXIS AND Q-AXIS REACTANCES (SYNDUCTION)

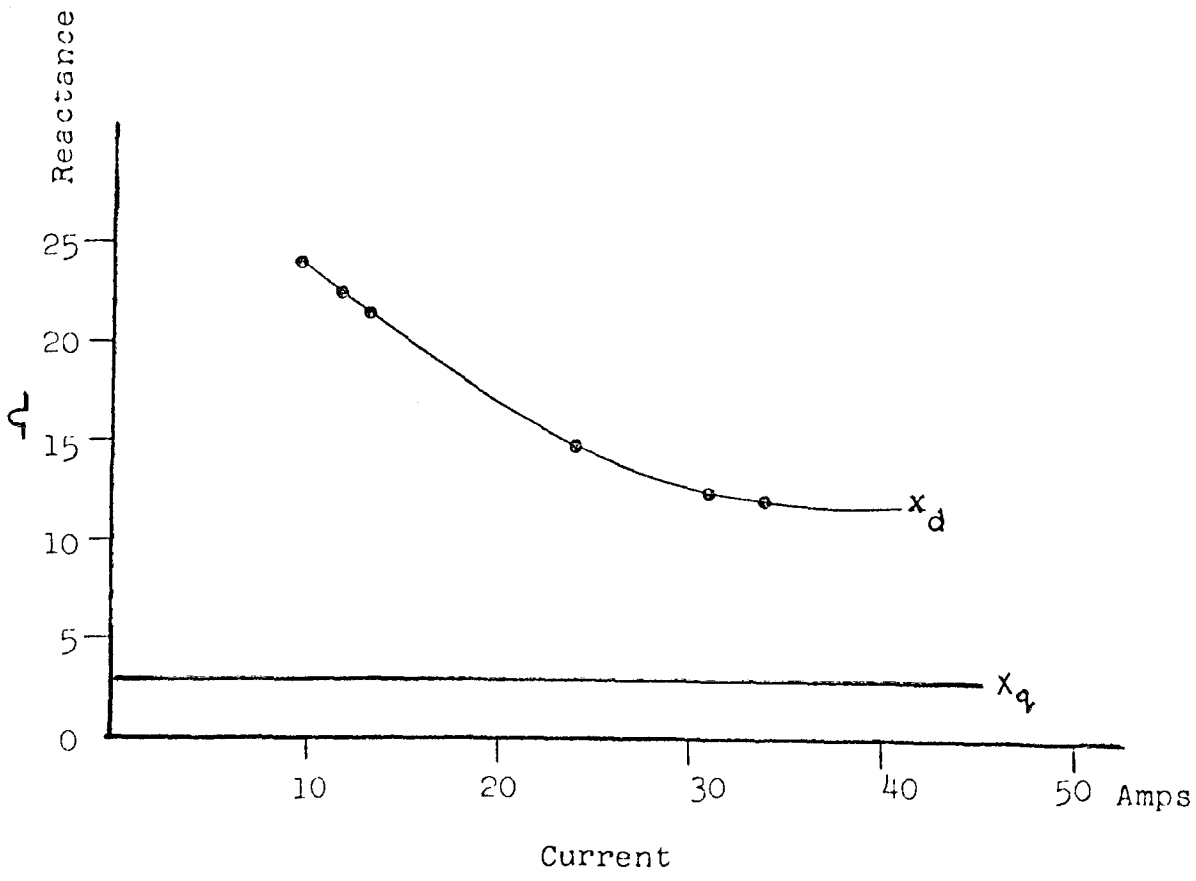

FIGURE 10.9 D-AXIS AND Q-AXIS REACTANCES (ANISOTROPIC)

Pull In Test

The generator connected to the motor was excited with field current corresponding to 12 KW load. The load switch between the generator and the load was kept closed. The motor was started at 480V and the motor pulled into synchronism with the load of 12 KW connected to it and a flywheel inertia 140#ft.^{2} attached to the motor shaft.

As the motor is rated for 575V, the pull in torque would be equal to:

$$T_{pi} = 12 \left(\frac{575}{480}\right)^2 = 17 \text{ KW}$$

and the inertia connected to the shaft is 140#ft.^{2} which is 10 x rotor inertia.

So $T_{\text{pull in}}$ - 1.15 p.u.

As far as the Synduction motor is concerned, the actual load test for pull in could not be taken, but the data is obtained from the curves of Allis-Chalmers, who produce the Synduction motors. From the curves $T_{\text{pull in}}$ = 0.2 p.u. for load inertia being 10 times the rotor inertia.

CHAPTER 11

SOLUTION TO DYNAMIC EQUATION

The equation for dynamic performance of the reluctance motor was established in Chapter 6. It was found that the equation is a second order nonlinear differential equation and could be solved or analogue computer by numerical integration.

By numerical integration, solution is approximate since the time interval cannot be made to be sufficiently small enough to make the step by step integration to be practical.

Since the equation is nonlinear and of the second order, the solution is best obtained by use of analogue computer. The program for the evaluation by the computer is in "BASIC" language using System Simulation Program (S. S. P.).

The various parameters used inthe equations are first evaluated in the following pages. The time constants T_d'' and T_q'' are then evaluated by the equivalent circuits.

The following assumptions are made:

(a) Saturation is neglected.

(b) The armature resistance in relation to the reactances is neglected.

(c) Core loss component in the equivalent circuit is neglected.

The disturbance chosen for the machine consists of 50% load on the machine running at no load. Hence the initial torque angle θ_o is taken as zero.

The general expression is

$$\frac{T_m}{s}\frac{d^2\theta}{dt^2} = N_L -$$

$$V^2\left\{\left[\left(\frac{1}{X''_d} - \frac{1}{X_q}\right)\mathrm{Sin}\theta\mathrm{Cos}\theta - \left(\frac{1}{X''_d} - \frac{1}{X_d}\right)\mathrm{Sin}\theta\mathrm{Cos}\theta_o + \left(\frac{1}{X''_q} - \frac{1}{X_q}\right)\mathrm{Cos}\theta\mathrm{Sin}\theta_o\right]\right.$$

$$\left. + \frac{1}{\omega}\left[\left(\frac{1}{X''_d} - \frac{1}{X_d}\right)T''_d\,\mathrm{Sin}^2\theta + \left(\frac{1}{X''_q} - \frac{1}{X_q}\right)T''_q\,\mathrm{Cos}^2\theta\right]\left(\frac{d\theta}{dt}\right)\right\};$$

Where the various terms are previously explained

substituting $\theta_o = 0$

$V = 1$

$N_L = .5$

and the various reactances and time constants calculated in the following pages and expressed in per unit quantities, the equation becomes after simplification,

$$\frac{d^2\theta}{dt^2} = 11.274 - (6.07\ \mathrm{Sin}2\theta - 112.8\ \mathrm{Sin}\theta) - \frac{d\theta}{dt}\ (2.427 + .695\ \mathrm{Cos}2\theta)$$

Figure 11.1 shows the results of the computer print-out showing variation of torque angle θ against time.

The system stabilizes to new torque angle θ, in about nine cycles.

Final angle is θ, = .323 radians (mechanical)

= .646 radians (electrical)

This is in excellent agreement with the test results observed under the above disturbance. However it was observed that there were fewer oscillations. This is explained by the fact that the above approximations were made and also certain amount of damping in the actual machine due to pole face losses and other eddy current losses were not taken into calculation.

However, the pattern of oscillations and the final torque angle obtained by the computer analysis of dynamical equation is so close to the test observations, that the calculations and approximations assumed become justified.

Calculation of Parameters From Design Values

In the following pages the following parameters are calculated:

R_{Dd} = Resistance of damper in d-axis

R_{Dq} = Resistance of damper in q-axis

X''_d = Transient d-axis reactance

X''_q = Transient q-axis reactance

T''_d = Short circuit time constant d-axis

T''_q = Short circuit time constant q-axis

T_m = Inertial time constant

Rotor circuit.

(a) d-axis resistance

$$R_{Dd(bar)} = P \frac{L_b}{K_b A_b} Z_D,$$

$$R_{Dd(ring)} = \frac{2P}{K_r} \frac{\gamma_{sD}}{A_r} \frac{Z_D^2}{4}$$

Substituting physical parameters

$$R_{Dd(total)} = (0.538)\ 10^{-5} \text{ ohms}$$

(b) q-axis resistance

$$\text{Similarly } R_{Dq(bar)} = P \frac{L_b}{K_b A_b} Z_D$$

$$R_{Dq(ring)} = P \left(\frac{L_b}{K_b A_b} + \frac{\gamma_p - Z_D \gamma_{sD/2}}{K_r A_r} \right) Z_D$$

On substitution,

$$R_{Dq(total)} = (1.635)\ 10^{-5} \text{ ohms}$$

Reducing the above resistances into stator terms by multiplying by the appropriate reduction factors, the following direct and quadrature axis resistances are obtained:

R'_{Dd} = .373 ohms i.e. 0.036 p.u.

R'_{Dq} = 0.563 ohms i.e. 0.054 p.u.

(c) d-axis reactance

(1) Slot reactance $X_{Dds} = (3.25)\ 10^{-5}$ ohms.

(2) End leakage reactance $X_{Dd} = (5.17)\ 10^{-5}$ ohms.

(3) Harmonic leakage reactance--negligable

Total $X_{Dd} = (8.42)\ 10^{-5}$ ohms

In terms of stator X'_{Dd} = 1.45 ohms i.e. 0.14 p.u.

(d) q-axis reactance

(1) Slot reactance $X_{Dqs} = (23.10)\ 10^{-5}$ ohms.

(2) End reactance $X_{Dq} = (7.33)\ 10^{-5}$ ohms.

(3) Harmonic reactance--negligable

Total X_{Dq} = 30.43 ohms

In terms of stator X'_{Dq} = 2.63 ohms i.e. 0.254 p.u.

Parameters of The Equivalent Circuit.

X_{al} = .4923 ohms = .0476 p.u.

X_{aq} = 3.5 ohms = .338 p.u.

X_{ad} = 14 ohms = 1.3 p.u.

X_{Dq} = 2.63 ohms = .254 p.u.

X_{Dd} = 1.45 ohms = .14 p.u.

r_{Dq} = .563 ohms = .054 p.u.

r_{Dd} = .373 ohms = .036 p.u.

Time constant.

d-axis

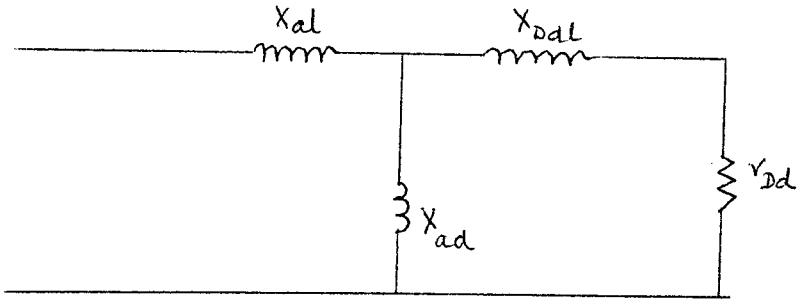

$$T_d'' = \frac{.14 + \frac{1.3\ (.0476)}{1.3 + .0476}}{.036}$$

= 5.16 radians

= 13.7 milliseconds

q-axis

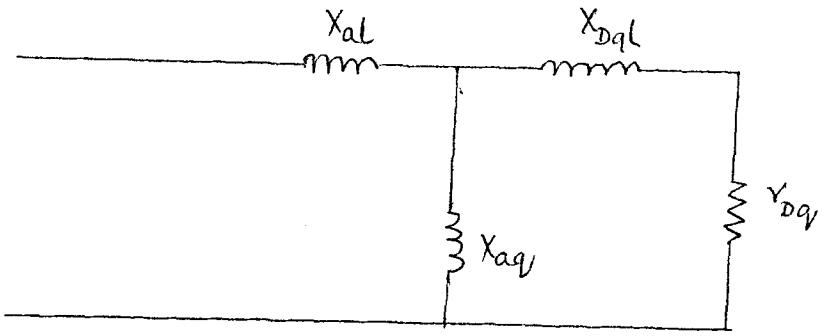

$$T_q'' = \frac{.254 + \frac{(.338)\ (.0476)}{.338 + .0476}}{.054}$$

$$= 5.476 \text{ radians}$$

$$= 14.52 \text{ milliseconds}$$

$$X_d = 1.35$$

$$X_q = 0.3858$$

$$X_d'' = .0476 + \frac{(1.3)\ (.14)}{1.3 + .14} = 0.174 \text{ p.u.}$$

$$X_q'' = .0476 + \frac{(.338)\ (.254)}{(.338 + .254)} = 0.192 \text{ p.u.}$$

Mechanical Time Constant.

$$WR^2 = 140\#ft.^2$$

$$T_m = \frac{WR^2\ (1800)}{308(T)}; \quad T = \frac{25 \times 7.04}{1.800} = 97\#ft.$$

$$= \frac{140\ (1800)}{308\ (97)} = 8.36 \text{ seconds}$$

Dynamic Equation (General).

$$\frac{T_m}{s}\frac{d^2\theta}{dt^2} = N_L -$$

$$V^2\left\{\left[\left(\frac{1}{X_d''} - \frac{1}{X_q''}\right)\text{Sin}\ \theta\text{Cos}\theta - \left(\frac{1}{X_d''} - \frac{1}{X_d}\right)\text{Sin}\theta\text{Cos}\theta_o + \left(\frac{1}{X_q''} - \frac{1}{X_q}\right)\text{Cos}\theta\text{Sin}\theta_o\right]\right.$$

$$\left. + \frac{1}{\omega}\left[\left(\frac{1}{X_d''} - \frac{1}{X_d}\right)\ T_d''\ \text{Sin}^2\theta + \left(\frac{1}{X_q''} - \frac{1}{X_q}\right)\ T_q''\ \text{Cos}^2\theta\right]\ \frac{d\theta}{dt}\right\}$$

Where,

θ_o = 0 at t = 0

N_L = 0.5

V = 1

ω_s = 188.5 rad/sec

T_m = 8.36 seconds

T_d'' = 5.16 radians

T_q'' = 5.476 radians

Substituting the preceding values, we have

$$.04435 \frac{d^2\theta}{dt} = .5 - \left(.2694 \text{ Sin } 2\theta - 5.006 \text{ Sin } \theta\right) - \frac{1}{186.5} \frac{d\theta}{dt} (30.07 + 5.75 \text{ Cos } 2\theta)$$

$$\frac{d^2\theta}{dt^2} = 11.274 - (6.07 \text{ Sin } 2\theta - 112.8 \text{ Sin } \theta) - \frac{d\theta}{dt} (2.426 + .695 \text{ Cos } 2\theta) ;$$

The above dynamic equation was set up on a computer for solution of torque angle θ as a function of time. A disturbance of suddenly applied load of 0.5 p.u. in magnitude was applied on a machine running under no load steady state condition where torque angle θ_o was considered equal to zero. The interval of computation time was chosen as 0.1 seconds and it took a total time of 5 to 7 seconds for all the oscillations of torque angle to settle down (see Figure 11.2). The computer print-out has the torque angle in mechanical radians plotted along Y-axis and time t in seconds plotted along X-axis.

The program was written in S.S.P. (System Simulation Program). The flow chart in drawn in Figure 11.1.

Flow Chart

Figure 11.1 depicts the flow chart set up for programming for the solution of the dynamical equation. Fifteen function blocks numbering from one to fifteen are chosen, each representing an algebraic or trigonometric function as shown on the diagram. The function block numbers, as well as the function they represent, are shown on the flow chart. The symbols used are according to the System Simulator Block definitions of the S.S.P. language.

Program

Table 11.1 depicts the program written in S.S.P. A short description and explanation of the program write-up is in order at this stage.

The program control is accomplished by two lines of data and a third line for the plot of torque angle θ against time.

The first line consists of the following:

(a) Fixed/free input indicator: 1 for free format

(b) Print interval: 0.1 sec.

(c) Total time: 10 sec.

(d) Initial condition of independent variable:
t = 0 sec.

(e) Error criteria: .00005

(f) Minimum integration interval = print interval/64.

Second line consists of the following:

(a) Four output block numbers: 15, 14, 5, 10.

(b) Number of runs: 1

(c) Function generator indicator: 0 as no arbitrary function generator is used.

(d) Total program Reset: 0 for single run.

(e) Sorted sequence print out indicator: 1 for sorted block sequence print out required.

(f) Number of plots: 1

Third line consists of the following:

(a) The number of output block to be plotted against the independent variable: 15 in the line indicates the value of θ to be printed.

(b) Any other output blocks to be printed to a maximum: In the program these are represented by 0's, as no other block print out was required.

The above three lines of the program form the program control description, the block description data lines are written. The free field input format is used. Each data line consists of the following:

(a) Element number: 2 - multiplication by constant
4 - integration
6 - constant
9 - sum

12 - Sin function

13 - Cos function

57 - List program.

(b) Block Number: Number of the block being operated.

(c) Input Blocks: Three must be specified.

(d) Numeric field: 0.

There are as many block description data lines as there are function blocks, and an additional line at the end having element 57 to indicate to the computer to list the program once the program is fed into the machine.

As decided by the second line of the program control data, the values of output blocks 15, 14, 5, 10 are printed out against the indpendent variable time from zero to ten seconds at intervals of 0.1 second.

In this instant, only output block 15 consisting of the dependent variable θ against time was desired as dictated by the third line of the program control data. The output is plotted and is shown in Figure 11.2.

From Figure 11.2 is seen the behavoir of the machine for a sudden disturbance from no load to half load condition. The rotor oscillations are depicted as well as the final position of rotor corresponding to load torque angle. The pattern of oscillations and the final torque angle very closely check with the observation during actual tests on the machine.

PROGRAM

```
:JOB, EE301
:PROG, SSP, 7
S. C. RAO

.1, .1, 10,  0, 3, 1
15, 14,  5, 10, 1, 0, 0, 1, 1
 0, 15,  0, 0, 0, 0



 2,  1, 15,   0,   0, 2
13,  2,  1,   0,   0, 0
 2,  3,  2,   0,   0, .695
 6,  4,  0,   0,   0, 2.426
 9,  5,  4,   3,   0, 0
12,  6,  1,   0,   0, 0
 2,  7,  6,   0,   0, 6.07
12,  8, 15,   0,   0, 0
 2,  9,  8,   0,   0, 112.8
 9, 10,  7,   9,   0, 0
 8, 11, 14,   5,   0, 0
 6, 12,  0,   0,   0, 11.274
 9, 13, 12, -10, -11  0
 4, 14, 13,   0,   0, 0
 4, 15, 14,   0,   0, 0
57,  0,  0,   0,   0, 0
```

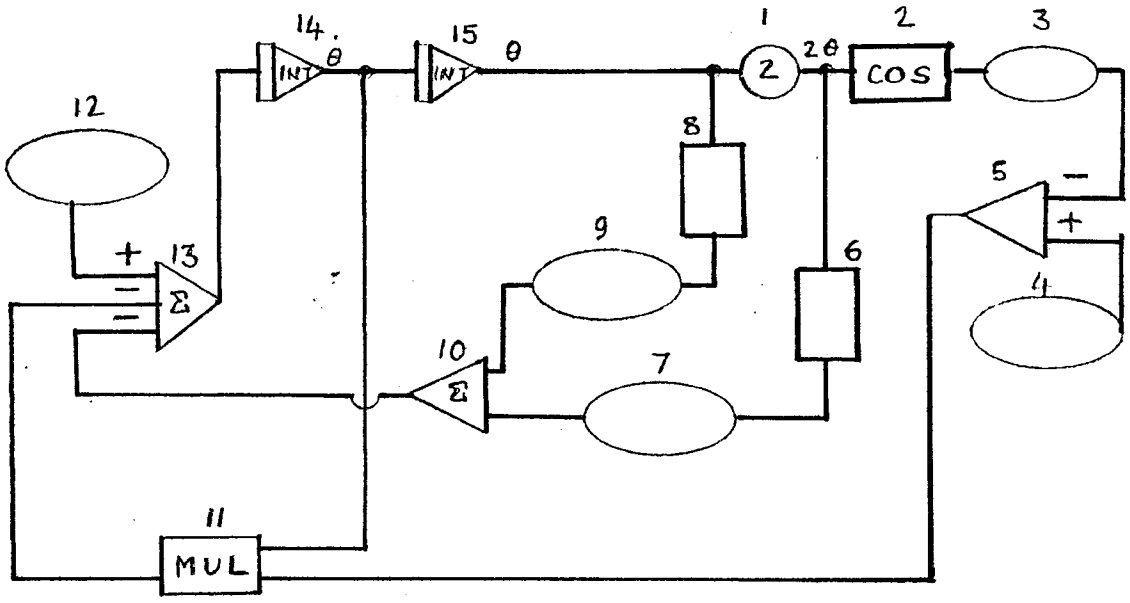

FIGURE 11.1 FLOW CHART FOR COMPUTER PROGRAM

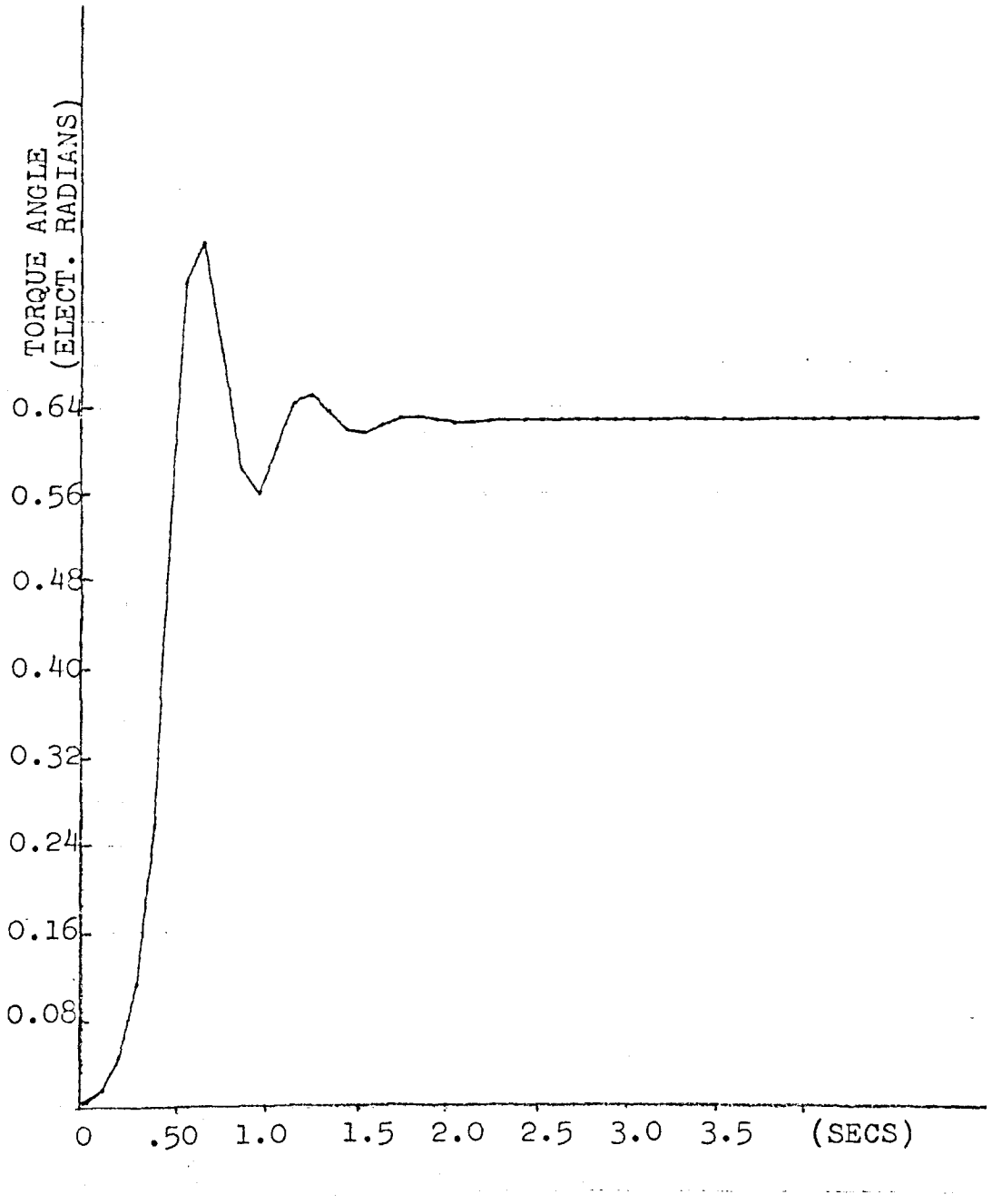

FIGURE 11.2 PLOT OF RESPONSE OF MOTOR FOR SUDDEN APPLICATION OF LOAD

CHAPTER 12

CONCLUSIONS

The superiority of the Anisotropic rotor over the Synduction is established in more than one aspect.

The torque of any synchronous machine depends on the ratio of x_d/x_q. It has been established both by analysis in Chapter 9 and tests in Chapter 10 that this ratio is higher in the case of Anisotropic rotor. In a conventional reluctance motor (as well as in synchronous motor), the ratio is 2:1 approximately. In the case of Synduction it is about 4:1 and in the case of Anisotropic a ratio of 6:1 or even better is obtainable.

Comparison of pull out torques from test data for the two machines also shows the same trend. At 480V input the pull out power in Synduction was only 12.5 KW compared to 23 KW in the Anisotropic rotor.

Thirdly, the power factors are compared from test data. The maximum power factor reached on Synduction motor at 575 volt operation was only about 0.56 obtained at load torque of 60 ft.lbs. In the case of Anisotropic, the power factor was 0.8 for 575 volt operation and a load of 120 ft. lbs.

Similarly the input line current for 575 volt operation and 60 ft.lbs. torque for Synduction motor is about 31 amps, where as in Anisotropic for the same conditions it is only 26 amps thereby resulting in improved efficiency.

Finally, the pull in characteristic is also considerably improved in the case of Anisotropic rotor. With a load inertia connected to the shaft, being approximately 10 times the normal rotor inertia, the Anisotropic motor was able to pull in with 1.15 p.u. electrical load connected. This compared favorably with the ratio of only 0.2 for $T_{pull\ in}/T_{rated}$ ratio for Synduction motor. This latter number is taken from the curves for commercially available Synduction motors.

So it is clearly seen that the Anisotropic rotor is superior in performance to the reluctance or Synduction motors. In fact the Anisotropic motor can be considered as a 40 HP in the same frame in which the Synduction motor developed only 25 HP.

As far as the author is aware of, some of the characteristics obtained above have far exceeded the performance obtained by any type of reluctance motor built so far.

With rugged and reliable construction and no rotating windings, this version is a serious challenge to synchronous

motors for many applications and will easily outweigh the conventional reluctance or Synduction motor in practically all applications in view of improved performance. Some of the many applications include textile mill drives and such where several motors have to run locked in step and run synchronously.

Summary of Performance

For the sake of comparison, the performance of the two types of motors, Synduction and Anisotropic, are listed below in tabular form.

The comparison is made on the basis of tests conducted and detailed in the previous chapter.

PERFORMANCE	SYNDUCTION	ANISOTROPIC
Ratio of $\frac{X_d}{X_q}$ at 15 amps stator current.	3.3	6.8
Maximum power factor at 480V input.	0.56	0.8
Input current for 55ft# torque at 480V.	37 amps	23.5 amps
Pull out torque at 480V.	57ft#	102ft#
Pull in torque at 480V with 10 times rotor inertia.	12ft#	58ft#

From the preceding, the superiority of the Anisotropic motor over the Synduction is clearly established. The thermal rating of Anisotropic could be almost 1.5 times and the pull out rating almost two times the Synduction for the same frame size. Also in view of greatly improved power factor of the order of 0.8, which is never hitherto achieved in other reluctance machines, the efficiency of the Anisotropic motor also works out to be higher, and the motor more readily acceptable in industrial applications.

REFERENCES

1. Alger, P. L., The Induction Machines--Their Behavoir and Uses. Second Edition. Gordon and Breach Science Publishers.

2. Crouse, C. H., "A Design Method for Polyphase Reluctance Synchronous Motors," AIEE Trans., vol. 70, 1951, pp. 957-962.

3. Douglas, John F.H., "The Theory of Anisotropic Field Structures in Synchronous Machines," AIEE Trans., April, 1956, pp. 84-86.

4. Fong, W., "New Type of Reluctance Motor," Proc. IEE, vol. 117, No. 3, March, 1970, pp. 545-551.

5. Honsinger, V. B., "The Inductances L_d and L_q of Reluctance Machines," IEEE Trans., vol. Pas-90, No. 1, pp. 299-304.

6. Honsinger, V. B., "Steady State Performance of Reluctance Machines," IEEE Trans., vol. Pas-90, No. 1, pp. 305-317.

7. Jain, G. C., Design, Operation and Testing of Synchronous Machines. Bombay, India: Asia Publishing House.

8. Kron, Gabriel, "Generalized Theory of Electric Machinery," AIEE Trans., vol. 49, 1930, pp. 666-683.

9. Kron Gabriel, "Steady State Equivalent Circuits of Synchronous Machines," AIEE Trans., vol. 67, 1948, pp. 175-181.

10. Kron, Gabriel, Tensors for Circuits. Dover Press, 1959.

11. Lawrenson, P. J. and Gupta, S. K., "Segmental Rotor Reluctance Motors," Proc. IEE, May, 1967, vol. 114, No. 5, pp. 645-653.

12. Lawrenson, P. J. and Agu, L. A., "Theory and Performance of Polyphase Reluctance Machines," Proc. IEE, vol. 111, No. 8, August, 1964, pp. 1435-1445.

13. Liwschitz-Garik and Whipple, Electric Machinery, Vol. II, AC Machines. Fifth Printing. New York: D. Van Nostrand Company, Inc., 1946.

14. Menzies, R. W., "Theory and Operation of Reluctance Motors With Magnetically Anisotropic Rotors, Part I Analysis," IEEE Trans., vol. Pas-91, No. 1, January 1972, pp. 35-41.

15. Menzies, Mathur and Lee, "Theory and Operation of Reluctance Motors With Magnetically Anisotropic Rotors, Part II Analysis," IEEE Trans., vol. Pas-91, No. 1, January, 1972, pp. 42-45.

16. Puchstein, Lloyd and Conrad, Alternating-Current Machines. Third Edition. New York: John Wiley & Sons, Inc., June, 1958.

17. Seely, Samuel, Electromechanical Energy Conversion. McGraw Hill Book Company, 1962.

18. Trickey, P. H., "The Non-Excited Synchronous Motor," Pittsbugh, Elec. Jour., 1933, No. 30, pp. 160.